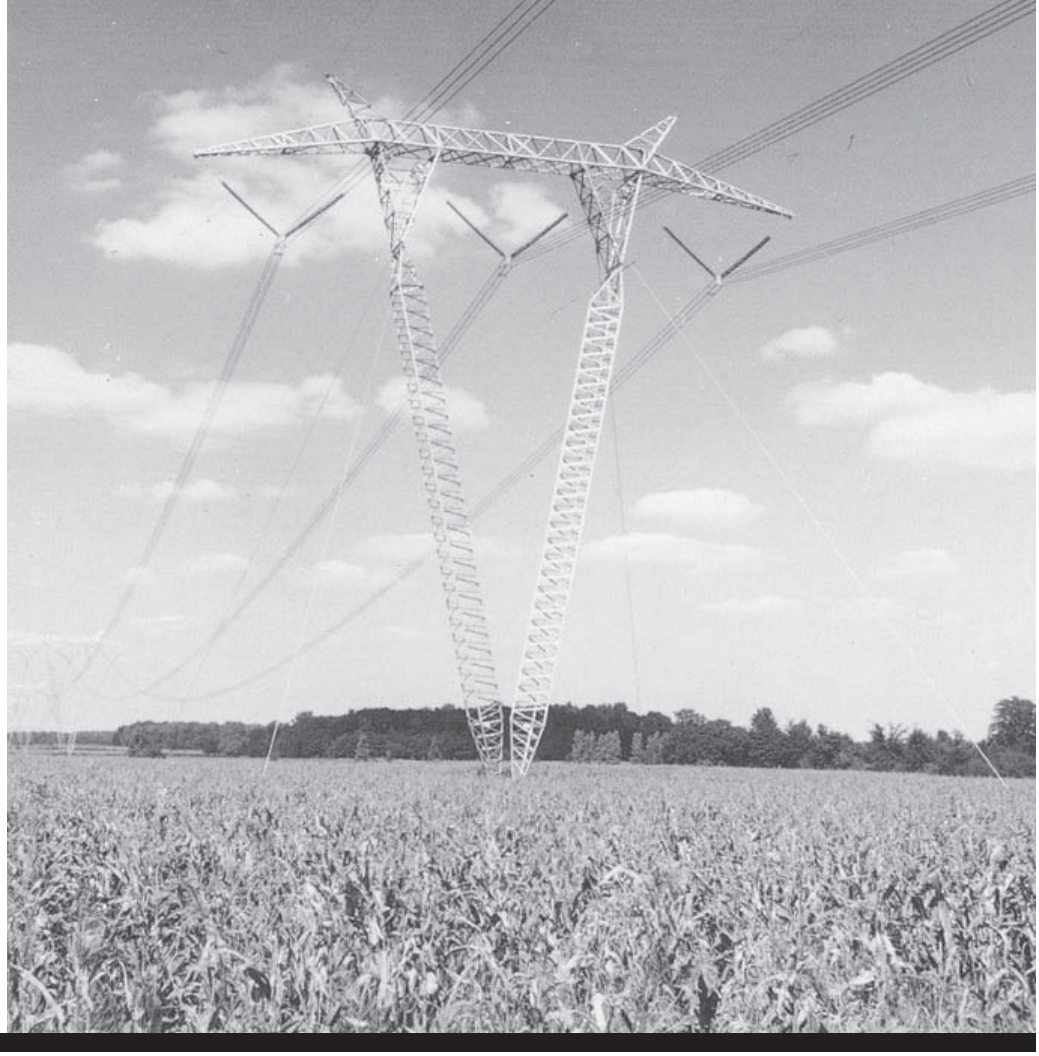

765-kV transmission line with aluminum guyed-V towers (Courtesy of American Electric Power Company)

4

TRANSMISSION LINE PARAMETERS

In this chapter, we discuss the four basic transmission-line parameters: series resistance, series inductance. shunt capacitance, and shunt conductance. We also investigate transmission-line electric and magnetic fields.

Series resistance accounts for ohmic (I^2R) line losses. Series impedance, including resistance and inductive reactance, gives rise to series-voltage drops along the line. Shunt capacitance gives rise to line-charging currents. Shunt conductance accounts for V^2G line losses due to leakage currents between conductors or between conductors and ground. Shunt conductance of overhead lines is usually neglected.

Although the ideas developed in this chapter can be applied to underground transmission and distribution, the primary focus here is on overhead lines. Underground transmission in the United States presently accounts for less than 1% of total transmission, and is found mostly in large cities or under

waterways. There is, however, a large application for underground cable in distribution systems.

CASE STUDY Two transmission articles are presented here. The first article covers transmission conductor technologies including conventional conductors, high-temperature conductors, and emerging conductor technologies [10]. Conventional conductors include the aluminum conductor steel reinforced (ACSR), the homogeneous all aluminum alloy conductor (AAAC), the aluminum conductor alloy reinforced (ACAR), and others. High-temperature conductors are based on aluminum-zirconium alloys that resist the annealing effects of high temperatures. Emerging conductor designs make use of composite material technology. The second article describes trends in transmission and distribution line insulators for six North American electric utilities [12]. Insulator technologies include porcelain, toughened glass, and polymer (also known as composite or non-ceramic). All three technologies are widely used. Current trends favor polymer insulators for distribution (less than 69 kV) because they are lightweight, easy to handle, and economical. Porcelain remains in wide use for bulk power transmission lines, but maintenance concerns associated with management and inspection of aging porcelain insulators are driving some utilities to question their use. Life-cycle cost considerations and ease of inspection for toughened glass insulators are steering some utilities toward glass technology.

Transmission Line Conductor Design Comes of Age

ART J. PETERSON JR. AND SVEN HOFFMANN

Deregulation and competition have changed power flows across transmission networks significantly. Meanwhile, demand for electricity continues to grow, as do the increasing challenges of building new transmission circuits. As a result, utilities need innovative ways to increase circuit capacities to reduce congestion and maintain reliability.

National Grid is monitoring transmission conductor technologies with the intent of testing and deploying innovative conductor technologies within the United States over the next few years. In the UK, National Grid has been using conductor replacement as a means of increasing circuit capacity since the mid 1980s, most recently involving the high-temperature, low-sag "Gap-type" conductor. As a first step in developing a global conductor deployment strategy, National Grid embarked on an overall assessment of overhead transmission line conductor technologies, examining innovative, and emerging technologies.

("Transmission Line Conductor Design Comes of Age" by Art J. Peterson Jr. and Sven Hoffmann, Transmission & Distribution World Magazine, (Aug/2006). Reprinted with permission of Penton Media)

About National Grid

National Grid USA is a subsidiary of National Grid Transco, an international energy-delivery business with principal activities in the regulated electric and gas industries. National Grid is the largest transmission business in the northeast United States, as well as one of the 10 largest electric utilities in the United States National Grid achieved this by combining New England Electric System, Eastern Utilities Associates and Niagara Mohawk between March 2000 and January 2002. Its electricity-delivery network includes 9000 miles (14,484 km) of transmission lines and 72,000 miles (115,872 km) of distribution lines.

National Grid UK is the owner, operator and developer of the high-voltage electricity transmission network in England and Wales, comprising approximately 9000* circuit-miles of overhead line and 600* circuit-miles of underground cable at 275 and 400 kV, connecting more than 300 substations.

**9000 circuit-miles = 14,500 circuit-km*
**600 circuit-miles = 1000 circuit-km*

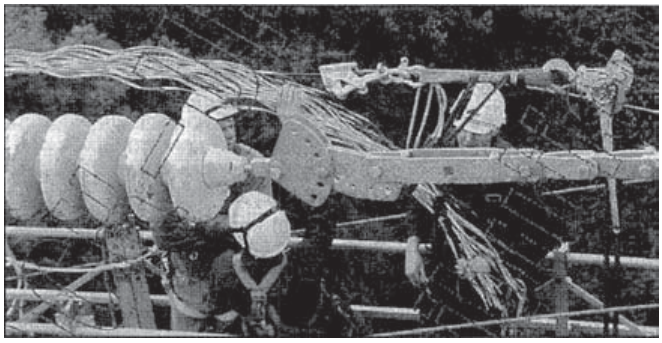

De-stranding the Gap conductor for field installation

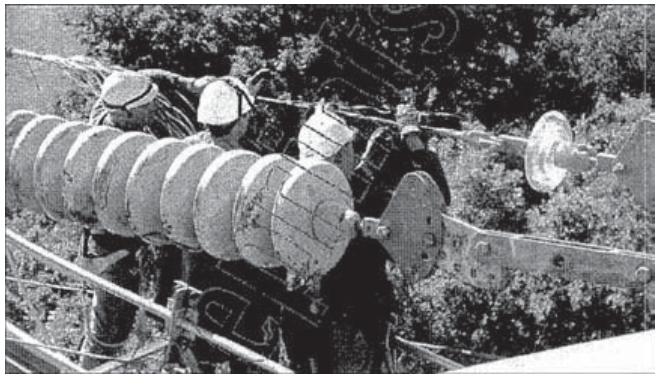

Re-stranding of conductor

CONVENTIONAL CONDUCTORS

The reality is that there is no single "wonder material." As such, the vast majority of overhead line conductors are nonhomogeneous (made up of more than one material). Typically, this involves a high-strength core material surrounded by a high-conductivity material. The most common conductor type is the aluminum conductor steel reinforced (ACSR), which has been in use for more than 80 years. By varying the relative cross-sectional areas of steel and aluminum, the conductor can be made stronger at the expense of conductivity (for areas with high ice loads, for example), or it can be made more conductive at the expense of strength where it's not required.

More recently, in the last 15 to 20 years, the homogeneous all-aluminum alloy conductor (AAAC) has become quite popular, especially for National Grid in the UK where it is now the standard conductor type employed for new and refurbished lines. Conductors made up of this alloy (a heat treatable aluminum-magnesium-silicon alloy) are, for the same diameter as an ACSR, stronger, lighter, and more conductive although they are a little more expensive and have a higher expansion coefficient. However, their high strength-to-weight ratio allows them to be strung to much lower initial sags, which allows higher operating temperatures. The resulting tension levels are relatively high, which could result in increased vibration and early fatigue of the conductors. In the UK, with favorable terrain, wind conditions and dampers, these tensions are acceptable and have allowed National Grid to increase the capacities of some lines by up to 50%.

For the purpose of this article, the three materials mentioned so far—steel, aluminum and aluminum alloy—are considered to be the materials from which conventional conductors are made. The ACSR and AAAC are two examples of such conductors. Other combinations available include aluminum conductor alloy reinforced (ACAR), aluminum alloy conductor steel reinforced (AACSR) and the less common all-aluminum conductor (AAC).

Conductors of these materials also are available in other forms, such as compacted conductors, where the strands are shaped so as not to leave any voids within the conductor's cross section (a standard conductor uses round strands), increasing the amount of conducting material without increasing the diameter. These conductors are designated trapezoidal-wire (TW) or, for example, ACSR/TW and AACSR/TW. Other shaped conductors are available that have noncircular cross sections designed to minimize the effects of wind-induced motions and vibrations.

HIGH-TEMPERATURE CONDUCTORS

Research in Japan in the 1960s produced a series of aluminum-zirconium alloys that resisted the annealing effects of high temperatures. These alloys can retain their strength at temperatures up to 230 °C (446 °F). The most common of these alloys—TA1, ZTA1 and XTA1—are the basis of a variety of high-temperature conductors.

Clamp used for Gap conductor

The thermal expansion coefficients of all the conventional steel-cored conductors are governed by both materials together, resulting in a value between that of the steel and that of the aluminum. This behavior relies on the fact that both components are carrying mechanical stress.

However, because the expansion coefficient of aluminum is twice that of steel, stress will be increasingly transferred to the steel core as the conductor's temperature rises. Eventually the core bears all the stress in the conductor. From this point on, the conductor as a whole essentially takes on the expansion coefficient of the core. For a typical 54/7 ACSR (54 aluminum strands, 7 steel) this transition point (also known as the "knee-point") occurs around 100 °C (212 °F).

For lines built to accommodate relatively large sags, the T-aluminum conductor, steel reinforced (TACSR) conductor was developed. (This is essentially identical to ACSR but uses the heat-resistant aluminum alloy designated TA1). Because this conductor can be used at high temperatures with no strength loss, advantage can be taken of the low-sag behavior above the knee-point.

If a conductor could be designed with a core that exhibited a lower expansion coefficient than steel, or that exhibited a lower knee-point temperature, more advantage could be taken of the high-temperature alloys. A conductor that exhibits both of these properties uses Invar, an alloy of iron and nickel. Invar has an expansion coefficient about one-third of steel (2.8 microstrain per Kelvin up to 100 °C, and 3.6 over 100 °C, as opposed to 11.5 for steel). T-aluminum conductor Invar reinforced (TACIR) is capable of operation up to 150 °C (302 °F), with ZTACIR and XTACIR capable of 210 °C (410 °F) and 230 °C (446 °F), respectively.

Further, the transition temperature, although dependent on many factors, is typically lower than that for an ACSR, allowing use of the high temperatures within lower sag limits than required for the TACSR conductors. One disadvantage of this conductor is that Invar is considerably weaker than steel. Therefore, for high-strength applications (to resist ice loading, for example), the core needs to make up a greater proportion of the conductor's area, reducing or even negating the high-temperature benefits. As a result, the ACIR-type conductors are used in favorable areas in Japan and Asia, but are not commonly used in the United States or Europe.

There will still be instances, however, where insufficient clearance is available to take full advantage of the transitional behavior of the ACIR conductors. A conductor more suitable for uprating purposes would exhibit a knee-point at much lower temperatures. Two conductors are available that exhibit this behavior: the Gap-type conductor and a variant of the ACSR that uses fully annealed aluminum.

Developed in Japan during the 1970s, Gap-type ZT-aluminum conductor steel reinforced (GZTACSR) uses heat-resistant aluminum over a steel core. It has been used in Japan, Saudi Arabia, and Malaysia, and is being extensively implemented by National Grid in the UK. The principle of the Gap-type conductor is that it can be tensioned on the steel core alone during erection. A small annular Gap exists between a high-strength steel core and the first layer of trapezoidal-shaped aluminum strands, which allows this to be achieved. The result is a conductor with a knee-point at the erection temperature. Above this, thermal expansion is that of steel (11.5 microstrain per Kelvin), while below it is that of a comparable ACSR (approximately 18). This construction allows for low-sag properties above the erection temperature and good strength below it as the aluminum alloy can take up significant load.

For example, the application of GZTACSR by National Grid in the UK allowed a 90 °C (194 °F) rated 570 mm^2 AAAC to be replaced with a 620 mm^2 GZTACSR (Matthew). The Gap-type conductor, being of compacted construction, actually had a smaller diameter than the AAAC, despite having a larger nominal area. The low-sag properties allowed

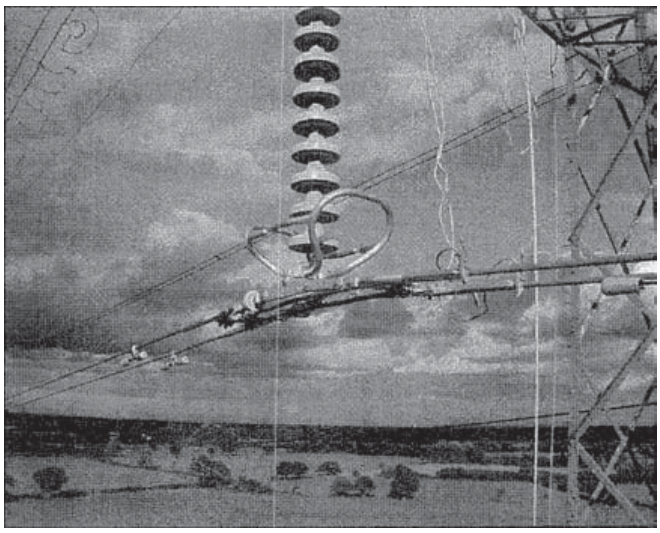

Semi-strain assembly installed on line in a rural area of the UK

a rated temperature of 170 °C (338 °F) and gave a 30% increase in rating for the same sag.

The principal drawback of the Gap-type conductor is its complex installation procedure, which requires destranding the aluminum alloy to properly install on the joints. There is also the need for "semi-strain" assemblies for long line sections (typically every five spans). Experience in the UK has shown that a Gap-type conductor requires about 25% more time to install than an ACSR.

A semi-strain assembly is, in essence, a pair of back-to-back compression anchors at the bottom of a suspension insulator set. It is needed to avoid potential problems caused by the friction that developes between the steel core and the aluminum layers when using running blocks. This helps to prevent the steel core from hanging up within the conductor.

During 1999 and 2000, in the UK, National Grid installed 8 km (single circuit) of Matthew GZTACSR. Later this year and continuing through to next year, National Grid will be refurbishing a 60 km (37-mile) double-circuit (120 circuit-km) route in the UK with Matthew.

A different conductor of a more standard construction is aluminum conductor steel supported (ACSS), formerly known as SSAC. Introduced in the 1980s, this conductor uses fully annealed aluminum around a steel core. The steel core provides the entire conductor support. The aluminum strands are "dead soft," thus the conductor may be operated at temperatures in excess of 200 °C without loss of strength. The maximum operating temperature of the conductor is limited by the coating used on the steel core. Conventional galvanized coatings deteriorate rapidly at temperatures above 245 °C (473 °F). If a zinc-5% aluminum mischmetal alloy coated steel core is used, temperatures of 250 °C are possible.

Since the fully annealed aluminum cannot support significant stress, the conductor has a thermal expansion similar to that of steel. Tension in the aluminum strands is normally low. This helps to improve the conductor's self-damping characteristics and helps to reduce the need for dampers.

For some applications there will be concern over the lack of strength in the aluminum, as well as the possibility of damage to the relatively soft outer layers. However, ACSS is available as ACSS/TW, improving, its strength. ACSS requires special care when installing. The soft annealed aluminum wires can be easily damaged and "bird-caging" can occur. As with the other high-temperature conductors, the heat requires the use of special suspension clamps, high-temperature deadends, and high-temperature splices to avoid hardware damage.

EMERGING CONDUCTOR TECHNOLOGIES

Presently, all the emerging designs have one thing in common—the use of composite material technology.

Aluminum conductor carbon fiber reinforced (ACFR) from Japan makes use of the very-low-expansion coefficient of carbon fiber, resulting in a conductor with a lower knee-point of around 70 °C (158 °F). The core is a resin-matrix composite containing carbon fiber. This composite is capable of withstanding temperatures up to 150 °C. The ACFR is about 30% lighter and has an expansion coefficient (above the knee-point) that is 8% that of an ACSR of the same stranding, giving a rating increase of around 50% with no structural work required.

Meanwhile, in the United States, 3M has developed the Aluminum Conductor Composite Reinforced (ACCR). The core is an aluminum-matrix

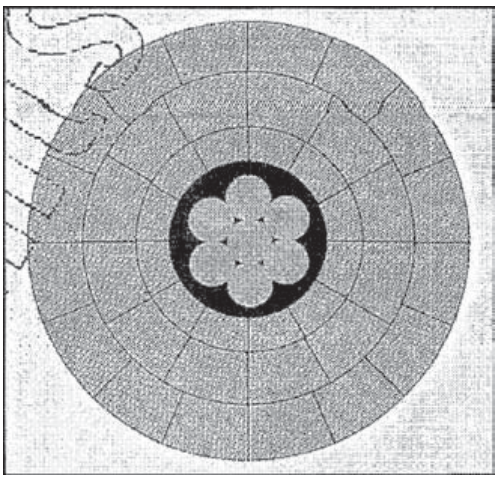

A cross section of the Gap conductor

composite containing alumina fibers, with the outer layers made from a heat-resistant aluminum alloy. As with the ACFR, the low-expansion coefficient of the core contributes to a fairly low knee-point, allowing the conductor to make full use of the heat resistant alloy within existing sag constraints. Depending on the application, rating increases between 50% and 200% are possible as the conductor can be rated up to 230 °C.

Also in the United States, two more designs based on glass-fiber composites are emerging. Composite Technology Corp. (CTC; Irvine, California, U.S.) calls it the aluminum conductor composite core (ACCC), and W. Brandt Goldsworthy and Associates (Torrance, California) are developing composite reinforced aluminum conductor (CRAC). These conductors are expected to offer between 40% and 100% increases in ratings.

Over the next few years, National Grid plans to install ACSS and the Gap conductor techology within its U.S. transmission system. Even a test span of one or more of the new composite conductors is being considered.

Art J. Peterson Jr. is a senior engineer in National Grid's transmission line engineering and project management department in Syracuse, New York. Peterson received a BS degree in physics from Le Moyne College in Syracuse; a MS degree in physics from Clarkson University in Potsdam, New York; a M. Eng. degree in nuclear engineering from Pennsylvania State University in State College, Pennsylvania; and a Ph.D. in organization and management from Capella University in Minneapolis, Minnesota. He has 20 years of experience in electric generation and transmission.

Art.Peterson@us.ngrid.com

Sven Hoffmann is the circuits forward policy team leader in National Grid's asset strategy group in Coventry, United Kingdom. Hoffmann has a bachelor's in engineering degree from the University of Birmingham in England. He is a chartered engineer with the Institution of Electrical Engineers, and the UK Regular Member for CIGRE Study Committee B2. Hoffmann has been working at National Grid, specializing in thermal and mechanical aspects of overhead lines for eight years.

sven.hoffmann@uk.ngrid.com

Six Utilities Share Their Perspectives on Insulators

APR 1, 2010 12:00 PM

BY RAVI S. GORUR, ARIZONA STATE UNIVERSITY

Trends in the changing landscape of high-voltage insulators are revealed through utility interviews.

("Six Utilities Share Their Perspectives on Insulators" by Ravi S. Gorur, *Transmission & Distribution World Magazine* (April/2010). *Reprinted with permission of Penton Media)*

The high-voltage transmission system in North America is the result of planning and execution initiated soon after World War II. Ambitious goals, sound engineering and the vertically integrated structure of utilities at that time all contributed to high reliability and good quality of electric power.

The high-voltage transmission infrastructure development peaked in the 1970s. From then on until the turn of the century, load growth was not as high as anticipated, resulting in a drastic reduction in transmission activity. Consequently, the system was pushed to its limits, which led to a few large-scale blackouts. The consensus is that the existing system is bursting at its seams, continuing to age and needs refurbishment; at the same time, new lines are needed to handle load growth and transfer massive amounts of power from remote regions to load centers.

Today, several thousand kilometers of transmission lines at voltages from 345 kV ac to 765 kV ac and high-voltage dc lines are either in the planning or construction stages. A catalyst for this renewed interest in transmission line construction is renewable energy. It is clear that in order to reap the benefits of green and clean energy (mostly solar and wind), there is an urgent need to build more lines to transfer power from locations rich in these resources to load centers quite distant from them.

For this upcoming surge of new high-voltage projects and refurbishment of older lines, insulators play a critical and often grossly underestimated role in power delivery. Over many decades, the utility perspective regarding insulation technologies has changed in several ways.

INSULATOR TYPES

When the *original transmission system* was built, the porcelain insulator industry was strong in North America and utilities preferred to use domestic products. Toughened glass insulators were introduced in Europe in the 1950s and gained worldwide acceptance. In the United States, many users adopted the new technology in the 1960s and 1970s, while others were reluctant to use them because of perceived concerns with vandalism. However, the use of glass insulators in the United States continued to expand.

Polymer (also known as composite or nonceramic) insulators were introduced in the 1970s and have been widely used in North America since the 1980s. With the advent of polymers, it seemed the use of glass and porcelain suspension insulators started to decline. Polymers are particularly suited for compact line construction. Such compact lines minimized right-of-way requirements and facilitated the permitting of new transmission corridors in congested and urban areas.

With the growing number of high-voltage lines now reaching their life expectancy, many utilities are turning their attention to the fast-growing population of aging porcelain insulators. Deterioration of porcelain insulators typically stems from impurities or voids in the porcelain dielectric and expansion of the cement in the pin region, which leads to radial cracks in the shell. As internal cracks or punctures in porcelain cannot be visually detected and require tools, the labor-intensive process is expensive and requires special training of the work force.

SUPPLY CHAIN

Today, there is no domestic supplier of porcelain suspension insulators in North America. However, there are quite a few suppliers of porcelain insulators in several other countries, but most of them have limited or no experience in North America. This naturally has raised concerns among many utilities in North America about the quality and consistency of such productions.

Polymer insulators have been widely used at all voltages but largely in the 230-kV and below range. There are still unresolved issues with degradation, life expectancy and live-line working—all of which are hindering large-scale acceptance at higher voltages. The *Electric Power Research Institute (EPRI)* recently suggested that composite insulators for voltages in the range of 115 kV to 161 kV may require corona rings, which would not only increase the cost of composites but could create possible confusion as the corona rings offered vary from one manufacturer to another. With respect to toughened glass, not much has been published or discussed in the United States.

SALT RIVER PROJECT, ARIZONA

Salt River Project (SRP) serves the central and eastern parts of Arizona. Except for small pockets in the eastern parts, which are subject to contamination from the mining industry, SRP's service

territory is fairly clean and dry. Its bulk transmission and distribution networks are based largely on porcelain insulators. The utility began to use polymer insulators in the early 1980s and has successfully used them at all voltages. Polymers are favored for line post construction and account for the majority of 69-kV through 230-kV constructions in the last 30 years. The 500-kV ac Mead-Phoenix line, operational since 1990, was one of the first long transmission lines in the country to use silicone rubber composite insulators. The utility's service experience with these has been excellent.

The need for corona rings for composite insulators at 230 kV and higher voltage was recognized in the early 1980s by many users that experience fairly high wet periods in addition to contamination. This was not a concern for *SRP;* consequently, the first batch of composite insulators installed in the 1980s on several 230-kV lines had no corona rings. These insulators were inspected visually and with a corona camera about 10 years ago and most recently in 2009.

Some 230-kV lines are constructed with polymer insulators and no corona rings, and the insulators are in remarkably good condition. The relatively clean and dry environment in Arizona creates a corona-free setting most of the time, and this contributes greatly to SRP's problem-free experience with all types of insulators. In keeping with industry practice, all 230-kV suspension composite insulators subsequently installed by SRP have a corona ring at the line end, and those installed on 500-kV lines have rings at the line and tower ends.

SRP performs helicopter inspections of its transmission lines annually. Insulators with visual damage are replaced. Like many utilities, SRP trains and equips its linemen to perform line maintenance under energized (live or hot) conditions. Even though most maintenance is done with the lines de-energized, it is considered essential to preserve the ability to work on energized 500-kV lines. Future conditions may make outages unobtainable or unreasonably expensive.

Because there is no industry standard on live-line working with composite insulators and because of the difficulty in getting an outage on its 500-kV lines, which are co-owned by several utilities, SRP decided not to use polymer insulators at 500 kV. After reviewing the service experience of toughened glass insulators, SRP decided to consider them equal to porcelain in bid processes. This has resulted in the installation of toughened glass insulators on a portion of the utility's recent 500-kV line construction. The ease of detection of damaged glass bells was a factor, although not the most important one as its service experience with porcelain has been excellent.

PUBLIC SERVICE ELECTRIC & GAS, NEW JERSEY

Public Service Electric & Gas (PSE&G) has experienced problems with loss of dielectric strength and punctures on porcelain insulators from some suppliers. Lines with such insulators are being examined individually using a buzzer or electric field probe, but the results are not always reliable.

The utility has used composite insulators extensively on compact lines (line post configuration) up to 69 kV, and the experience has been good. It has experienced degradation (erosion, corona cutting) on some composite suspension insulators at 138 kV. These insulators were installed without a corona ring as is common practice. In one instance, PSE&G was fortunate to remove a composite insulator with part of the fiberglass core exposed before any mechanical failure (brittle fracture) could occur.

In the last five years, the utility has been using toughened glass insulators on new construction and as a replacement of degraded porcelain insulators on 138-kV and higher lines. Since many of these lines are shared with other utilities, PSE&G needs to have the ability to maintain them live; it calls itself a live-line utility. A major factor for using glass was the ease of spotting damaged bells. For example, the utility flies about 6 miles (10 km) per day and inspects roughly 30 towers; in contrast, a ground crew climbing and inspecting averages about three towers per day. In many cases, the entire circuit using glass insulators can be inspected in a single day with helicopters. PSE&G has estimated the maintenance of porcelain insulators can be up to 25 times more than that of glass insulators.

The utility is working to make its specifications for porcelain insulators more stringent than dictated by present ANSI standards, so that only good-quality insulators can be selected.

PACIFIC GAS AND ELECTRIC CO., CALIFORNIA

Pacific Gas and Electric Co. (PG&E) operates its extra-high-voltage lines at either 230 kV or 500 kV. The primary insulator type used is ceramic or glass. The exceptions are in vandalism-prone locations and areas with high insulator wash cycles, where composite insulators are used. Composite insulators are also used at lower voltages. However, fairly recently, corona cutting and cracks have been found on some 115-kV composite insulators installed without corona rings, which was the normal practice.

PG&E has reduced the use of composite insulators somewhat at all voltages in the last five years. In addition to aging-related issues, the utility has experienced damage by birds, specifically crows.

The utility has approved two offshore suppliers of porcelain insulators and expects several more vying for acceptance. While PG&E does not differentiate between porcelain and glass in the specification, design and installation, it is seeing an increase in the use of toughened glass insulators at all voltages in the 69-kV to 500-kV range. The utility attributes this to better education of the work force and performance characteristics associated with glass insulators.

The utility performs an aerial helicopter inspection annually, wherein insulators with visible damage are noted. A detailed ground inspection is done every five years. Climbing inspections are performed only if triggered by a specific condition.

XCEL ENERGY, MINNESOTA

Xcel Energy recently updated its standard designs by voltage. All technologies—porcelain, toughened glass and polymer—may be used for voltages below 69 kV. For 69 kV to 345 kV, polymers are used for suspension, braced and unbraced line post applications. For deadend application in this range and higher voltages, only toughened glass insulators are used. This change was driven by problems encountered with porcelain and early generation polymers.

For example, several porcelain suspension and deadend insulators on 115-kV and 345-kV lines in critical locations failed mechanically, attributable to cement growth. The age of these insulators was in excess of 20 years. As most of the porcelain insulators in the system are of this vintage or older, the utility has instituted a rigorous maintenance procedure where lines are examined regularly by fixed wing, helicopter and foot patrols. Those identified for detailed inspection are worked by linemen from buckets using the buzz technique. Needless to say, this is a very expensive undertaking and adds to the life-cycle cost of porcelain insulators.

Xcel has also experienced failures (brittle fracture) with early generation composites, primarily on 115-kV and 345-kV installations, and is concerned about longevity in 345-kV and higher applications. The utility evaluated life-cycle costs with the three insulator technologies before proceeding with revisions to its design philosophy.

HYDRO ONE, ONTARIO

Hydro One has excellent experience with all three insulator technologies for lines up to 230 kV. For higher voltages, it uses porcelain and glass, and does not use polymer insulators because issues with live-line working, bird damage, corona and aging have not been fully resolved. Porcelain and glass insulators on Hydro One's system in many places are 60 years or older for some porcelain. The porcelain insulators are tested on a regular basis for punctures and cracks attributed to cement expansion, which have caused primarily mechanical failures of several strings across the high-voltage system.

The utility has success using thermovision equipment, and punctured bells show a temperature difference of up to 10 °C (18 °F) under damp conditions. In the last two years, Hydro One has examined more than 3000 porcelain strings at 230-kV and 500-kV lines. With a five-man crew, the utility can inspect five towers per day. Indeed, this is a time- and labor-intensive, not to mention expensive, undertaking.

Owing to the ease of visually detecting damaged units on toughened glass insulator strings, Hydro

One will be using such insulators on its new construction of 230-kV and 500-kV lines.

NORTHWESTERN ENERGY, MONTANA

NorthWestern Energy has been using toughened glass insulators on its 500-kV lines since the 1980s. It has had very good experience with them and will continue this practice on its new construction of a 430-mile (692-km) 500-kV line being built for the Mountain State Transmission Intertie project. The utility performs much of its maintenance under live conditions; it calls itself a live-line-friendly utility. Since most of North Western's lines are in remote locations, routine inspections by helicopter occur four times a year on the 500-kV lines and once per year for all other lines. More detailed inspections are done on a five- to 10-year cycle. The utility has experienced problems due to vandalism in some pockets, but since the damaged glass insulators are easy to spot, it finds that glass is advantageous over other options.

NorthWestern has had good experience with porcelain at 230-kV and lower voltage lines. It inspects these insulators under de-energized conditions. Owing to the relatively dry climate in Montana, the utility has many thousands of porcelain insulators well in excess of 60 years old. Composite insulators are the preferred choice for lines of 115 kV and below. At 161 kV and 230 kV, composites are used on a limited basis for project-specific needs.

Porcelain is still the preferred choice for the bulk transmission lines. NorthWestern has experienced problems with many of the early vintage composite insulators due to corona cutting and moisture ingress. One severe example of this was a 161-kV line built in the early 1990s with composite horizontal line post insulators. The line has only been operated at 69 kV since construction, yet moisture ingress failures, believed to occur during manufacturing, have occurred on the 161-kV insulators, forcing NorthWestern to replace them recently.

OVERALL PERSPECTIVE

It seems a shift is occurring in the use of the various insulator technologies for high-voltage lines in North America. Users pointed out that, for distribution (less than 69 kV), polymers are favored, because they are lightweight, easy to handle and low cost; however, several utilities are limiting the use of polymers at higher voltages. Polymers seem to be established as the technological choice for compact line applications (line posts and braced posts). Maintenance concerns associated with the management of aging porcelain insulators and associated inspection costs are driving some utilities to question the use of porcelain insulators, while life-cycle cost considerations and ease of inspection associated with toughened glass insulators are steering other utilities toward this latter technology.

Clearly, all three insulation technologies are still very much alive, and decisions made with regard to insulation systems for the refurbishment of older lines and the upcoming surge of new high-voltage projects will depend on past experience and the expected performance and life-cycle cost criteria utilities set for the operation of their systems.

Ravi Gorur (ravi.gorur@asu.edu) is a professor in the school of electrical, computer and energy engineering at Arizona State University, Tempe. He has authored a textbook and more than 150 publications on the subject of outdoor insulators. He is the U.S. representative to CIGRÉ Study Committee DI (Materials and Emerging Technologies) and is actively involved in various IEEE working groups and task forces related to insulators. Gorur is a fellow of the IEEE.

The purpose of this article is to provide a current review of the trends in insulator technologies through interviews with several utilities, all familiar with and having experience in the three technologies. The utilities selected for soliciting input cover a wide range of geographic and climatic conditions from the U.S. West Coast to the East Coast, including one major Canadian utility. The author gratefully acknowledges input from the following:

- J. Hunt, Salt River Project
- G. Giordanella, Public Service Electric and Gas
- D.H. Shaffner, Pacific Gas and Electric
- D. Berklund, Xcel Energy
- H. Crockett, Hydro One
- T. Pankratz, North Western Energy.

4.1

TRANSMISSION LINE DESIGN CONSIDERATIONS

An overhead transmission line consists of conductors, insulators, support structures, and, in most cases, shield wires.

CONDUCTORS

Aluminum has replaced copper as the most common conductor metal for overhead transmission. Although a larger aluminum cross-sectional area is required to obtain the same loss as in a copper conductor, aluminum has a lower cost and lighter weight. Also, the supply of aluminum is abundant, whereas that of copper is limited.

One of the most common conductor types is aluminum conductor, steel-reinforced (ACSR), which consists of layers of aluminum strands surrounding a central core of steel strands (Figure 4.1). Stranded conductors are easier to manufacture, since larger conductor sizes can be obtained by simply adding successive layers of strands. Stranded conductors are also easier to handle and more flexible than solid conductors, especially in larger sizes. The use of steel strands gives ACSR conductors a high strength-to-weight ratio. For purposes of heat dissipation, overhead transmission-line conductors are bare (no insulating cover).

Other conductor types include the all-aluminum conductor (AAC), all-aluminum-alloy conductor (AAAC), aluminum conductor alloy-reinforced (ACAR), and aluminum-clad steel conductor (Alumoweld). Higher-temperature conductors capable of operation in excess of 150 °C include the aluminum conductor steel supported (ACSS), which uses fully annealed aluminum around a steel core, and the gap-type ZT-aluminum conductor (GTZACSR) which uses heat-resistant aluminum over a steel core with a small annular gap between the steel and first layer of aluminum strands. Emerging technologies use composite materials, including the aluminum conductor carbon reinforced (ACFR), whose core is a resinmatrix composite containing carbon fiber, and the aluminum conductor composite reinforced (ACCR), whose core is an aluminum-matrix containing aluminum fibers [10].

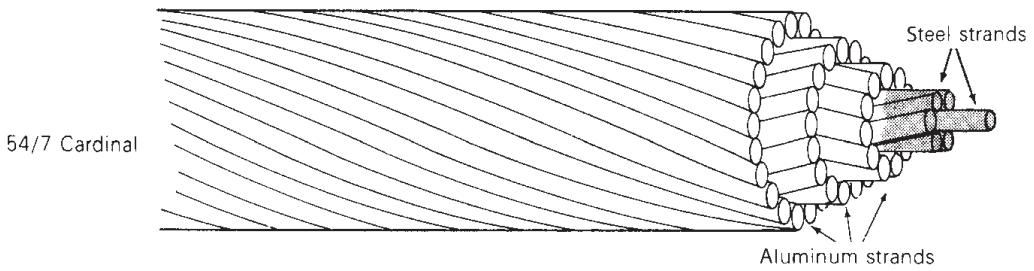

FIGURE 4.1
Typical ACSR conductor

FIGURE 4.2

A 765-kV transmission line with self-supporting lattice steel towers (Courtesy of the American Electric Power Company)

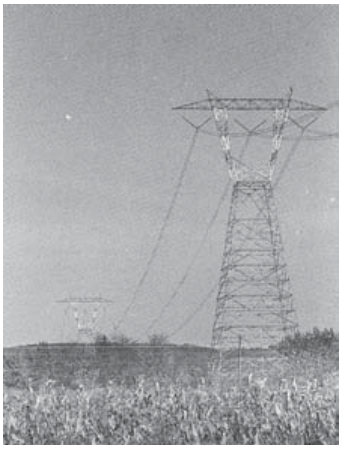

FIGURE 4.3

A 345-kV double-circuit transmission line with self-supporting lattice steel towers (Courtesy of NSTAR, formerly Boston Edison Company)

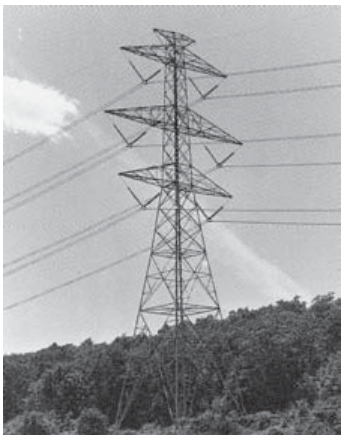

EHV lines often have more than one conductor per phase; these conductors are called a *bundle*. The 765-kV line in Figure 4.2 has four conductors per phase, and the 345-kV double-circuit line in Figure 4.3 has two conductors per phase. Bundle conductors have a lower electric field strength at the conductor surfaces, thereby controlling corona. They also have a smaller series reactance.

INSULATORS

Insulators for transmission lines above 69 kV are typically suspension-type insulators, which consist of a string of discs constructed porcelain, toughened glass, or polymer. The standard disc (Figure 4.4) has a 0.254-m (10-in.) diameter, 0.146-m ($5\frac{3}{4}$-in.) spacing between centers of adjacent discs, and a mechanical strength of 7500 kg. The 765-kV line in Figure 4.2 has two strings

FIGURE 4.4

Cut-away view of a standard porcelain insulator disc for suspension insulator strings (Courtesy of Ohio Brass)

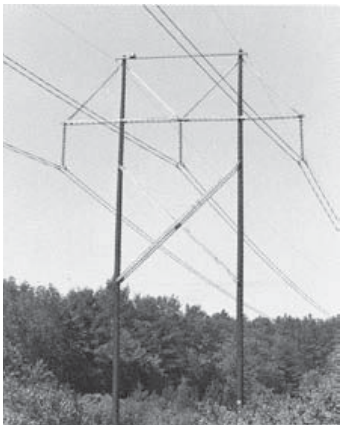

FIGURE 4.5

Wood frame structure for a 345-kV line (Courtesy of NSTAR, formerly Boston Edison Company)

per phase in a V-shaped arrangement, which helps to restrain conductor swings. The 345-kV line in Figure 4.5 has one vertical string per phase. The number of insulator discs in a string increases with line voltage (Table 4.1). Other types of discs include larger units with higher mechanical strength and fog insulators for use in contaminated areas.

SUPPORT STRUCTURES

Transmission lines employ a variety of support structures. Figure 4.2 shows a self-supporting, lattice steel tower typically used for 500- and 765-kV lines. Double-circuit 345-kV lines usually have self-supporting steel towers with the phases arranged either in a triangular configuration to reduce tower height or in a vertical configuration to reduce tower width (Figure 4.3). Wood frame configurations are commonly used for voltages of 345 kV and below (Figure 4.5).

TABLE 4.1

Typical transmission-line characteristics [1, 2] (Electric Power Research Institute (EPRI), EPRI AC Transmission Line Reference Book—200 kV and Above (Palo Alto, CA: EPRI, www.epri.com, December 2005); Westinghouse Electric Corporation, Electrical Transmission and Distribution Reference Book, 4th ed. (East Pittsburgh, PA, 1964))

Nominal Voltage	Phase Conductors				
				Minimum Clearances	
(kV)	Number of Conductors per Bundle	Aluminum Cross-Section Area per Conductor (ACSR) (kcmil)*	Bundle Spacing (cm)	Phase-to-Phase (m)	Phase-to-Ground (m)
69	1	—	—	—	—
138	1	300–700	—	4 to 5	—
230	1	400–1000	—	6 to 9	—
345	1	2000–2500	—	6 to 9	7.6 to 11
345	2	800–2200	45.7	6 to 9	7.6 to 11
500	2	2000–2500	45.7	9 to 11	9 to 14
500	3	900–1500	45.7	9 to 11	9 to 14
765	4	900–1300	45.7	13.7	12.2

*1 kcmil = 0.5 mm^2

Nominal Voltage	Suspension Insulator String		Shield Wires		
(kV)	Number of Strings per Phase	Number of Standard Insulator Discs per Suspension String	Type	Number	Diameter (cm)
69	1	4 to 6	Steel	0, 1 or 2	—
138	1	8 to 11	Steel	0, 1 or 2	—
230	1	12 to 21	Steel or ACSR	1 or 2	1.1 to 1.5
345	1	18 to 21	Alumoweld	2	0.87 to 1.5
345	1 and 2	18 to 21	Alumoweld	2	0.87 to 1.5
500	2 and 4	24 to 27	Alumoweld	2	0.98 to 1.5
500	2 and 4	24 to 27	Alumoweld	2	0.98 to 1.5
765	2 and 4	30 to 35	Alumoweld	2	0.98

SHIELD WIRES

Shield wires located above the phase conductors protect the phase conductors against lightning. They are usually high- or extra-high-strength steel, Alumoweld, or ACSR with much smaller cross section than the phase conductors. The number and location of the shield wires are selected so that almost all lightning strokes terminate on the shield wires rather than on the phase conductors. Figures 4.2, 4.3, and 4.5 have two shield wires. Shield wires are grounded to the tower. As such, when lightning strikes a shield wire, it flows harmlessly to ground, provided the tower impedance and tower footing resistance are small.

The decision to build new transmission is based on power-system planning studies to meet future system requirements of load growth and new generation. The points of interconnection of each new line to the system, as well as the power and voltage ratings of each, are selected based on these studies. Thereafter, transmission-line design is based on optimization of electrical, mechanical, environmental, and economic factors.

ELECTRICAL FACTORS

Electrical design dictates the type, size, and number of bundle conductors per phase. Phase conductors are selected to have sufficient thermal capacity to meet continuous, emergency overload, and short-circuit current ratings. For EHV lines, the number of bundle conductors per phase is selected to control the voltage gradient at conductor surfaces, thereby reducing or eliminating corona.

Electrical design also dictates the number of insulator discs, vertical or V-shaped string arrangement, phase-to-phase clearance, and phase-to-tower clearance, all selected to provide adequate line insulation. Line insulation must withstand transient overvoltages due to lightning and switching surges, even when insulators are contaminated by fog, salt, or industrial pollution. Reduced clearances due to conductor swings during winds must also be accounted for.

The number, type, and location of shield wires are selected to intercept lightning strokes that would otherwise hit the phase conductors. Also, tower footing resistance can be reduced by using driven ground rods or a buried conductor (called *counterpoise*) running parallel to the line. Line height is selected to satisfy prescribed conductor-to-ground clearances and to control ground-level electric field and its potential shock hazard.

Conductor spacings, types, and sizes also determine the series impedance and shunt admittance. Series impedance affects line-voltage drops, I^2R losses, and stability limits (Chapters 5, 13). Shunt admittance, primarily capacitive, affects line-charging currents, which inject reactive power into the power system. Shunt reactors (inductors) are often installed on lightly loaded EHV lines to absorb part of this reactive power, thereby reducing overvoltages.

MECHANICAL FACTORS

Mechanical design focuses on the strength of the conductors, insulator strings, and support structures. Conductors must be strong enough to support a specified thickness of ice and a specified wind in addition to their own weight. Suspension insulator strings must be strong enough to support the phase conductors with ice and wind loadings from tower to tower (span length). Towers that satisfy minimum strength requirements, called suspension towers, are designed to support the phase conductors and shield wires

with ice and wind loadings, and, in some cases, the unbalanced pull due to breakage of one or two conductors. Dead-end towers located every mile or so satisfy the maximum strength requirement of breakage of all conductors on one side of the tower. Angles in the line employ angle towers with intermediate strength. Conductor vibrations, which can cause conductor fatigue failure and damage to towers, are also of concern. Vibrations are controlled by adjustment of conductor tensions, use of vibration dampers, and—for bundle conductors—large bundle spacing and frequent use of bundle spacers.

ENVIRONMENTAL FACTORS

Environmental factors include land usage and visual impact. When a line route is selected, the effect on local communities and population centers, land values, access to property, wildlife, and use of public parks and facilities must all be considered. Reduction in visual impact is obtained by aesthetic tower design and by blending the line with the countryside. Also, the biological effects of prolonged exposure to electric and magnetic fields near transmission lines is of concern. Extensive research has been and continues to be done in this area.

ECONOMIC FACTORS

The optimum line design meets all the technical design criteria at lowest overall cost, which includes the total installed cost of the line as well as the cost of line losses over the operating life of the line. Many design factors affect cost. Utilities and consulting organizations use digital computer programs combined with specialized knowledge and physical experience to achieve optimum line design.

4.2

RESISTANCE

The dc resistance of a conductor at a specified temperature T is

$$R_{dc,T} = \frac{\rho_T l}{A} \quad \Omega \tag{4.2.1}$$

where ρ_T = conductor resistivity at temperature T

l = conductor length

A = conductor cross-sectional area

Two sets of units commonly used for calculating resistance, SI and English units, are summarized in Table 4.2. In this text we will use SI units throughout except where manufacturers' data is in English units. To interpret American manufacturers' data, it is useful to learn the use of English units in resistance calculations. In English units, conductor cross-sectional area is

TABLE 4.2

Comparison of SI and English units for calculating conductor resistance

Quantity	Symbol	SI Units	English Units
Resistivity	ρ	Ωm	Ω-cmil/ft
Length	ℓ	m	ft
Cross-sectional area	A	m^2	cmil
dc resistance	$R_{dc} = \frac{\rho\ell}{A}$	Ω	Ω

expressed in circular mils (cmil). One inch (2.54 cm) equals 1000 mils and 1 cmil equals $\pi/4$ sq mil. A circle with diameter D inches, or (D in.) (1000 mil/in.) = 1000 D mil = d mil, has an area

$$A = \left(\frac{\pi}{4}\ D^2\ \text{in.}^2\right)\left(1000\frac{\text{mil}}{\text{in.}}\right)^2 = \frac{\pi}{4}(1000\ D)^2 = \frac{\pi}{4}d^2 \quad \text{sq mil}$$

or

$$A = \left(\frac{\pi}{4}d^2\ \text{sq mil}\right)\left(\frac{1\ \text{cmil}}{\pi/4\ \text{sq mil}}\right) = d^2 \quad \text{cmil} \tag{4.2.2}$$

1000 cmil or 1 kcmil is equal to 0.506 mm^2, often approximated to 0.5 mm^2.

Resistivity depends on the conductor metal. Annealed copper is the international standard for measuring resistivity ρ (or conductivity σ, where $\sigma = 1/\rho$). Resistivity of conductor metals is listed in Table 4.3. As shown, hard-drawn aluminum, which has 61% of the conductivity of the international standard, has a resistivity at 20 °C of 2.83×10^{-8} Ωm.

Conductor resistance depends on the following factors:

1. Spiraling
2. Temperature
3. Frequency ("skin effect")
4. Current magnitude—magnetic conductors

These are described in the following paragraphs.

TABLE 4.3

% Conductivity, resistivity, and temperature constant of conductor metals

		$\rho_{20°C}$	T
		Resistivity at 20 °C	Temperature Constant
Material	% Conductivity	Ωm × 10^{-8}	°C
Copper:			
Annealed	100%	1.72	234.5
Hard-drawn	97.3%	1.77	241.5
Aluminum			
Hard-drawn	61%	2.83	228.1
Brass	20–27%	6.4–8.4	480
Iron	17.2%	10	180
Silver	108%	1.59	243
Sodium	40%	4.3	207
Steel	2–14%	12–88	180–980

For stranded conductors, alternate layers of strands are spiraled in opposite directions to hold the strands together. Spiraling makes the strands 1 or 2% longer than the actual conductor length. As a result, the dc resistance of a stranded conductor is 1 or 2% larger than that calculated from (4.2.1) for a specified conductor length.

Resistivity of conductor metals varies linearly over normal operating temperatures according to

$$\rho_{T2} = \rho_{T1}\left(\frac{T_2 + T}{T_1 + T}\right) \tag{4.2.3}$$

where ρ_{T2} and ρ_{T1} are resistivities at temperatures T_2 and T_1 °C, respectively. T is a temperature constant that depends on the conductor material, and is listed in Table 4.3.

The ac resistance or *effective* resistance of a conductor is

$$R_{ac} = \frac{P_{loss}}{|I|^2} \quad \Omega \tag{4.2.4}$$

where P_{loss} is the conductor real power loss in watts and I is the rms conductor current. For dc, the current distribution is uniform throughout the conductor cross section, and (4.2.1) is valid. However, for ac, the current distribution is nonuniform. As frequency increases, the current in a solid cylindrical conductor tends to crowd toward the conductor surface, with smaller current density at the conductor center. This phenomenon is called *skin effect*. A conductor with a large radius can even have an oscillatory current density versus the radial distance from the conductor center.

With increasing frequency, conductor loss increases, which, from (4.2.4), causes the ac resistance to increase. At power frequencies (60 Hz), the ac resistance is at most a few percent higher than the dc resistance. Conductor manufacturers normally provide dc, 50-Hz, and 60-Hz conductor resistance based on test data (see Appendix Tables A.3 and A.4).

For magnetic conductors, such as steel conductors used for shield wires, resistance depends on current magnitude. The internal flux linkages, and therefore the iron or magnetic losses, depend on the current magnitude. For ACSR conductors, the steel core has a relatively high resistivity compared to the aluminum strands, and therefore the effect of current magnitude on ACSR conductor resistance is small. Tables on magnetic conductors list resistance at two current levels (see Table A.4).

EXAMPLE 4.1 Stranded conductor: dc and ac resistance

Table A.3 lists a 4/0 copper conductor with 12 strands. Strand diameter is 0.3373 cm (0.1328 in.). For this conductor:

a. Verify the total copper cross-sectional area of 107.2 mm^2 (211,600 cmil in the table).

b. Verify the dc resistance at 50 °C of 0.1876 Ω/km or 0.302 Ω/mi. Assume a 2% increase in resistance due to spiraling.

c. From Table A.3, determine the percent increase in resistance at 60 Hz versus dc.

SOLUTION

a. The strand diameter is $d = (0.3373 \text{ cm})\ (10 \text{ mm/cm}) = 3.373$ mm, and, from (4.2.2), the strand area is

$$A = \frac{12\pi d^2}{4} = 3\pi(3.373)^2 = 107.2 \quad \text{mm}^2$$

which agrees with the value given in Table A.3.

b. Using (4.2.3) and hard-drawn copper data from Table 4.3,

$$\rho_{50\,^\circ\text{C}} = 1.77 \times 10^{-8}\left(\frac{50 + 241.5}{20 + 241.5}\right) = 1.973 \times 10^{-8} \quad \Omega\text{-m}$$

From (4.2.1), the dc resistance at 50 °C for a conductor length of 1 km is

$$R_{\text{dc, }50\,^\circ\text{C}} = \frac{(1.973 \times 10^{-8})(10^3 \times 1.02)}{107.2 \times 10^{-6}} = 0.1877 \quad \Omega/\text{km}$$

which agrees with the value listed in Table A.3.

c. From Table A.3,

$$\frac{R_{60\text{ Hz, }50\,^\circ\text{C}}}{R_{\text{dc, }50\,^\circ\text{C}}} = \frac{0.1883}{0.1877} = 1.003 \qquad \frac{R_{60\text{ Hz, }25\,^\circ\text{C}}}{R_{\text{dc, }25\,^\circ\text{C}}} = \frac{0.1727}{0.1715} = 1.007$$

Thus, the 60-Hz resistance of this conductor is about 0.3–0.7% higher than the dc resistance. The variation of these two ratios is due to the fact that resistance in Table A.3 is given to only three significant figures. ■

4.3

CONDUCTANCE

Conductance accounts for real power loss between conductors or between conductors and ground. For overhead lines, this power loss is due to leakage currents at insulators and to corona. Insulator leakage current depends on the amount of dirt, salt, and other contaminants that have accumulated on insulators, as well as on meteorological factors, particularly the presence of moisture. Corona occurs when a high value of electric field strength at a conductor surface causes the air to become electrically ionized and to conduct. The real power loss due to corona, called *corona loss*, depends on meteorological conditions, particularly rain, and on conductor surface irregularities. Losses due to insulator leakage and corona are usually small compared to conductor I^2R loss. Conductance is usually neglected in power system studies because it is a very small component of the shunt admittance.

4.4

INDUCTANCE: SOLID CYLINDRICAL CONDUCTOR

The inductance of a magnetic circuit that has a constant permeability μ can be obtained by determining the following:

1. Magnetic field intensity H, from Ampere's law
2. Magnetic flux density B ($B = \mu H$)
3. Flux linkages λ
4. Inductance from flux linkages per ampere ($\mathrm{L} = \lambda/I$)

As a step toward computing the inductances of more general conductors and conductor configurations, we first compute the internal, external, and total inductance of a solid cylindrical conductor. We also compute the flux linking one conductor in an array of current-carrying conductors.

Figure 4.6 shows a 1-meter section of a solid cylindrical conductor with radius r, carrying current I. For simplicity, assume that the conductor (1) is sufficiently long that end effects are neglected, (2) is nonmagnetic ($\mu = \mu_0 = 4\pi \times 10^{-7}$ H/m), and (3) has a uniform current density (skin effect is neglected). From (3.1.1), Ampere's law states that

$$\oint H_{\tan}\, dl = I_{\text{enclosed}} \tag{4.4.1}$$

To determine the magnetic field inside the conductor, select the dashed circle of radius $x < r$ shown in Figure 4.6 as the closed contour for Ampere's law. Due to symmetry, H_x is constant along the contour. Also, there is no radial component of H_x, so H_x is tangent to the contour. That is, the conductor has a concentric magnetic field. From (4.4.1), the integral of H_x around the selected contour is

$$H_x(2\pi x) = I_x \qquad \text{for } x < r \tag{4.4.2}$$

FIGURE 4.6

Internal magnetic field of a solid cylindrical conductor

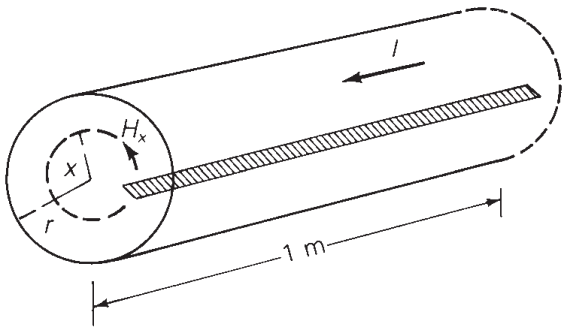

where I_x is the portion of the total current enclosed by the contour. Solving (4.4.2)

$$H_x = \frac{I_x}{2\pi x} \quad \text{A/m} \tag{4.4.3}$$

Now assume a uniform current distribution within the conductor, that is

$$I_x = \left(\frac{x}{r}\right)^2 I \qquad \text{for } x < r \tag{4.4.4}$$

Using (4.4.4) in (4.4.3)

$$H_x = \frac{xI}{2\pi r^2} \quad \text{A/m} \tag{4.4.5}$$

For a nonmagnetic conductor, the magnetic flux density B_x is

$$B_x = \mu_0 H_x = \frac{\mu_0 xI}{2\pi r^2} \quad \text{Wb/m}^2 \tag{4.4.6}$$

The differential flux $d\Phi$ per-unit length of conductor in the cross-hatched rectangle of width dx shown in Figure 4.6 is

$$d\Phi = B_x\, dx \quad \text{Wb/m} \tag{4.4.7}$$

Computation of the differential flux linkage $d\lambda$ in the rectangle is tricky since only the fraction $(x/r)^2$ of the total current I is linked by the flux. That is,

$$d\lambda = \left(\frac{x}{r}\right)^2 d\Phi = \frac{\mu_0 I}{2\pi r^4} x^3\, dx \quad \text{Wb-t/m} \tag{4.4.8}$$

Integrating (4.4.8) from $x = 0$ to $x = r$ determines the total flux linkages λ_{int} inside the conductor

$$\lambda_{\text{int}} = \int_0^r d\lambda = \frac{\mu_0 I}{2\pi r^4} \int_0^r x^3\, dx = \frac{\mu_0 I}{8\pi} = \frac{1}{2} \times 10^{-7} I \quad \text{Wb-t/m} \tag{4.4.9}$$

The internal inductance L_{int} per-unit length of conductor due to this flux linkage is then

$$\mathrm{L}_{\text{int}} = \frac{\lambda_{\text{int}}}{I} = \frac{\mu_0}{8\pi} = \frac{1}{2} \times 10^{-7} \quad \text{H/m} \tag{4.4.10}$$

Next, in order to determine the magnetic field outside the conductor, select the dashed circle of radius $x > r$ shown in Figure 4.7 as the closed contour for Ampere's law. Noting that this contour encloses the entire current I, integration of (4.4.1) yields

$$H_x(2\pi x) = I \tag{4.4.11}$$

which gives

$$H_x = \frac{I}{2\pi x} \quad \text{A/m} \qquad x > r \tag{4.4.12}$$

FIGURE 4.7

External magnetic field of a solid cylindrical conductor

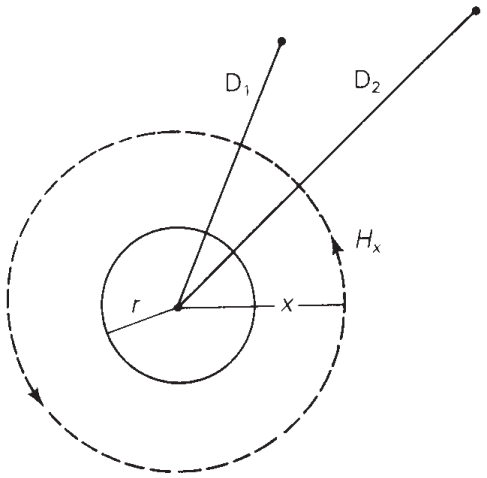

Outside the conductor, $\mu = \mu_0$ and

$$B_x = \mu_0 H_x = (4\pi \times 10^{-7}) \frac{I}{2\pi x} = 2 \times 10^{-7} \frac{I}{x} \quad \text{Wb/m}^2 \tag{4.4.13}$$

$$d\Phi = B_x \, dx = 2 \times 10^{-7} \frac{I}{x} \, dx \quad \text{Wb/m} \tag{4.4.14}$$

Since the entire current I is linked by the flux outside the conductor,

$$d\lambda = d\Phi = 2 \times 10^{-7} \frac{I}{x} \, dx \quad \text{Wb-t/m} \tag{4.4.15}$$

Integrating (4.4.15) between two external points at distances D_1 and D_2 from the conductor center gives the external flux linkage λ_{12} between D_1 and D_2:

$$\begin{aligned} \lambda_{12} &= \int_{D_1}^{D_2} d\lambda = 2 \times 10^{-7} I \int_{D_1}^{D_2} \frac{dx}{x} \\ &= 2 \times 10^{-7} I \ln\left(\frac{D_2}{D_1}\right) \quad \text{Wb-t/m} \end{aligned} \tag{4.4.16}$$

The external inductance L_{12} per-unit length due to the flux linkages between D_1 and D_2 is then

$$L_{12} = \frac{\lambda_{12}}{I} = 2 \times 10^{-7} \ln\left(\frac{D_2}{D_1}\right) \quad \text{H/m} \tag{4.4.17}$$

The total flux λ_P linking the conductor out to external point P at distance D is the sum of the internal flux linkage, (4.4.9), and the external flux linkage, (4.4.16) from $D_1 = r$ to $D_2 = D$. That is

$$\lambda_P = \frac{1}{2} \times 10^{-7} I + 2 \times 10^{-7} I \ln \frac{D}{r} \tag{4.4.18}$$

Using the identity $\frac{1}{2} = 2 \ln e^{1/4}$ in (4.4.18), a more convenient expression for λ_P is obtained:

$$\begin{aligned}\lambda_P &= 2 \times 10^{-7} I \left(\ln e^{1/4} + \ln \frac{D}{r} \right) \\ &= 2 \times 10^{-7} I \ln \frac{D}{e^{-1/4} r} \\ &= 2 \times 10^{-7} I \ln \frac{D}{r'} \quad \text{Wb-t/m}\end{aligned} \tag{4.4.19}$$

where

$$r' = e^{-1/4} r = 0.7788 r \tag{4.4.20}$$

Also, the total inductance L_P due to both internal and external flux linkages out to distance D is

$$L_P = \frac{\lambda_P}{I} = 2 \times 10^{-7} \ln \left(\frac{D}{r'} \right) \quad \text{H/m} \tag{4.4.21}$$

Finally, consider the array of M solid cylindrical conductors shown in Figure 4.8. Assume that each conductor m carries current I_m referenced out of the page. Also assume that the sum of the conductor currents is zero—that is,

$$I_1 + I_2 + \cdots + I_M = \sum_{m=1}^{M} I_m = 0 \tag{4.4.22}$$

The flux linkage λ_{kPk}, which links conductor k out to point P due to current I_k, is, from (4.4.19),

$$\lambda_{kPk} = 2 \times 10^{-7} I_k \ln \frac{D_{Pk}}{r'_k} \tag{4.4.23}$$

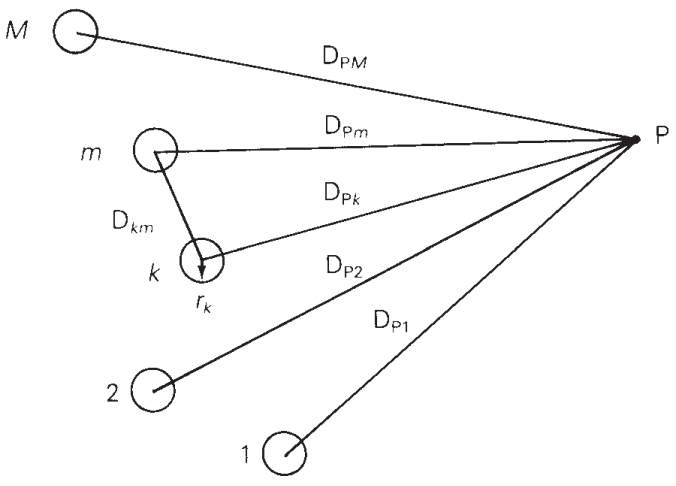

FIGURE 4.8
Array of M solid cylindrical conductors

Note that $\lambda_{k\mathrm{P}k}$ includes both internal and external flux linkages due to I_k. The flux linkage $\lambda_{k\mathrm{P}m}$, which links conductor k out to P due to I_m, is, from (4.4.16),

$$\lambda_{k\mathrm{P}m} = 2 \times 10^{-7} I_m \ln \frac{\mathrm{D}_{\mathrm{P}m}}{\mathrm{D}_{km}} \tag{4.4.24}$$

In (4.4.24) we use D_{km} instead of $(\mathrm{D}_{km} - r_k)$ or $(\mathrm{D}_{km} + r_k)$, which is a valid approximation when D_{km} is much greater than r_k. It can also be shown that this is a good approximation even when D_{km} is small. Using superposition, the total flux linkage $\lambda_{k\mathrm{P}}$, which links conductor k out to P due to all the currents, is

$$\begin{aligned}\lambda_{k\mathrm{P}} &= \lambda_{k\mathrm{P}1} + \lambda_{k\mathrm{P}2} + \cdots + \lambda_{k\mathrm{P}M} \\ &= 2 \times 10^{-7} \sum_{m=1}^{M} I_m \ln \frac{\mathrm{D}_{\mathrm{P}m}}{\mathrm{D}_{km}}\end{aligned} \tag{4.4.25}$$

where we define $\mathrm{D}_{kk} = r_k' = e^{-1/4} r_k$ when $m = k$ in the above summation. Equation (4.4.25) is separated into two summations:

$$\lambda_{k\mathrm{P}} = 2 \times 10^{-7} \sum_{m=1}^{M} I_m \ln \frac{1}{\mathrm{D}_{km}} + 2 \times 10^{-7} \sum_{m=1}^{M} I_m \ln \mathrm{D}_{\mathrm{P}m} \tag{4.4.26}$$

Removing the last term from the second summation we get:

$$\lambda_{k\mathrm{P}} = 2 \times 10^{-7} \left[\sum_{m=1}^{M} I_m \ln \frac{1}{\mathrm{D}_{km}} + \sum_{m=1}^{M-1} I_m \ln \mathrm{D}_{\mathrm{P}m} + I_M \ln \mathrm{D}_{\mathrm{P}M} \right] \tag{4.4.27}$$

From (4.4.22),

$$I_M = -(I_1 + I_2 + \cdots + I_{M-1}) = -\sum_{m=1}^{M-1} I_m \tag{4.4.28}$$

Using (4.4.28) in (4.4.27)

$$\begin{aligned}\lambda_{k\mathrm{P}} &= 2 \times 10^{-7} \left[\sum_{m=1}^{M} I_m \ln \frac{1}{\mathrm{D}_{km}} + \sum_{m=1}^{M-1} I_m \ln \mathrm{D}_{\mathrm{P}m} - \sum_{m=1}^{M-1} I_m \ln \mathrm{D}_{\mathrm{P}M} \right] \\ &= 2 \times 10^{-7} \left[\sum_{m=1}^{M} I_m \ln \frac{1}{\mathrm{D}_{km}} + \sum_{m=1}^{M-1} I_m \ln \frac{\mathrm{D}_{\mathrm{P}m}}{\mathrm{D}_{\mathrm{P}M}} \right]\end{aligned} \tag{4.4.29}$$

Now, let λ_k equal the total flux linking conductor k out to infinity. That is, $\lambda_k = \lim_{\mathrm{P} \to \infty} \lambda_{k\mathrm{P}}$. As $\mathrm{P} \to \infty$, all the distances $\mathrm{D}_{\mathrm{P}m}$ become equal, the ratios $\mathrm{D}_{\mathrm{P}m}/\mathrm{D}_{\mathrm{P}M}$ become unity, and $\ln(\mathrm{D}_{\mathrm{P}m}/\mathrm{D}_{\mathrm{P}M}) \to 0$. Therefore, the second summation in (4.4.29) becomes zero as $\mathrm{P} \to \infty$, and

$$\lambda_k = 2 \times 10^{-7} \sum_{m=1}^{M} I_m \ln \frac{1}{\mathrm{D}_{km}} \quad \text{Wb-t/m} \tag{4.4.30}$$

Equation (4.4.30) gives the total flux linking conductor k in an array of M conductors carrying currents $I_1, I_2, \ldots, I_M$, whose sum is zero. This equation is valid for either dc or ac currents. λ_k is a dc flux linkage when the currents are dc, and λ_k is a phasor flux linkage when the currents are phasor representations of sinusoids.

4.5

INDUCTANCE: SINGLE-PHASE TWO-WIRE LINE AND THREE-PHASE THREE-WIRE LINE WITH EQUAL PHASE SPACING

The results of the previous section are used here to determine the inductances of two relatively simple transmission lines: a single-phase two-wire line and a three-phase three-wire line with equal phase spacing.

Figure 4.9(a) shows a single-phase two-wire line consisting of two solid cylindrical conductors x and y. Conductor x with radius r_x carries phasor current $I_x = I$ referenced out of the page. Conductor y with radius r_y carries return current $I_y = -I$. Since the sum of the two currents is zero, (4.4.30) is valid, from which the total flux linking conductor x is

$$\begin{aligned}\lambda_x &= 2 \times 10^{-7}\left(I_x \ln \frac{1}{\mathrm{D}_{xx}} + I_y \ln \frac{1}{\mathrm{D}_{xy}}\right) \\ &= 2 \times 10^{-7}\left(I \ln \frac{1}{r'_x} - I \ln \frac{1}{\mathrm{D}}\right) \\ &= 2 \times 10^{-7} I \ln \frac{\mathrm{D}}{r'_x} \quad \text{Wb-t/m}\end{aligned} \tag{4.5.1}$$

where $r'_x = e^{-1/4} r_x = 0.7788 r_x$.

The inductance of conductor x is then

$$\mathrm{L}_x = \frac{\lambda_x}{I_x} = \frac{\lambda_x}{I} = 2 \times 10^{-7} \ln \frac{\mathrm{D}}{r'_x} \quad \text{H/m per conductor} \tag{4.5.2}$$

FIGURE 4.9
Single-phase two-wire line

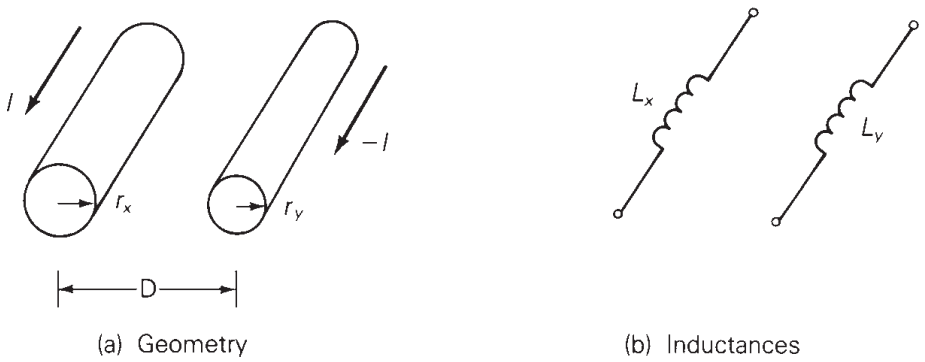

(a) Geometry (b) Inductances

Similarly, the total flux linking conductor y is

$$\begin{aligned}\lambda_y &= 2\times 10^{-7}\left(I_x \ln\frac{1}{\mathrm{D}_{yx}} + I_y \ln\frac{1}{\mathrm{D}_{yy}}\right)\\ &= 2\times 10^{-7}\left(I \ln\frac{1}{\mathrm{D}} - I \ln\frac{1}{r'_y}\right)\\ &= -2\times 10^{-7} I \ln\frac{\mathrm{D}}{r'_y}\end{aligned} \tag{4.5.3}$$

and

$$\mathrm{L}_y = \frac{\lambda_y}{I_y} = \frac{\lambda_y}{-I} = 2\times 10^{-7}\ln\frac{\mathrm{D}}{r'_y} \quad \mathrm{H/m\ per\ conductor} \tag{4.5.4}$$

The total inductance of the single-phase circuit, also called *loop inductance*, is

$$\begin{aligned}\mathrm{L} = \mathrm{L}_x + \mathrm{L}_y &= 2\times 10^{-7}\left(\ln\frac{\mathrm{D}}{r'_x} + \ln\frac{\mathrm{D}}{r'_y}\right)\\ &= 2\times 10^{-7}\ln\frac{\mathrm{D}^2}{r'_x r'_y}\\ &= 4\times 10^{-7}\ln\frac{\mathrm{D}}{\sqrt{r'_x r'_y}} \quad \mathrm{H/m\ per\ circuit}\end{aligned} \tag{4.5.5}$$

Also, if $r'_x = r'_y = r'$, the total circuit inductance is

$$\mathrm{L} = 4\times 10^{-7}\ln\frac{\mathrm{D}}{r'} \quad \mathrm{H/m\ per\ circuit} \tag{4.5.6}$$

The inductances of the single-phase two-wire line are shown in Figure 4.9(b).

Figure 4.10(a) shows a three-phase three-wire line consisting of three solid cylindrical conductors a, b, c, each with radius r, and with equal phase spacing D between any two conductors. To determine inductance, assume balanced positive-sequence currents I_a, I_b, I_c that satisfy $I_a + I_b + I_c = 0$. Then (4.4.30) is valid and the total flux linking the phase a conductor is

FIGURE 4.10

Three-phase three-wire line with equal phase spacing

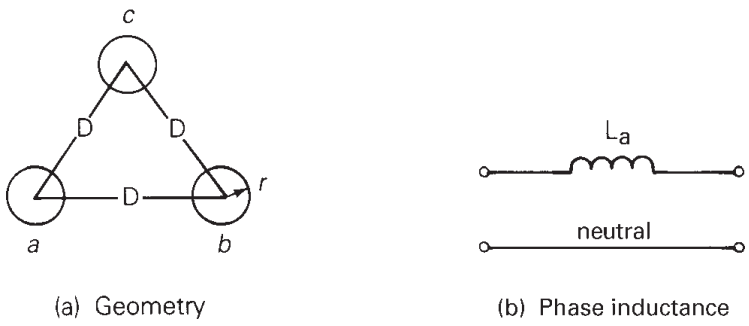

(a) Geometry (b) Phase inductance

$$\lambda_a = 2 \times 10^{-7}\left(I_a \ln\frac{1}{r'} + I_b \ln\frac{1}{\mathrm{D}} + I_c \ln\frac{1}{\mathrm{D}}\right)$$

$$= 2 \times 10^{-7}\left[I_a \ln\frac{1}{r'} + (I_b + I_c)\ln\frac{1}{\mathrm{D}}\right] \tag{4.5.7}$$

Using $(I_b + I_c) = -I_a$,

$$\lambda_a = 2 \times 10^{-7}\left(I_a \ln\frac{1}{r'} - I_a \ln\frac{1}{\mathrm{D}}\right)$$

$$= 2 \times 10^{-7} I_a \ln\frac{\mathrm{D}}{r'} \quad \text{Wb-t/m} \tag{4.5.8}$$

The inductance of phase a is then

$$\mathrm{L}_a = \frac{\lambda_a}{I_a} = 2 \times 10^{-7} \ln\frac{\mathrm{D}}{r'} \quad \text{H/m per phase} \tag{4.5.9}$$

Due to symmetry, the same result is obtained for $L_b = \lambda_b/I_b$ and for $\mathrm{L}_c = \lambda_c/I_c$. However, only one phase need be considered for balanced three-phase operation of this line, since the flux linkages of each phase have equal magnitudes and 120° displacement. The phase inductance is shown in Figure 4.10(b).

4.6

INDUCTANCE: COMPOSITE CONDUCTORS, UNEQUAL PHASE SPACING, BUNDLED CONDUCTORS

The results of Section 4.5 are extended here to include composite conductors, which consist of two or more solid cylindrical subconductors in parallel. A stranded conductor is one example of a composite conductor. For simplicity we assume that for each conductor, the subconductors are identical and share the conductor current equally.

Figure 4.11 shows a single-phase two-conductor line consisting of two composite conductors x and y. Conductor x has N identical subconductors, each with radius r_x and with current (I/N) referenced out of the page. Similarly, conductor y consists of M identical subconductors, each with radius r_y and with return current $(-I/M)$. Since the sum of all the currents is zero, (4.4.30) is valid and the total flux Φ_k linking subconductor k of conductor x is

$$\Phi_k = 2 \times 10^{-7}\left[\frac{I}{N}\sum_{m=1}^{N} \ln\frac{1}{\mathrm{D}_{km}} - \frac{I}{M}\sum_{m=1'}^{M} \ln\frac{1}{\mathrm{D}_{km}}\right] \tag{4.6.1}$$

Since only the fraction $(1/N)$ of the total conductor current I is linked by this flux, the flux linkage λ_k of (the current in) subconductor k is

FIGURE 4.11

Single-phase two-conductor line with composite conductors

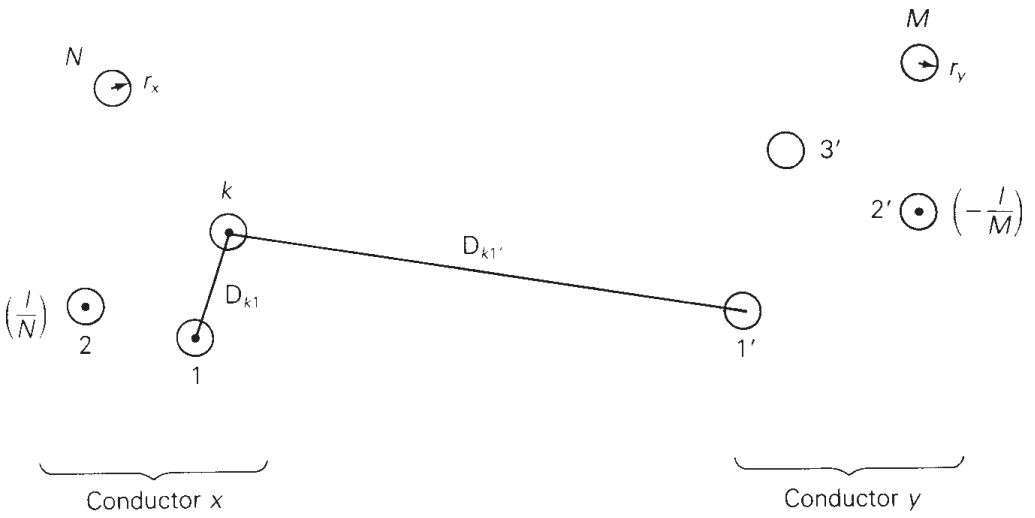

$$\lambda_k = \frac{\Phi_k}{N} = 2 \times 10^{-7} I \left[\frac{1}{N^2} \sum_{m=1}^{N} \ln \frac{1}{\mathrm{D}_{km}} - \frac{1}{NM} \sum_{m=1'}^{M} \ln \frac{1}{\mathrm{D}_{km}} \right] \tag{4.6.2}$$

The total flux linkage of conductor x is

$$\lambda_x = \sum_{k=1}^{N} \lambda_k = 2 \times 10^{-7} I \sum_{k=1}^{N} \left[\frac{1}{N^2} \sum_{m=1}^{N} \ln \frac{1}{\mathrm{D}_{km}} - \frac{1}{NM} \sum_{m=1'}^{M} \ln \frac{1}{\mathrm{D}_{km}} \right] \tag{4.6.3}$$

Using $\ln \mathrm{A}^{\alpha} = \alpha \ln \mathrm{A}$ and $\sum \ln \mathrm{A}_k = \ln \prod \mathrm{A}_k$ (sum of ln s = ln of products), (4.6.3) can be rewritten in the following form:

$$\lambda_x = 2 \times 10^{-7} I \ln \prod_{k=1}^{N} \frac{\left(\prod_{m=1'}^{M} \mathrm{D}_{km} \right)^{1/NM}}{\left(\prod_{m=1}^{N} \mathrm{D}_{km} \right)^{1/N^2}} \tag{4.6.4}$$

and the inductance of conductor x, $\mathrm{L}_x = \dfrac{\lambda_x}{I}$, can be written as

$$\mathrm{L}_x = 2 \times 10^{-7} \ln \frac{\mathrm{D}_{xy}}{\mathrm{D}_{xx}} \quad \mathrm{H/m \text{ per conductor}} \tag{4.6.5}$$

where

$$\mathrm{D}_{xy} = \sqrt[MN]{\prod_{k=1}^{N} \prod_{m=1'}^{M} \mathrm{D}_{km}} \tag{4.6.6}$$

$$\mathrm{D}_{xx} = \sqrt[N^2]{\prod_{k=1}^{N} \prod_{m=1}^{N} \mathrm{D}_{km}} \tag{4.6.7}$$

D_{xy}, given by (4.6.6), is the MNth root of the product of the MN distances from the subconductors of conductor x to the subconductors of conductor y. Associated with each subconductor k of conductor x are the M distances $D_{k1}', D_{k2}', \ldots, D_{kM}$ to the subconductors of conductor y. For N subconductors in conductor x, there are therefore MN of these distances. D_{xy} is called the *geometric mean distance* or GMD between conductors x and y.

Also, D_{xx}, given by (4.6.7), is the N^2 root of the product of the N^2 distances between the subconductors of conductor x. Associated with each subconductor k are the N distances $D_{k1}, D_{k2}, \ldots, D_{kk} = r', \ldots, D_{kN}$. For N subconductors in conductor x, there are therefore N^2 of these distances. D_{xx} is called the *geometric mean radius* or GMR of conductor x.

Similarly, for conductor y,

$$L_y = 2 \times 10^{-7} \ln \frac{D_{xy}}{D_{yy}} \quad \text{H/m per conductor} \tag{4.6.8}$$

where

$$D_{yy} = \sqrt[M^2]{\prod_{k=1'}^{M} \prod_{m=1'}^{M} D_{km}} \tag{4.6.9}$$

D_{yy}, the GMR of conductor y, is the M^2 root of the product of the M^2 distances between the subconductors of conductor y. The total inductance L of the single-phase circuit is

$$L = L_x + L_y \quad \text{H/m per circuit} \tag{4.6.10}$$

EXAMPLE 4.2 GMR, GMD, and inductance: single-phase two-conductor line

Expand (4.6.6), (4.6.7), and (4.6.9) for $N = 3$ and $M = 2'$. Then evaluate L_x, L_y, and L in H/m for the single-phase two-conductor line shown in Figure 4.12.

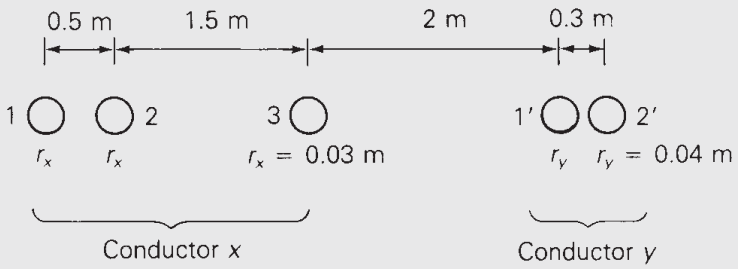

FIGURE 4.12 Single-phase two-conductor line for Example 4.2

SOLUTION For $N = 3$ and $M = 2'$, (4.6.6) becomes

$$\begin{aligned} \mathrm{D}_{xy} &= \sqrt[6]{\prod_{k=1}^{3}\prod_{m=1'}^{2'} \mathrm{D}_{km}} \\ &= \sqrt[6]{\prod_{k=1}^{3} \mathrm{D}_{k1'}\mathrm{D}_{k2'}} \\ &= \sqrt[6]{(\mathrm{D}_{11'}\mathrm{D}_{12'})(\mathrm{D}_{21'}\mathrm{D}_{22'})(\mathrm{D}_{31'}\mathrm{D}_{32'})} \end{aligned}$$

Similarly, (4.6.7) becomes

$$\begin{aligned} \mathrm{D}_{xx} &= \sqrt[9]{\prod_{k=1}^{3}\prod_{m=1}^{3} \mathrm{D}_{km}} \\ &= \sqrt[9]{\prod_{k=1}^{3} \mathrm{D}_{k1}\mathrm{D}_{k2}\mathrm{D}_{k3}} \\ &= \sqrt[9]{(\mathrm{D}_{11}\mathrm{D}_{12}\mathrm{D}_{13})(\mathrm{D}_{21}\mathrm{D}_{22}\mathrm{D}_{23})(\mathrm{D}_{31}\mathrm{D}_{32}\mathrm{D}_{33})} \end{aligned}$$

and (4.6.9) becomes

$$\begin{aligned} \mathrm{D}_{yy} &= \sqrt[4]{\prod_{k=1'}^{2'}\prod_{m=1'}^{2'} \mathrm{D}_{km}} \\ &= \sqrt[4]{\prod_{k=1'}^{2'} \mathrm{D}_{k1'}\mathrm{D}_{k2'}} \\ &= \sqrt[4]{(\mathrm{D}_{1'1'}\mathrm{D}_{1'2'})(\mathrm{D}_{2'1'}\mathrm{D}_{2'2'})} \end{aligned}$$

Evaluating D_{xy}, D_{xx}, and D_{yy} for the single-phase two-conductor line shown in Figure 4.12,

$$\mathrm{D}_{11'} = 4 \text{ m} \qquad \mathrm{D}_{12'} = 4.3 \text{ m} \qquad \mathrm{D}_{21'} = 3.5 \text{ m}$$

$$\mathrm{D}_{22'} = 3.8 \text{ m} \qquad \mathrm{D}_{31'} = 2 \text{ m} \qquad \mathrm{D}_{32'} = 2.3 \text{ m}$$

$$\mathrm{D}_{xy} = \sqrt[6]{(4)(4.3)(3.5)(3.8)(2)(2.3)} = 3.189 \text{ m}$$

$$\mathrm{D}_{11} = \mathrm{D}_{22} = \mathrm{D}_{33} = r_x' = e^{-1/4} r_x = (0.7788)(0.03) = 0.02336 \text{ m}$$

$$\mathrm{D}_{21} = \mathrm{D}_{12} = 0.5 \text{ m}$$

$$\mathrm{D}_{23} = \mathrm{D}_{32} = 1.5 \text{ m}$$

$$\mathrm{D}_{31} = \mathrm{D}_{13} = 2.0 \text{ m}$$

$$D_{xx} = \sqrt[9]{(0.02336)^3(0.5)^2(1.5)^2(2.0)^2} = 0.3128 \text{ m}$$

$$D_{1'1'} = D_{2'2'} = r'_y = e^{-1/4}r_y = (0.7788)(0.04) = 0.03115 \text{ m}$$

$$D_{1'2'} = D_{2'1'} = 0.3 \text{ m}$$

$$D_{yy} = \sqrt[4]{(0.03115)^2(0.3)^2} = 0.09667 \text{ m}$$

Then, from (4.6.5), (4.6.8), and (4.6.10):

$$L_x = 2 \times 10^{-7} \ln\left(\frac{3.189}{0.3128}\right) = 4.644 \times 10^{-7} \quad \text{H/m per conductor}$$

$$L_y = 2 \times 10^{-7} \ln\left(\frac{3.189}{0.09667}\right) = 6.992 \times 10^{-7} \quad \text{H/m per conductor}$$

$$L = L_x + L_y = 1.164 \times 10^{-6} \quad \text{H/m per circuit}$$ ■

It is seldom necessary to calculate GMR or GMD for standard lines. The GMR of standard conductors is provided by conductor manufacturers and can be found in various handbooks (see Appendix Tables A.3 and A.4). Also, if the distances between conductors are large compared to the distances between subconductors of each conductor, then the GMD between conductors is approximately equal to the distance between conductor centers.

EXAMPLE 4.3 Inductance and inductive reactance: single-phase line

A single-phase line operating at 60 Hz consists of two 4/0 12-strand copper conductors with 1.5 m spacing between conductor centers. The line length is 32 km. Determine the total inductance in H and the total inductive reactance in Ω.

SOLUTION The GMD between conductor centers is $D_{xy} = 1.5$ m. Also, from Table A.3, the GMR of a 4/0 12-strand copper conductor is $D_{xx} = D_{yy} = 0.01750$ ft or 0.5334 cm. From (4.6.5) and (4.6.8),

$$L_x = L_y = 2 \times 10^{-7} \ln\left(\frac{150}{0.5334}\right)\frac{\text{H}}{\text{m}} \times 32 \times 10^3$$

$$= 0.03609 \quad \text{H per conductor}$$

The total inductance is

$$L = L_x + L_y = 2 \times 0.03609 = 0.07218 \quad \text{H per circuit}$$

and the total inductive reactance is

$$X_L = 2\pi f L = (2\pi)(60)(0.07218) = 27.21 \quad \Omega \text{ per circuit}$$ ■

FIGURE 4.13

Completely transposed three-phase line

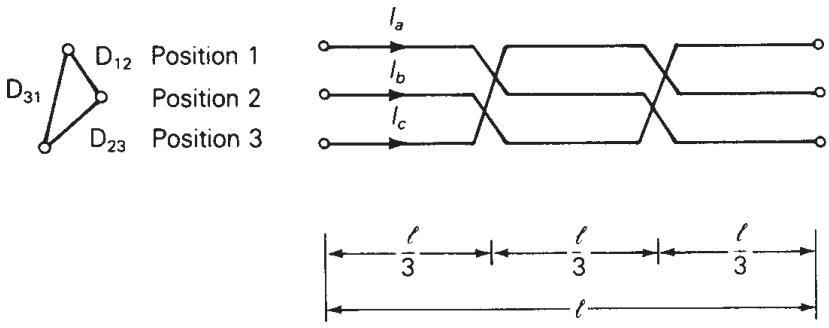

To calculate inductance for three-phase lines with stranded conductors and equal phase spacing, r' is replaced by the conductor GMR in (4.5.9). If the spacings between phases are unequal, then balanced positive-sequence flux linkages are not obtained from balanced positive-sequence currents. Instead, unbalanced flux linkages occur, and the phase inductances are unequal. However, balance can be restored by exchanging the conductor positions along the line, a technique called *transposition*.

Figure 4.13 shows a completely transposed three-phase line. The line is transposed at two locations such that each phase occupies each position for one-third of the line length. Conductor positions are denoted 1, 2, 3 with distances D_{12}, D_{23}, D_{31} between positions. The conductors are identical, each with GMR denoted D_S. To calculate inductance of this line, assume balanced positive-sequence currents I_a, I_b, I_c, for which $I_a + I_b + I_c = 0$. Again, (4.4.30) is valid, and the total flux linking the phase a conductor while it is in position 1 is

$$\lambda_{a1} = 2 \times 10^{-7}\left[I_a \ln \frac{1}{D_S} + I_b \ln \frac{1}{D_{12}} + I_c \ln \frac{1}{D_{31}}\right] \quad \text{Wb-t/m} \qquad (4.6.11)$$

Similarly, the total flux linkage of this conductor while it is in positions 2 and 3 is

$$\lambda_{a2} = 2 \times 10^{-7}\left[I_a \ln \frac{1}{D_S} + I_b \ln \frac{1}{D_{23}} + I_c \ln \frac{1}{D_{12}}\right] \quad \text{Wb-t/m} \qquad (4.6.12)$$

$$\lambda_{a3} = 2 \times 10^{-7}\left[I_a \ln \frac{1}{D_S} + I_b \ln \frac{1}{D_{31}} + I_c \ln \frac{1}{D_{23}}\right] \quad \text{Wb-t/m} \qquad (4.6.13)$$

The average of the above flux linkages is

$$\lambda_a = \frac{\lambda_{a1}\left(\frac{l}{3}\right) + \lambda_{a2}\left(\frac{l}{3}\right) + \lambda_{a3}\left(\frac{l}{3}\right)}{l} = \frac{\lambda_{a1} + \lambda_{a2} + \lambda_{a3}}{3}$$

$$= \frac{2\times 10^{-7}}{3}\left[3I_a \ln \frac{1}{D_S} + I_b \ln \frac{1}{D_{12}D_{23}D_{31}} + I_c \ln \frac{1}{D_{12}D_{23}D_{31}}\right] \qquad (4.6.14)$$

Using $(I_b + I_c) = -I_a$ in (4.6.14),

$$\lambda_a = \frac{2 \times 10^{-7}}{3}\left[3I_a \ln \frac{1}{D_S} - I_a \ln \frac{1}{D_{12}D_{23}D_{31}}\right]$$

$$= 2 \times 10^{-7} I_a \ln \frac{\sqrt[3]{D_{12}D_{23}D_{31}}}{D_S} \quad \text{Wb-t/m} \tag{4.6.15}$$

and the average inductance of phase a is

$$L_a = \frac{\lambda_a}{I_a} = 2 \times 10^{-7} \ln \frac{\sqrt[3]{D_{12}D_{23}D_{31}}}{D_S} \quad \text{H/m per phase} \tag{4.6.16}$$

The same result is obtained for $L_b = \lambda_b/I_b$ and for $L_c = \lambda_c/I_c$. However, only one phase need be considered for balanced three-phase operation of a completely transposed three-phase line. Defining

$$D_{eq} = \sqrt[3]{D_{12}D_{23}D_{31}} \tag{4.6.17}$$

we have

$$L_a = 2 \times 10^{-7} \ln \frac{D_{eq}}{D_S} \quad \text{H/m} \tag{4.6.18}$$

D_{eq}, the cube root of the product of the three-phase spacings, is the geometric mean distance between phases. Also, D_S is the conductor GMR for stranded conductors, or r' for solid cylindrical conductors.

EXAMPLE 4.4 Inductance and inductive reactance: three-phase line

A completely transposed 60-Hz three-phase line has flat horizontal phase spacing with 10 m between adjacent conductors. The conductors are 806 mm^2 (1,590,000 cmil) ACSR with 54/3 stranding. Line length is 200 km. Determine the inductance in H and the inductive reactance in Ω.

SOLUTION From Table A.4, the GMR of a 806 mm^2 (1,590,000 cmil) 54/3 ACSR conductor is

$$D_S = 0.0520 \text{ ft} \frac{1 \text{ m}}{3.28 \text{ ft}} = 0.0159 \text{ m}$$

Also, from (4.6.17) and (4.6.18),

$$D_{eq} = \sqrt[3]{(10)(10)(20)} = 12.6 \text{ m}$$

$$L_a = 2 \times 10^{-7} \ln\left(\frac{12.6}{0.0159}\right) \frac{\text{H}}{\text{m}} \times \frac{1000 \text{ m}}{\text{km}} \times 200 \text{ km}$$

$$= 0.267 \quad \text{H}$$

The inductive reactance of phase a is

$$X_a = 2\pi f L_a = 2\pi(60)(0.267) = 101 \quad \Omega$$

■

FIGURE 4.14
Bundle conductor configurations

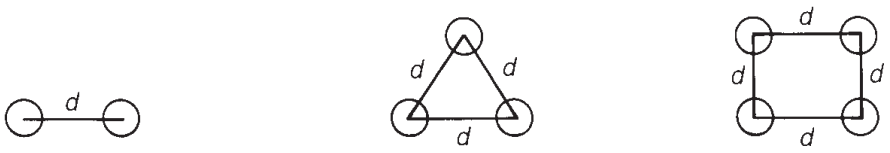

It is common practice for EHV lines to use more than one conductor per phase, a practice called *bundling*. Bundling reduces the electric field strength at the conductor surfaces, which in turn reduces or eliminates corona and its results: undesirable power loss, communications interference, and audible noise. Bundling also reduces the series reactance of the line by increasing the GMR of the bundle.

Figure 4.14 shows common EHV bundles consisting of two, three, or four conductors. The three-conductor bundle has its conductors on the vertices of an equilateral triangle, and the four-conductor bundle has its conductors on the corners of a square. To calculate inductance, D_S in (4.6.18) is replaced by the GMR of the bundle. Since the bundle constitutes a composite conductor, calculation of bundle GMR is, in general, given by (4.6.7). If the conductors are stranded and the bundle spacing d is large compared to the conductor outside radius, each stranded conductor is first replaced by an equivalent solid cylindrical conductor with GMR $= D_S$. Then the bundle is replaced by one equivalent conductor with GMR $= D_{SL}$, given by (4.6.7) with $n = 2$, 3, or 4 as follows:

Two-conductor bundle:

$$D_{SL} = \sqrt[4]{(D_S \times d)^2} = \sqrt{D_S d} \tag{4.6.19}$$

Three-conductor bundle:

$$D_{SL} = \sqrt[9]{(D_S \times d \times d)^3} = \sqrt[3]{D_S d^2} \tag{4.6.20}$$

Four-conductor bundle:

$$D_{SL} = \sqrt[16]{(D_S \times d \times d \times d\sqrt{2})^4} = 1.091\sqrt[4]{D_S d^3} \tag{4.6.21}$$

The inductance is then

$$L_a = 2 \times 10^{-7} \ln \frac{D_{eq}}{D_{SL}} \quad \text{H/m} \tag{4.6.22}$$

If the phase spacings are large compared to the bundle spacing, then sufficient accuracy for D_{eq} is obtained by using the distances between bundle centers.

EXAMPLE 4.5 Inductive reactance: three-phase line with bundled conductors

Each of the 806 mm^2 conductors in Example 4.4 is replaced by two 403 mm^2 ACSR 26/2 conductors, as shown in Figure 4.15. Bundle spacing is 0.40 m.

FIGURE 4.15

Three-phase bundled conductor line for Example 4.5

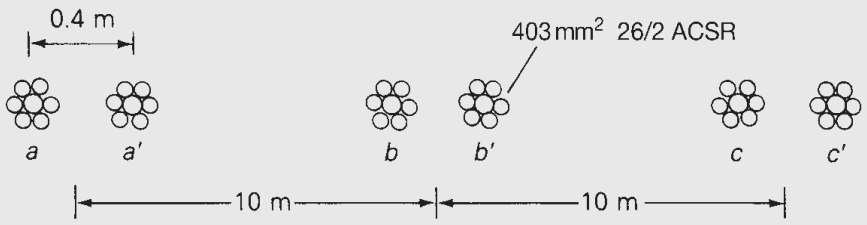

Flat horizontal spacing is retained, with 10 m between adjacent bundle centers. Calculate the inductive reactance of the line and compare it with that of Example 4.4.

SOLUTION From Table A.4, the GMR of a 403 mm^2 (795,000 cmil) 26/2 ACSR conductor is

$$D_S = 0.0375 \text{ ft} \times \frac{1 \text{ m}}{3.28 \text{ ft}} = 0.0114 \text{ m}$$

From (4.6.19), the two-conductor bundle GMR is

$$D_{SL} = \sqrt{(0.0114)(0.40)} = 0.0676 \text{ m}$$

Since $D_{eq} = 12.6$ m is the same as in Example 4.4,

$$L_a = 2 \times 10^{-7} \ln\left(\frac{12.6}{0.0676}\right)(1000)(200) = 0.209 \text{ H}$$

$$X_a = 2\pi f L_1 = (2\pi)(60)(0.209) = 78.8 \ \Omega$$

The reactance of the bundled line, 78.8 Ω, is 22% less than that of Example 4.4, even though the two-conductor bundle has the same amount of conductor material (that is, the same cmil per phase). One advantage of reduced series line reactance is smaller line-voltage drops. Also, the loadability of medium and long EHV lines is increased (see Chapter 5). ■

4.7

SERIES IMPEDANCES: THREE-PHASE LINE WITH NEUTRAL CONDUCTORS AND EARTH RETURN

In this section, we develop equations suitable for computer calculation of the series impedances, including resistances and inductive reactances, for the three-phase overhead line shown in Figure 4.16. This line has three phase conductors *a*, *b*, and *c*, where bundled conductors, if any, have already been replaced by equivalent conductors, as described in Section 4.6. The line also has *N* neutral conductors denoted $n1, n2, \ldots, nN$.* All the neutral conductors

*Instead of *shield wire* we use the term *neutral conductor*, which applies to distribution as well as transmission lines.

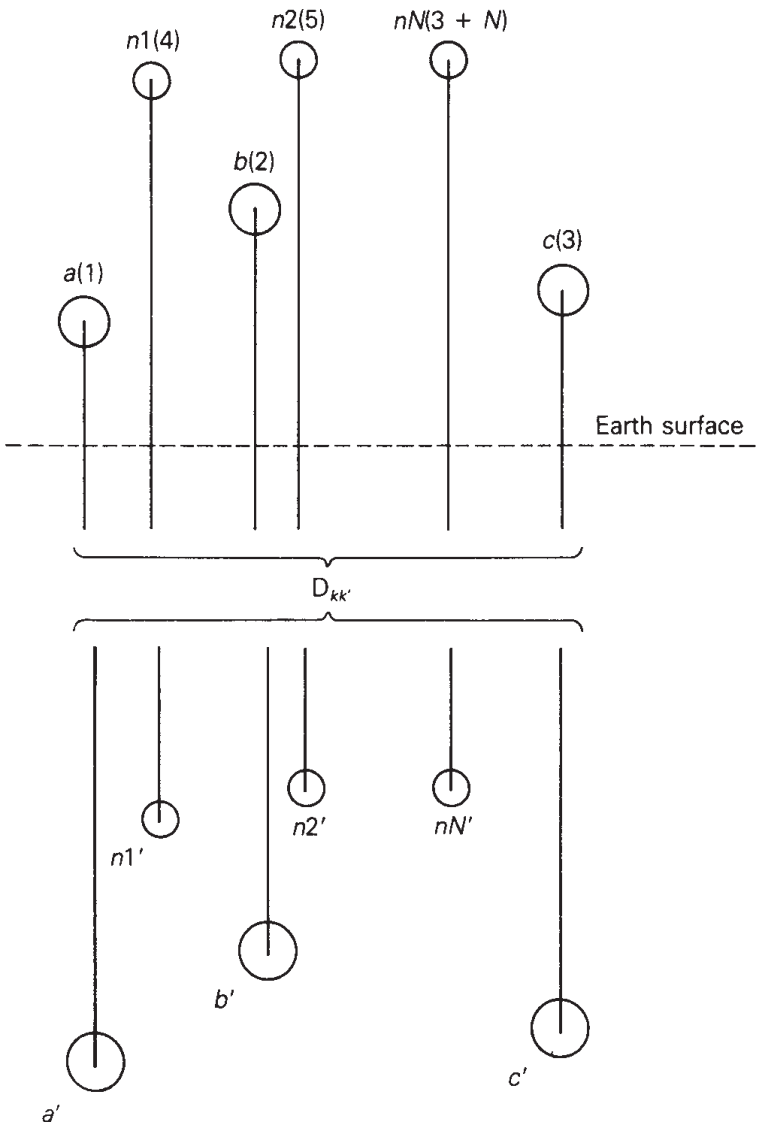

FIGURE 4.16

Three-phase transmission line with earth replaced by earth return conductors

are connected in parallel and are grounded to the earth at regular intervals along the line. Any isolated neutral conductors that carry no current are omitted. The phase conductors are insulated from each other and from earth.

If the phase currents are not balanced, there may be a return current in the grounded neutral wires and in the earth. The earth return current will spread out under the line, seeking the lowest impedance return path. A classic paper by Carson [4], later modified by others [5, 6], shows that the earth can be replaced by a set of "earth return" conductors located directly under the overhead conductors, as shown in Figure 4.16. Each earth return conductor carries the negative of its overhead conductor current, has a GMR denoted $D_{k'k'}$, distance $D_{kk'}$ from its overhead conductor, and resistance $R_{k'}$ given by:

TABLE 4.4

Earth resistivities and 60-Hz equivalent conductor distances

Type of Earth	Resistivity (Ωm)	$D_{kk'}$ (m)
Sea water	0.01–1.0	8.50–85.0
Swampy ground	10–100	269–850
Average damp earth	100	850
Dry earth	1000	2690
Pure slate	10^7	269,000
Sandstone	10^9	2,690,000

$$D_{k'k'} = D_{kk} \quad \text{m} \tag{4.7.1}$$

$$D_{kk'} = 658.5\sqrt{\rho/f} \quad \text{m} \tag{4.7.2}$$

$$R_{k'} = 9.869 \times 10^{-7} f \quad \Omega/\text{m} \tag{4.7.3}$$

where ρ is the earth resistivity in ohm-meters and f is frequency in hertz. Table 4.4 lists earth resistivities and 60-Hz equivalent conductor distances for various types of earth. It is common practice to select $\rho = 100$ Ωm when actual data are unavailable.

Note that the GMR of each earth return conductor, $D_{k'k'}$, is the same as the GMR of its corresponding overhead conductor, D_{kk}. Also, all the earth return conductors have the same distance $D_{kk'}$ from their overhead conductors and the same resistance $R_{k'}$.

For simplicity, we renumber the overhead conductors from 1 to $(3 + N)$, beginning with the phase conductors, then overhead neutral conductors, as shown in Figure 4.16. Operating as a transmission line, the sum of the currents in all the conductors is zero. That is,

$$\sum_{k=1}^{(6+2N)} I_k = 0 \tag{4.7.4}$$

Equation (4.4.30) is therefore valid, and the flux linking overhead conductor k is

$$\lambda_k = 2 \times 10^{-7} \sum_{m=1}^{(3+N)} I_m \ln \frac{D_{km'}}{D_{km}} \quad \text{Wb-t/m} \tag{4.7.5}$$

In matrix format, (4.7.5) becomes

$$\boldsymbol{\lambda} = \mathbf{L}\boldsymbol{I} \tag{4.7.6}$$

where

$\boldsymbol{\lambda}$ is a $(3 + N)$ vector

$\boldsymbol{I}$ is a $(3 + N)$ vector

$\mathbf{L}$ is a $(3 + N) \times (3 + N)$ matrix whose elements are:

$$L_{km} = 2 \times 10^{-7} \ln \frac{D_{km'}}{D_{km}} \tag{4.7.7}$$

FIGURE 4.17

Circuit representation of series-phase impedances

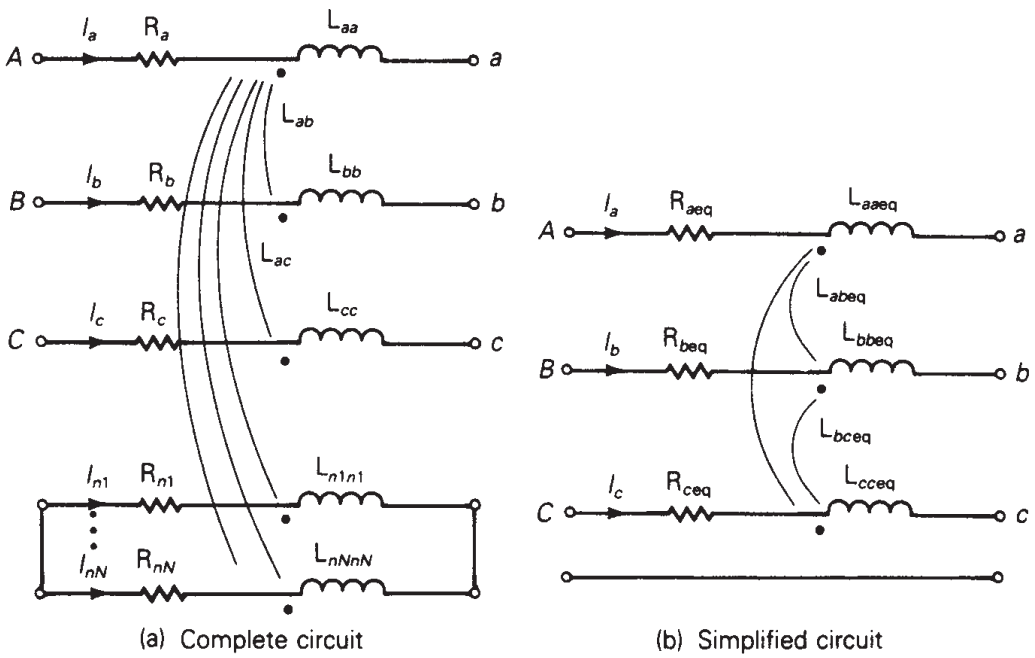

When $k = m$, D_{kk} in (4.7.7) is the GMR of (bundled) conductor k. When $k \neq m$, D_{km} is the distance between conductors k and m.

A circuit representation of a 1-meter section of the line is shown in Figure 4.17(a). Using this circuit, the vector of voltage drops across the conductors is:

$$\begin{bmatrix} E_{Aa} \\ E_{Bb} \\ E_{Cc} \\ 0 \\ 0 \\ \vdots \\ 0 \end{bmatrix} = (\mathbf{R} + j\omega\mathbf{L}) \begin{bmatrix} I_a \\ I_b \\ I_c \\ I_{n1} \\ \vdots \\ I_{nN} \end{bmatrix} \tag{4.7.8}$$

where $\mathbf{L}$ is given by (4.7.7) and $\mathbf{R}$ is a $(3 + N) \times (3 + N)$ matrix of conductor resistances.

$$\mathbf{R} = \begin{bmatrix} (R_a + R_{k'})R_{k'} \cdots & & R_{k'} \\ R_{k'}(R_b + R_{k'})R_{k'} \cdots & & \vdots \\ & (R_c + R_{k'})R_{k'} \cdots & \\ & & (R_{n1} + R_{k'})R_{k'} \cdots \\ & \ddots & \\ R_{k'} & & (R_{nN} + R_{k'}) \end{bmatrix} \Omega/\text{m} \tag{4.7.9}$$

The resistance matrix of (4.7.9) includes the resistance R_k of each overhead conductor and a mutual resistance $\mathrm{R}_{k'}$ due to the image conductors. R_k of each overhead conductor is obtained from conductor tables such as Appendix Table A.3 or A.4, for a specified frequency, temperature, and current. $\mathrm{R}_{k'}$ of all the image conductors is the same, as given by (4.7.3).

Our objective now is to reduce the $(3 + N)$ equations in (4.7.8) to three equations, thereby obtaining the simplified circuit representations shown in Figure 4.17(b). We partition (4.7.8) as follows:

$$\begin{bmatrix} E_{Aa} \\ E_{Bb} \\ E_{Cc} \\ \hline 0 \\ \cdots \\ 0 \end{bmatrix} = \overbrace{\left[\begin{array}{ccc|ccc} Z_{11} & Z_{12} & Z_{13} & Z_{14} & \cdots & Z_{1(3+N)} \\ Z_{21} & Z_{22} & Z_{23} & Z_{24} & \cdots & Z_{2(3+N)} \\ Z_{31} & Z_{32} & Z_{33} & Z_{34} & \cdots & Z_{3(3+N)} \\ \hline Z_{41} & Z_{42} & Z_{43} & Z_{44} & \cdots & Z_{4(3+N)} \\ & & & & & \\ Z_{(3+N)1} & Z_{(3+N)2} & Z_{(3+N)3} & Z_{(3+N)4} & \cdots & Z_{(3+N)(3+N)} \end{array}\right]}^{\substack{Z_A \quad\quad\quad\quad\quad Z_B \\ \\ \underbrace{\qquad\qquad\qquad\qquad\qquad\qquad}_{Z_C \qquad\qquad\qquad\qquad\qquad Z_D}}} \begin{bmatrix} I_a \\ I_b \\ I_c \\ \hline I_{n1} \\ I_{nN} \\ \vdots \end{bmatrix} \tag{4.7.10}$$

The diagonal elements of this matrix are

$$Z_{kk} = \mathrm{R}_k + \mathrm{R}_{k'} + j\omega 2 \times 10 \ln \frac{\mathrm{D}_{kk'}}{\mathrm{D}_{kk}} \quad \Omega/\mathrm{m} \tag{4.7.11}$$

And the off-diagonal elements, for $k \neq m$, are

$$Z_{km} = \mathrm{R}_{k'} + j\omega 2 \times 10 \ln \frac{\mathrm{D}_{km'}}{\mathrm{D}_{km}} \quad \Omega/\mathrm{m} \tag{4.7.12}$$

Next, (4.7.10) is partitioned as shown above to obtain

$$\left[\begin{array}{c} \boldsymbol{E}_{\mathrm{P}} \\ \hline \mathbf{0} \end{array}\right] = \left[\begin{array}{c|c} \boldsymbol{Z}_A & \boldsymbol{Z}_B \\ \hline \boldsymbol{Z}_C & \boldsymbol{Z}_D \end{array}\right] \left[\begin{array}{c} \boldsymbol{I}_{\mathrm{P}} \\ \hline \boldsymbol{I}_n \end{array}\right] \tag{4.7.13}$$

where

$$\boldsymbol{E}_{\mathrm{P}} = \begin{bmatrix} E_{Aa} \\ E_{Bb} \\ E_{Cc} \end{bmatrix}; \quad \boldsymbol{I}_{\mathrm{P}} = \begin{bmatrix} I_a \\ I_b \\ I_c \end{bmatrix}; \quad \boldsymbol{I}_n = \begin{bmatrix} I_{n1} \\ \vdots \\ I_{nN} \end{bmatrix}$$

$\boldsymbol{E}_{\mathrm{P}}$ is the three-dimensional vector of voltage drops across the phase conductors (including the neutral voltage drop). $\boldsymbol{I}_{\mathrm{P}}$ is the three-dimensional vector of phase currents and $\boldsymbol{I}_n$ is the N vector of neutral currents. Also, the $(3 + N) \times (3 + N)$ matrix in (4.7.10) is partitioned to obtain the following matrices:

$\boldsymbol{Z}_A$ with dimension 3×3

$\boldsymbol{Z}_B$ with dimension $3 \times N$

$\boldsymbol{Z}_C$ with dimension $N \times 3$

$\boldsymbol{Z}_D$ with dimension $N \times N$

Equation (4.7.13) is rewritten as two separate matrix equations:

$$\boldsymbol{E}_{\mathrm{P}} = \boldsymbol{Z}_A \boldsymbol{I}_{\mathrm{P}} + \boldsymbol{Z}_B \boldsymbol{I}_n \tag{4.7.14}$$

$$\boldsymbol{0} = \boldsymbol{Z}_C \boldsymbol{I}_{\mathrm{P}} + \boldsymbol{Z}_D \boldsymbol{I}_n \tag{4.7.15}$$

Solving (4.7.15) for $\boldsymbol{I}_n$,

$$\boldsymbol{I}_n = -\boldsymbol{Z}_D^{-1} \boldsymbol{Z}_C \boldsymbol{I}_{\mathrm{P}} \tag{4.7.16}$$

Using (4.7.16) in (4.7.14):

$$\boldsymbol{E}_{\mathrm{P}} = [\boldsymbol{Z}_A - \boldsymbol{Z}_B \boldsymbol{Z}_D^{-1} \boldsymbol{Z}_C] \boldsymbol{I}_{\mathrm{P}} \tag{4.7.17}$$

or

$$\boldsymbol{E}_{\mathrm{P}} = \boldsymbol{Z}_{\mathrm{P}} \boldsymbol{I}_{\mathrm{P}} \tag{4.7.18}$$

where

$$\boldsymbol{Z}_{\mathrm{P}} = \boldsymbol{Z}_A - \boldsymbol{Z}_B \boldsymbol{Z}_D^{-1} \boldsymbol{Z}_C \tag{4.7.19}$$

Equation (4.7.17), the desired result, relates the phase-conductor voltage drops (including neutral voltage drop) to the phase currents. $\boldsymbol{Z}_{\mathrm{P}}$ given by (4.7.19) is the 3×3 series-phase impedance matrix, whose elements are denoted

$$\boldsymbol{Z}_{\mathrm{P}} = \begin{bmatrix} Z_{aa\mathrm{eq}} & Z_{ab\mathrm{eq}} & Z_{ac\mathrm{eq}} \\ Z_{ab\mathrm{eq}} & Z_{bb\mathrm{eq}} & Z_{bc\mathrm{eq}} \\ Z_{ac\mathrm{eq}} & Z_{bc\mathrm{eq}} & Z_{cc\mathrm{eq}} \end{bmatrix} \quad \Omega/\mathrm{m} \tag{4.7.20}$$

If the line is completely transposed, the diagonal and off-diagonal elements are averaged to obtain

$$\hat{\boldsymbol{Z}}_{\mathrm{P}} = \begin{bmatrix} \hat{Z}_{aa\mathrm{eq}} & \hat{Z}_{ab\mathrm{eq}} & \hat{Z}_{ab\mathrm{eq}} \\ \hat{Z}_{ab\mathrm{eq}} & \hat{Z}_{aa\mathrm{eq}} & \hat{Z}_{ab\mathrm{eq}} \\ \hat{Z}_{ab\mathrm{eq}} & \hat{Z}_{ab\mathrm{eq}} & \hat{Z}_{aa\mathrm{eq}} \end{bmatrix} \quad \Omega/\mathrm{m} \tag{4.7.21}$$

where

$$\hat{Z}_{aa\mathrm{eq}} = \tfrac{1}{3}(Z_{aa\mathrm{eq}} + Z_{bb\mathrm{eq}} + Z_{cc\mathrm{eq}}) \tag{4.7.22}$$

$$\hat{Z}_{ab\mathrm{eq}} = \tfrac{1}{3}(Z_{ab\mathrm{eq}} + Z_{ac\mathrm{eq}} + Z_{bc\mathrm{eq}}) \tag{4.7.23}$$

4.8

ELECTRIC FIELD AND VOLTAGE: SOLID CYLINDRICAL CONDUCTOR

The capacitance between conductors in a medium with constant permittivity ε can be obtained by determining the following:

1. Electric field strength E, from Gauss's law
2. Voltage between conductors
3. Capacitance from charge per unit volt $(C = q/V)$

As a step toward computing capacitances of general conductor configurations, we first compute the electric field of a uniformly charged, solid cylindrical conductor and the voltage between two points outside the conductor. We also compute the voltage between two conductors in an array of charged conductors.

Gauss's law states that the total electric flux leaving a closed surface equals the total charge within the volume enclosed by the surface. That is, the normal component of electric flux density integrated over a closed surface equals the charge enclosed:

$$\oiint D_\perp \, ds = \oiint \varepsilon E_\perp \, ds = Q_{\text{enclosed}} \tag{4.8.1}$$

where $D_\perp$ denotes the normal component of electric flux density, $E_\perp$ denotes the normal component of electric field strength, and ds denotes the differential surface area. From Gauss's law, electric charge is a source of electric fields. Electric field lines originate from positive charges and terminate at negative charges.

Figure 4.18 shows a solid cylindrical conductor with radius r and with charge q coulombs per meter (assumed positive in the figure), uniformly distributed on the conductor surface. For simplicity, assume that the conductor is (1) sufficiently long that end effects are negligible, and (2) a perfect conductor (that is, zero resistivity, $\rho = 0$).

Inside the perfect conductor, Ohm's law gives $E_{\text{int}} = \rho J = 0$. That is, the internal electric field E_{int} is zero. To determine the electric field outside the conductor, select the cylinder with radius $x > r$ and with 1-meter length, shown in Figure 4.18, as the closed surface for Gauss's law. Due to the uniform charge distribution, the electric field strength E_x is constant on the cylinder. Also, there is no tangential component of E_x, so the electric field is radial to the conductor. Then, integration of (4.8.1) yields

$$\varepsilon E_x (2\pi x)(1) = q(1)$$

$$E_x = \frac{q}{2\pi\varepsilon x} \quad \text{V/m} \tag{4.8.2}$$

where, for a conductor in free space, $\varepsilon = \varepsilon_0 = 8.854 \times 10^{-12}$ F/m.

FIGURE 4.18

Perfectly conducting solid cylindrical conductor with uniform charge distribution

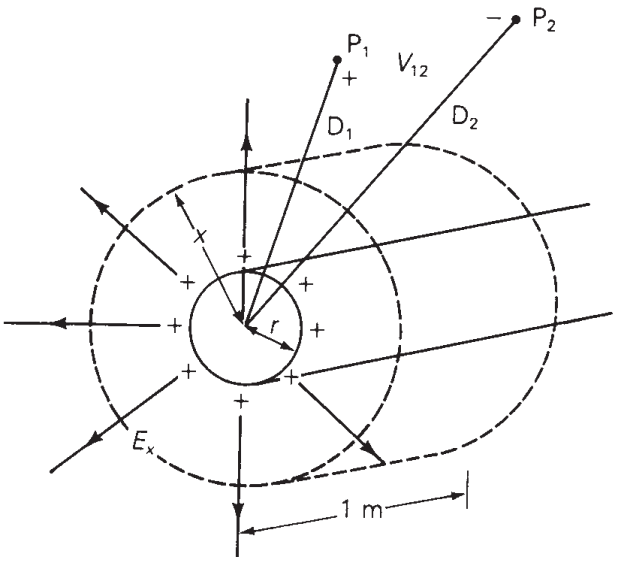

A plot of the electric field lines is also shown in Figure 4.18. The direction of the field lines, denoted by the arrows, is from the positive charges where the field originates, to the negative charges, which in this case are at infinity. If the charge on the conductor surface were negative, then the direction of the field lines would be reversed.

Concentric cylinders surrounding the conductor are constant potential surfaces. The potential difference between two concentric cylinders at distances D_1 and D_2 from the conductor center is

$$V_{12} = \int_{D_1}^{D_2} E_x \, dx \tag{4.8.3}$$

Using (4.8.2) in (4.8.1),

$$V_{12} = \int_{D_1}^{D_2} \frac{q}{2\pi\varepsilon x} \, dx = \frac{q}{2\pi\varepsilon} \ln \frac{D_2}{D_1} \quad \text{volts} \tag{4.8.4}$$

Equation (4.8.4) gives the voltage V_{12} between two points, P_1 and P_2, at distances D_1 and D_2 from the conductor center, as shown in Figure 4.18. Also, in accordance with our notation, V_{12} is the voltage at P_1 with respect to P_2. If q is positive and D_2 is greater than D_1, as shown in the figure, then V_{12} is positive; that is, P_1 is at a higher potential than P_2. Equation (4.8.4) is also valid for either dc or ac. For ac, V_{12} is a phasor voltage and q is a phasor representation of a sinusoidal charge.

Now apply (4.8.4) to the array of M solid cylindrical conductors shown in Figure 4.19. Assume that each conductor m has an ac charge q_m C/m uniformly distributed along the conductor. The voltage V_{kim} between conductors k and i due to the charge q_m acting alone is

$$V_{kim} = \frac{q_m}{2\pi\varepsilon} \ln \frac{D_{im}}{D_{km}} \quad \text{volts} \tag{4.8.5}$$

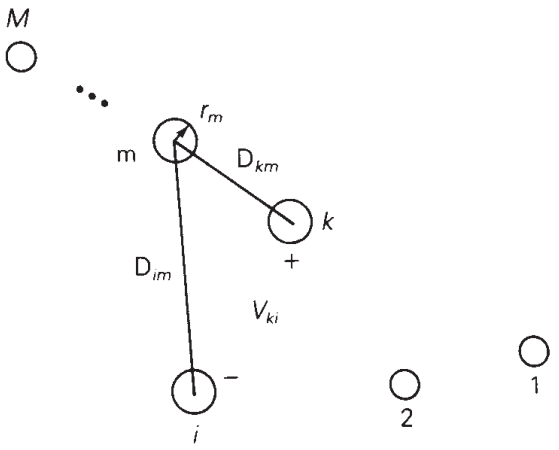

FIGURE 4.19
Array of M solid cylindrical conductors

where $D_{mm} = r_m$ when $k = m$ or $i = m$. In (4.8.5) we have neglected the distortion of the electric field in the vicinity of the other conductors, caused by the fact that the other conductors themselves are constant potential surfaces. V_{kim} can be thought of as the voltage between cylinders with radii D_{km} and D_{im} concentric to conductor m at points on the cylinders remote from conductors, where there is no distortion.

Using superposition, the voltage V_{ki} between conductors k and i due to all the changes is

$$V_{ki} = \frac{1}{2\pi\varepsilon}\sum_{m=1}^{M} q_m \ln\frac{D_{im}}{D_{km}} \quad \text{volts} \tag{4.8.6}$$

4.9

CAPACITANCE: SINGLE-PHASE TWO-WIRE LINE AND THREE-PHASE THREE-WIRE LINE WITH EQUAL PHASE SPACING

The results of the previous section are used here to determine the capacitances of the two relatively simple transmission lines considered in Section 4.5, a single-phase two-wire line and a three-phase three-wire line with equal phase spacing.

First we consider the single-phase two-wire line shown in Figure 4.9. Assume that the conductors are energized by a voltage source such that conductor x has a uniform charge q C/m and, assuming conservation of charge, conductor y has an equal quantity of negative charge $-q$. Using (4.8.6) with $k = x$, $i = y$, and $m = x, y$,

$$\begin{aligned} V_{xy} &= \frac{1}{2\pi\varepsilon}\left[q \ln\frac{D_{yx}}{D_{xx}} - q \ln\frac{D_{yy}}{D_{xy}}\right] \\ &= \frac{q}{2\pi\varepsilon} \ln\frac{D_{yx}D_{xy}}{D_{xx}D_{yy}} \end{aligned} \tag{4.9.1}$$

Using $D_{xy} = D_{yx} = D$, $D_{xx} = r_x$, and $D_{yy} = r_y$, (4.9.1) becomes

$$V_{xy} = \frac{q}{\pi\varepsilon} \ln \frac{D}{\sqrt{r_x r_y}} \quad \text{volts} \tag{4.9.2}$$

For a 1-meter line length, the capacitance between conductors is

$$C_{xy} = \frac{q}{V_{xy}} = \frac{\pi\varepsilon}{\ln\left(\dfrac{D}{\sqrt{r_x r_y}}\right)} \quad \text{F/m line-to-line} \tag{4.9.3}$$

and if $r_x = r_y = r$,

$$C_{xy} = \frac{\pi\varepsilon}{\ln(D/r)} \quad \text{F/m line-to-line} \tag{4.9.4}$$

If the two-wire line is supplied by a transformer with a grounded center tap, then the voltage between each conductor and ground is one-half that given by (4.9.2). That is,

$$V_{xn} = V_{yn} = \frac{V_{xy}}{2} \tag{4.9.5}$$

and the capacitance from either line to the grounded neutral is

$$C_n = C_{xn} = C_{yn} = \frac{q}{V_{xn}} = 2C_{xy}$$

$$= \frac{2\pi\varepsilon}{\ln(D/r)} \quad \text{F/m line-to-neutral} \tag{4.9.6}$$

Circuit representations of the line-to-line and line-to-neutral capacitances are shown in Figure 4.20. Note that if the neutral is open in Figure 4.20(b), the two line-to-neutral capacitances combine in series to give the line-to-line capacitance.

Next consider the three-phase line with equal phase spacing shown in Figure 4.10. We shall neglect the effect of earth and neutral conductors here. To determine the positive-sequence capacitance, assume positive-sequence charges q_a, q_b, q_c such that $q_a + q_b + q_c = 0$. Using (4.8.6) with $k = a$, $i = b$, and $m = a, b, c$, the voltage V_{ab} between conductors a and b is

$$V_{ab} = \frac{1}{2\pi\varepsilon}\left[q_a \ln \frac{D_{ba}}{D_{aa}} + q_b \ln \frac{D_{bb}}{D_{ab}} + q_c \ln \frac{D_{bc}}{D_{ac}}\right] \tag{4.9.7}$$

Using $D_{aa} = D_{bb} = r$, and $D_{ab} = D_{ba} = D_{ca} = D_{cb} = D$, (4.9.7) becomes

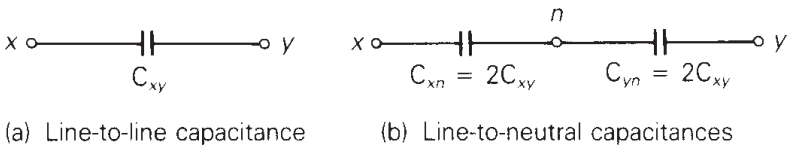

(a) Line-to-line capacitance (b) Line-to-neutral capacitances

FIGURE 4.20
Circuit representation of capacitances for a single-phase two-wire line

$$V_{ab} = \frac{1}{2\pi\varepsilon}\left[q_a \ln\frac{\mathrm{D}}{r} + q_b \ln\frac{r}{\mathrm{D}} + q_c \ln\frac{\mathrm{D}}{\mathrm{D}}\right]$$
$$= \frac{1}{2\pi\varepsilon}\left[q_a \ln\frac{\mathrm{D}}{r} + q_b \ln\frac{r}{\mathrm{D}}\right] \quad \text{volts} \tag{4.9.8}$$

Note that the third term in (4.9.8) is zero because conductors a and b are equidistant from conductor c. Thus, conductors a and b lie on a constant potential cylinder for the electric field due to q_c.

Similarly, using (4.8.6) with $k = a$, $i = c$, and $m = a, b, c$, the voltage V_{ac} is

$$V_{ac} = \frac{1}{2\pi\varepsilon}\left[q_a \ln\frac{\mathrm{D}_{ca}}{\mathrm{D}_{aa}} + q_b \ln\frac{\mathrm{D}_{cb}}{\mathrm{D}_{ab}} + q_c \ln\frac{\mathrm{D}_{cc}}{\mathrm{D}_{ac}}\right]$$
$$= \frac{1}{2\pi\varepsilon}\left[q_a \ln\frac{\mathrm{D}}{r} + q_b \ln\frac{\mathrm{D}}{\mathrm{D}} + q_c \ln\frac{r}{\mathrm{D}}\right]$$
$$= \frac{1}{2\pi\varepsilon}\left[q_a \ln\frac{\mathrm{D}}{r} + q_c \ln\frac{r}{\mathrm{D}}\right] \quad \text{volts} \tag{4.9.9}$$

Recall that for balanced positive-sequence voltages,

$$V_{ab} = \sqrt{3}V_{an}\underline{/+30^\circ} = \sqrt{3}V_{an}\left[\frac{\sqrt{3}}{2} + j\frac{1}{2}\right] \tag{4.9.10}$$

$$V_{ac} = -V_{ca} = \sqrt{3}V_{an}\underline{/-30^\circ} = \sqrt{3}V_{an}\left[\frac{\sqrt{3}}{2} - j\frac{1}{2}\right] \tag{4.9.11}$$

Adding (4.9.10) and (4.9.11) yields

$$V_{ab} + V_{ac} = 3V_{an} \tag{4.9.12}$$

Using (4.9.8) and (4.9.9) in (4.9.12),

$$V_{an} = \frac{1}{3}\left(\frac{1}{2\pi\varepsilon}\right)\left[2q_a \ln\frac{\mathrm{D}}{r} + (q_b + q_c)\ln\frac{r}{\mathrm{D}}\right] \tag{4.9.13}$$

and with $q_b + q_c = -q_a$,

$$V_{an} = \frac{1}{2\pi\varepsilon}q_a \ln\frac{\mathrm{D}}{r} \quad \text{volts} \tag{4.9.14}$$

The capacitance-to-neutral per line length is

$$\mathrm{C}_{an} = \frac{q_a}{V_{an}} = \frac{2\pi\varepsilon}{\ln\left(\dfrac{\mathrm{D}}{r}\right)} \quad \text{F/m line-to-neutral} \tag{4.9.15}$$

Due to symmetry, the same result is obtained for $\mathrm{C}_{bn} = q_b/V_{bn}$ and $\mathrm{C}_{cn} = q_c/V_{cn}$. For balanced three-phase operation, however, only one phase need be considered. A circuit representation of the capacitance-to-neutral is shown in Figure 4.21.

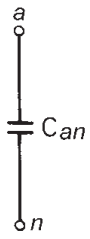

FIGURE 4.21
Circuit representation of the capacitance-to-neutral of a three-phase line with equal phase spacing

4.10

CAPACITANCE: STRANDED CONDUCTORS, UNEQUAL PHASE SPACING, BUNDLED CONDUCTORS

Equations (4.9.6) and (4.9.15) are based on the assumption that the conductors are solid cylindrical conductors with zero resistivity. The electric field inside these conductors is zero, and the external electric field is perpendicular to the conductor surfaces. Practical conductors with resistivities similar to those listed in Table 4.3 have a small internal electric field. As a result, the external electric field is slightly altered near the conductor surfaces. Also, the electric field near the surface of a stranded conductor is not the same as that of a solid cylindrical conductor. However, it is normal practice when calculating line capacitance to replace a stranded conductor by a perfectly conducting solid cylindrical conductor whose radius equals the outside radius of the stranded conductor. The resulting error in capacitance is small since only the electric field near the conductor surfaces is affected.

Also, (4.8.2) is based on the assumption that there is uniform charge distribution. But conductor charge distribution is nonuniform in the presence of other charged conductors. Therefore (4.9.6) and (4.9.15), which are derived from (4.8.2), are not exact. However, the nonuniformity of conductor charge distribution can be shown to have a negligible effect on line capacitance.

For three-phase lines with unequal phase spacing, balanced positive-sequence voltages are not obtained with balanced positive-sequence charges. Instead, unbalanced line-to-neutral voltages occur, and the phase-to-neutral capacitances are unequal. Balance can be restored by transposing the line such that each phase occupies each position for one-third of the line length. If equations similar to (4.9.7) for V_{ab} as well as for V_{ac} are written for each position in the transposition cycle, and are then averaged and used in (4.9.12)–(4.9.14), the resulting capacitance becomes

$$C_{an} = \frac{2\pi\varepsilon}{\ln(D_{eq}/r)} \quad \text{F/m} \tag{4.10.1}$$

where

$$D_{eq} = \sqrt[3]{D_{ab}D_{bc}D_{ac}} \tag{4.10.2}$$

Figure 4.22 shows a bundled conductor line with two conductors per bundle. To determine the capacitance of this line, assume balanced positive-sequence charges q_a, q_b, q_c for each phase such that $q_a + q_b + q_c = 0$. Assume that the conductors in each bundle, which are in parallel, share the charges equally. Thus conductors a and a' each have the charge $q_a/2$. Also assume that the phase spacings are much larger than the bundle spacings so that D_{ab} may be used instead of $(D_{ab} - d)$ or $(D_{ab} + d)$. Then, using (4.8.6) with $k = a$, $i = b$, $m = a, a', b, b', c, c'$,

FIGURE 4.22

Three-phase line with two conductors per bundle

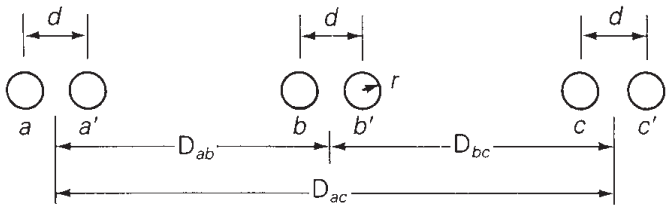

$$
\begin{aligned}
V_{ab} &= \frac{1}{2\pi\varepsilon}\left[\frac{q_a}{2}\ln\frac{D_{ba}}{D_{aa}} + \frac{q_a}{2}\ln\frac{D_{ba'}}{D_{aa'}} + \frac{q_b}{2}\ln\frac{D_{bb}}{D_{ab}}\right.\\
&\qquad \left. + \frac{q_b}{2}\ln\frac{D_{bb'}}{D_{ab'}} + \frac{q_c}{2}\ln\frac{D_{bc}}{D_{ac}} + \frac{q_c}{2}\ln\frac{D_{bc'}}{D_{ac'}}\right]\\
&= \frac{1}{2\pi\varepsilon}\left[\frac{q_a}{2}\left(\ln\frac{D_{ab}}{r} + \ln\frac{D_{ab}}{d}\right) + \frac{q_b}{2}\left(\ln\frac{r}{D_{ab}} + \ln\frac{d}{D_{ab}}\right)\right.\\
&\qquad \left. + \frac{q_c}{2}\left(\ln\frac{D_{bc}}{D_{ac}} + \ln\frac{D_{bc}}{D_{ac}}\right)\right]\\
&= \frac{1}{2\pi\varepsilon}\left[q_a\ln\frac{D_{ab}}{\sqrt{rd}} + q_b\ln\frac{\sqrt{rd}}{D_{ab}} + q_c\ln\frac{D_{bc}}{D_{ac}}\right] \qquad (4.10.3)
\end{aligned}
$$

Equation (4.10.3) is the same as (4.9.7), except that D_{aa} and D_{bb} in (4.9.7) are replaced by $\sqrt{rd}$ in this equation. Therefore, for a transposed line, derivation of the capacitance would yield

$$C_{an} = \frac{2\pi\varepsilon}{\ln(D_{eq}/D_{SC})} \quad \text{F/m} \qquad (4.10.4)$$

where

$$D_{SC} = \sqrt{rd} \quad \text{for a two-conductor bundle} \qquad (4.10.5)$$

Similarly,

$$D_{SC} = \sqrt[3]{rd^2} \quad \text{for a three-conductor bundle} \qquad (4.10.6)$$

$$D_{SC} = 1.091\sqrt[4]{rd^3} \quad \text{for a four-conductor bundle} \qquad (4.10.7)$$

Equation (4.10.4) for capacitance is analogous to (4.6.22) for inductance. In both cases D_{eq}, given by (4.6.17) or (4.10.2), is the geometric mean of the distances between phases. Also, (4.10.5)–(4.10.7) for D_{SC} are analogous to (4.6.19)–(4.6.21) for D_{SL}, except that the conductor outside radius r replaces the conductor GMR D_S.

The current supplied to the transmission-line capacitance is called *charging current*. For a single-phase circuit operating at line-to-line voltage $V_{xy} = V_{xy}\angle 0°$, the charging current is

$$I_{chg} = Y_{xy}V_{xy} = j\omega C_{xy}V_{xy} \quad \text{A} \qquad (4.10.8)$$

As shown in Chapter 2, a capacitor delivers reactive power. From (2.3.5), the reactive power delivered by the line-to-line capacitance is

$$Q_C = \frac{V_{xy}^2}{X_c} = Y_{xy}V_{xy}^2 = \omega C_{xy}V_{xy}^2 \quad \text{var} \tag{4.10.9}$$

For a completely transposed three-phase line that has balanced positive-sequence voltages with $V_{an} = V_{LN}\underline{/0^\circ}$, the phase a charging current is

$$I_{chg} = YV_{an} = j\omega C_{an}V_{LN} \quad \text{A} \tag{4.10.10}$$

and the reactive power delivered by phase a is

$$Q_{C1\phi} = YV_{an}^2 = \omega C_{an}V_{LN}^2 \quad \text{var} \tag{4.10.11}$$

The total reactive power supplied by the three-phase line is

$$Q_{C3\phi} = 3Q_{C1\phi} = 3\omega C_{an}V_{LN}^2 = \omega C_{an}V_{LL}^2 \quad \text{var} \tag{4.10.12}$$

EXAMPLE 4.6 Capacitance, admittance, and reactive power supplied: single-phase line

For the single-phase line in Example 4.3, determine the line-to-line capacitance in F and the line-to-line admittance in S. If the line voltage is 20 kV, determine the reactive power in kvar supplied by this capacitance.

SOLUTION From Table A.3, the outside radius of a 4/0 12-strand copper conductor is

$$r = \frac{0.552}{2} \text{ in.} = 0.7 \text{ cm}$$

and from (4.9.4),

$$C_{xy} = \frac{\pi(8.854 \times 10^{-12})}{\ln\left(\frac{150}{0.7}\right)} = 5.182 \times 10^{-12} \quad \text{F/m}$$

or

$$C_{xy} = 5.182 \times 10^{-12}\frac{\text{F}}{\text{m}} \times 32 \times 10^3 \text{ m} = 1.66 \times 10^{-7} \quad \text{F}$$

and the shunt admittance is

$$\begin{aligned} Y_{xy} &= j\omega C_{xy} = j(2\pi 60)(1.66 \times 10^{-7}) \\ &= j6.27 \times 10^{-5} \quad \text{S line-to-line} \end{aligned}$$

From (4.10.9),

$$Q_C = (6.27 \times 10^{-5})(20 \times 10^3)^2 = 25.1 \quad \text{kvar}$$ ■

EXAMPLE 4.7 Capacitance and shunt admittance; charging current and reactive power supplied: three-phase line

For the three-phase line in Example 4.5, determine the capacitance-to-neutral in F and the shunt admittance-to-neutral in S. If the line voltage is 345 kV, determine the charging current in kA per phase and the total reactive power in Mvar supplied by the line capacitance. Assume balanced positive-sequence voltages.

SOLUTION From Table A.4, the outside radius of a 403 mm^2 26/2 ACSR conductor is

$$r = \frac{1.108}{2} \text{ in.} \times 0.0254 \frac{\text{m}}{\text{in.}} = 0.0141 \quad \text{m}$$

From (4.10.5), the equivalent radius of the two-conductor bundle is

$$D_{SC} = \sqrt{(0.0141)(0.40)} = 0.0750 \quad \text{m}$$

$D_{eq} = 12.6$ m is the same as in Example 4.5. Therefore, from (4.10.4),

$$C_{an} = \frac{(2\pi)(8.854 \times 10^{-12})}{\ln\left(\dfrac{12.6}{0.0750}\right)} \frac{\text{F}}{\text{m}} \times 1000 \frac{\text{m}}{\text{km}} \times 200 \text{ km}$$

$$= 2.17 \times 10^{-6} \quad \text{F}$$

The shunt admittance-to-neutral is

$$Y_{an} = j\omega C_{an} = j(2\pi 60)(2.17 \times 10^{-6})$$

$$= j8.19 \times 10^{-4} \quad \text{S}$$

From (4.10.10),

$$I_{chg} = |I_{chg}| = (8.19 \times 10^{-4})\left(\frac{345}{\sqrt{3}}\right) = 0.163 \quad \text{kA/phase}$$

and from (4.10.12),

$$Q_{C3\phi} = (8.19 \times 10^{-4})(345)^2 = 97.5 \quad \text{Mvar}$$ ■

4.11

SHUNT ADMITTANCES: LINES WITH NEUTRAL CONDUCTORS AND EARTH RETURN

In this section, we develop equations suitable for computer calculation of the shunt admittances for the three-phase overhead line shown in Figure 4.16. We approximate the earth surface as a perfectly conducting horizontal plane,

FIGURE 4.23

Method of images

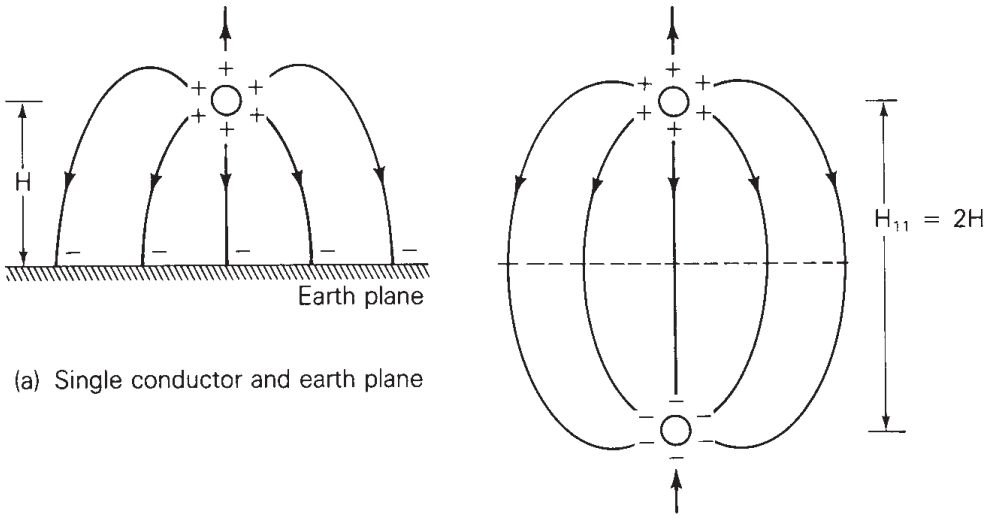

(a) Single conductor and earth plane

(b) Earth plane replaced by image conductor

even though the earth under the line may have irregular terrain and resistivities as shown in Table 4.4.

The effect of the earth plane is accounted for by the *method of images*, described as follows. Consider a single conductor with uniform charge distribution and with height H above a perfectly conducting earth plane, as shown in Figure 4.23(a). When the conductor has a positive charge, an equal quantity of negative charge is induced on the earth. The electric field lines will originate from the positive charges on the conductor and terminate at the negative charges on the earth. Also, the electric field lines are perpendicular to the surfaces of the conductor and earth.

Now replace the earth by the image conductor shown in Figure 4.23(b), which has the same radius as the original conductor, lies directly below the original conductor with conductor separation $H_{11} = 2H$, and has an equal quantity of negative charge. The electric field above the dashed line representing the location of the removed earth plane in Figure 4.23(b) is identical to the electric field above the earth plane in Figure 4.23(a). Therefore, the voltage between any two points above the earth is the same in both figures.

EXAMPLE 4.8 Effect of earth on capacitance: single-phase line

If the single-phase line in Example 4.6 has flat horizontal spacing with 5.49 m average line height, determine the effect of the earth on capacitance. Assume a perfectly conducting earth plane.

SOLUTION The earth plane is replaced by a separate image conductor for each overhead conductor, and the conductors are charged as shown in Figure 4.24. From (4.8.6), the voltage between conductors x and y is

FIGURE 4.24

Single-phase line for Example 4.8

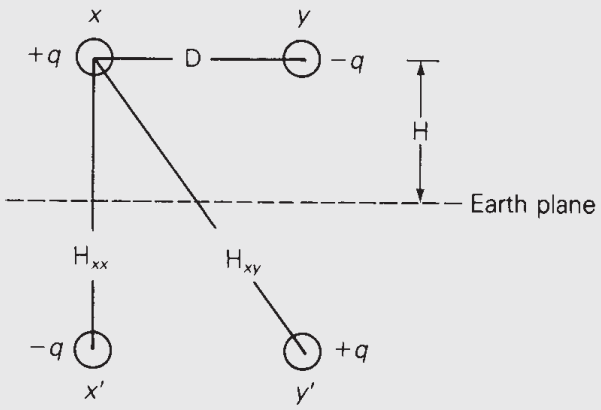

$$V_{xy} = \frac{q}{2\pi\varepsilon}\left[\ln\frac{D_{yx}}{D_{xx}} - \ln\frac{D_{yy}}{D_{xy}} - \ln\frac{H_{yx}}{H_{xx}} + \ln\frac{H_{yy}}{H_{xy}}\right]$$
$$= \frac{q}{2\pi\varepsilon}\left[\ln\frac{D_{yx}D_{xy}}{D_{xx}D_{yy}} - \ln\frac{H_{yx}H_{xy}}{H_{xx}H_{yy}}\right]$$
$$= \frac{q}{\pi\varepsilon}\left[\ln\frac{D}{r} - \ln\frac{H_{xy}}{H_{xx}}\right]$$

The line-to-line capacitance is

$$C_{xy} = \frac{q}{V_{xy}} = \frac{\pi\varepsilon}{\ln\dfrac{D}{r} - \ln\dfrac{H_{xy}}{H_{xx}}} \quad \text{F/m}$$

Using D = 1.5 m, r = 0.7 cm, $H_{xx} = 2H = 10.98$, and $H_{xy} = \sqrt{(10.98)^2 + (1.5)^2} = 11.08$ m,

$$C_{xy} = \frac{\pi(8.854 \times 10^{-12})}{\ln\dfrac{150}{0.7} - \ln\dfrac{11.08}{11}} = 5.189 \times 10^{-12} \quad \text{F/m}$$

compared with 5.182×10^{-12} F/m in Example 4.6. The effect of the earth plane is to slightly increase the capacitance. Note that as the line height H increases, the ratio H_{xy}/H_{xx} approaches 1, $\ln(H_{xy}/H_{xx}) \to 0$, and the effect of the earth becomes negligible. ■

For the three-phase line with N neutral conductors shown in Figure 4.25, the perfectly conducting earth plane is replaced by a separate image conductor for each overhead conductor. The overhead conductors a, b, c, $n1$, $n2, \ldots, nN$ carry charges $q_a, q_b, q_c, q_{n1}, \ldots, q_{nN}$, and the image conductors a', b', c', $n1', \ldots, nN'$ carry charges $-q_a$, $-q_b$, $-q_c$, $-q_{n1}, \ldots, -q_{nN}$. Applying (4.8.6) to determine the voltage $V_{kk'}$ between any conductor k and its image conductor k',

FIGURE 4.25

Three-phase line with neutral conductors and with earth plane replaced by image conductors

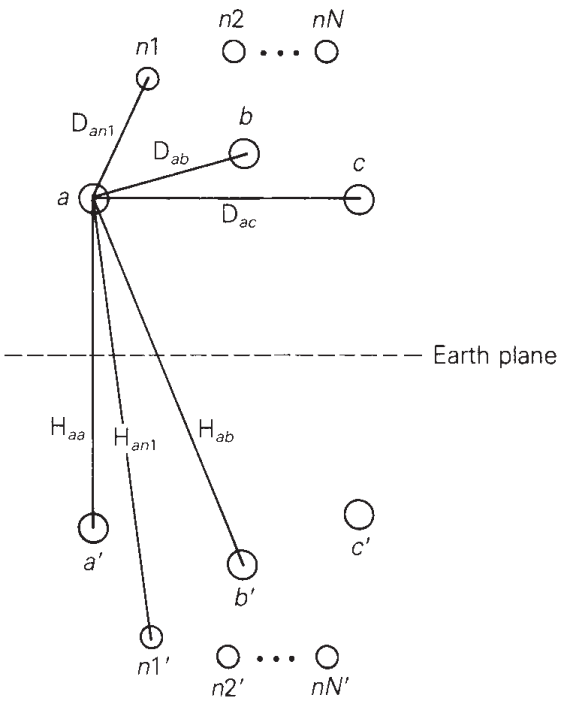

$$V_{kk'} = \frac{1}{2\pi\varepsilon}\left[\sum_{m=a}^{nN} q_m \ln\frac{\mathrm{H}_{km}}{\mathrm{D}_{km}} - \sum_{m=a}^{nN} q_m \ln\frac{\mathrm{D}_{km}}{\mathrm{H}_{km}}\right]$$

$$= \frac{2}{2\pi\varepsilon}\sum_{m=a}^{nN} q_m \ln\frac{\mathrm{H}_{km}}{\mathrm{D}_{km}} \tag{4.11.1}$$

where $\mathrm{D}_{kk} = r_k$ and D_{km} is the distance between overhead conductors k and m. H_{km} is the distance between overhead conductor k and image conductor m. By symmetry, the voltage V_{kn} between conductor k and the earth is one-half of $V_{kk'}$.

$$V_{kn} = \frac{1}{2}V_{kk'} = \frac{1}{2\pi\varepsilon}\sum_{m=a}^{nN} q_m \ln\frac{\mathrm{H}_{km}}{\mathrm{D}_{km}} \tag{4.11.2}$$

where

$$k = a, b, c, n1, n2, \ldots, nN$$

$$m = a, b, c, n1, n2, \ldots, nN$$

Since all the neutral conductors are grounded to the earth,

$$V_{kn} = 0 \qquad \text{for } k = n1, n2, \ldots, nN \tag{4.11.3}$$

In matrix format, (4.11.2) and (4.11.3) are

$$\begin{bmatrix} V_{an} \\ V_{bn} \\ V_{cn} \\ \hline 0 \\ \vdots \\ 0 \end{bmatrix} = \left[\begin{array}{ccc|ccc} \overbrace{\mathrm{P}_{aa} & \mathrm{P}_{ab} & \mathrm{P}_{ac}}^{\mathbf{P}_A} & \overbrace{\mathrm{P}_{an1} & \cdots & \mathrm{P}_{anN}}^{\mathbf{P}_B} \\ \mathrm{P}_{ba} & \mathrm{P}_{bb} & \mathrm{P}_{bc} & \mathrm{P}_{bn1} & \cdots & \mathrm{P}_{bnN} \\ \mathrm{P}_{ca} & \mathrm{P}_{cb} & \mathrm{P}_{cc} & \mathrm{P}_{cn1} & \cdots & \mathrm{P}_{cnN} \\ \hline \mathrm{P}_{n1a} & \mathrm{P}_{n1b} & \mathrm{P}_{n1c} & \mathrm{P}_{n1n1} & \cdots & \mathrm{P}_{n1nN} \\ \vdots & & & & & \\ \underbrace{\mathrm{P}_{nNa} & \mathrm{P}_{nNb} & \mathrm{P}_{nNc}}_{\mathbf{P}_C} & \underbrace{\mathrm{P}_{nNn1} & \cdots & \mathrm{P}_{nNnN}}_{\mathbf{P}_D} \end{array}\right] \begin{bmatrix} q_a \\ q_b \\ q_c \\ \hline q_{n1} \\ \vdots \\ q_{nN} \end{bmatrix} \tag{4.11.4}$$

The elements of the $(3+N)\times(3+N)$ matrix $\mathbf{P}$ are

$$\mathrm{P}_{km} = \frac{1}{2\pi\varepsilon}\ln\frac{\mathrm{H}_{km}}{\mathrm{D}_{km}} \quad \mathrm{m/F} \tag{4.11.5}$$

where

$$k = a, b, c, n1, \ldots, nN$$

$$m = a, b, c, n1, \ldots, nN$$

Equation (4.11.4) is now partitioned as shown above to obtain

$$\left[\begin{array}{c} \boldsymbol{V}_{\mathrm{P}} \\ \hline \mathbf{0} \end{array}\right] = \left[\begin{array}{c|c} \mathbf{P}_A & \mathbf{P}_B \\ \hline \mathbf{P}_C & \mathbf{P}_D \end{array}\right] \left[\begin{array}{c} \boldsymbol{q}_{\mathrm{P}} \\ \hline \boldsymbol{q}_n \end{array}\right] \tag{4.11.6}$$

$\boldsymbol{V}_{\mathrm{P}}$ is the three-dimensional vector of phase-to-neutral voltages. $\boldsymbol{q}_{\mathrm{P}}$ is the three-dimensional vector of phase-conductor charges and $\boldsymbol{q}_n$ is the N vector of neutral conductor charges. The $(3+N)\times(3+N)\mathbf{P}$ matrix is partitioned as shown in (4.11.4) to obtain:

$\mathbf{P}_A$ with dimension 3×3

$\mathbf{P}_B$ with dimension $3\times N$

$\mathbf{P}_C$ with dimension $N\times 3$

$\mathbf{P}_D$ with dimension $N\times N$

Equation (4.11.6) is rewritten as two separate equations:

$$\boldsymbol{V}_{\mathrm{P}} = \mathbf{P}_A\boldsymbol{q}_{\mathrm{P}} + \mathbf{P}_B\boldsymbol{q}_n \tag{4.11.7}$$

$$\mathbf{0} = \mathbf{P}_C\boldsymbol{q}_{\mathrm{P}} + \mathbf{P}_D\boldsymbol{q}_n \tag{4.11.8}$$

Then (4.11.8) is solved for $\boldsymbol{q}_n$, which is used in (4.11.7) to obtain

$$\boldsymbol{V}_{\mathrm{P}} = (\mathbf{P}_A - \mathbf{P}_B\mathbf{P}_D^{-1}\mathbf{P}_C)\boldsymbol{q}_{\mathrm{P}} \tag{4.11.9}$$

or

$$\boldsymbol{q}_{\mathrm{P}} = \mathbf{C}_{\mathrm{P}}\boldsymbol{V}_{\mathrm{P}} \tag{4.11.10}$$

where

$$\mathbf{C}_{\mathrm{P}} = (\mathbf{P}_A - \mathbf{P}_B\mathbf{P}_D^{-1}\mathbf{P}_C)^{-1} \quad \mathrm{F/m} \tag{4.11.11}$$

Equation (4.11.10), the desired result, relates the phase-conductor charges to the phase-to-neutral voltages. $\mathbf{C}_{\mathrm{P}}$ is the 3×3 matrix of phase capacitances whose elements are denoted

$$\mathbf{C}_{\mathrm{P}} = \begin{bmatrix} \mathrm{C}_{aa} & \mathrm{C}_{ab} & \mathrm{C}_{ac} \\ \mathrm{C}_{ab} & \mathrm{C}_{bb} & \mathrm{C}_{bc} \\ \mathrm{C}_{ac} & \mathrm{C}_{bc} & \mathrm{C}_{cc} \end{bmatrix} \quad \mathrm{F/m} \tag{4.11.12}$$

It can be shown that $\mathbf{C}_{\mathrm{P}}$ is a symmetric matrix whose diagonal terms C_{aa}, C_{bb}, C_{cc} are positive, and whose off-diagonal terms C_{ab}, C_{bc}, C_{ac} are negative. This indicates that when a positive line-to-neutral voltage is applied to one phase, a positive charge is induced on that phase and negative charges are induced on the other phases, which is physically correct.

If the line is completely transposed, the diagonal and off-diagonal elements of $\mathbf{C}_{\mathrm{P}}$ are averaged to obtain

$$\hat{\mathbf{C}}_{\mathrm{P}} = \begin{bmatrix} \hat{\mathrm{C}}_{aa} & \hat{\mathrm{C}}_{ab} & \hat{\mathrm{C}}_{ab} \\ \hat{\mathrm{C}}_{ab} & \hat{\mathrm{C}}_{aa} & \hat{\mathrm{C}}_{ab} \\ \hat{\mathrm{C}}_{ab} & \hat{\mathrm{C}}_{ab} & \hat{\mathrm{C}}_{aa} \end{bmatrix} \quad \mathrm{F/m} \tag{4.11.13}$$

where

$$\hat{\mathrm{C}}_{aa} = \tfrac{1}{3}(\mathrm{C}_{aa} + \mathrm{C}_{bb} + \mathrm{C}_{cc}) \quad \mathrm{F/m} \tag{4.11.14}$$

$$\hat{\mathrm{C}}_{ab} = \tfrac{1}{3}(\mathrm{C}_{ab} + \mathrm{C}_{bc} + \mathrm{C}_{ac}) \quad \mathrm{F/m} \tag{4.11.15}$$

$\hat{\mathrm{C}}_{\mathrm{P}}$ is a symmetrical capacitance matrix.

The shunt phase admittance matrix is given by

$$\boldsymbol{Y}_{\mathrm{P}} = j\omega\mathbf{C}_{\mathrm{P}} = j(2\pi f)\mathbf{C}_{\mathrm{P}} \quad \mathrm{S/m} \tag{4.11.16}$$

or, for a completely transposed line,

$$\hat{\boldsymbol{Y}}_{\mathrm{P}} = j\omega\hat{\mathbf{C}}_{\mathrm{P}} = j(2\pi f)\hat{\mathbf{C}}_{\mathrm{P}} \quad \mathrm{S/m} \tag{4.11.17}$$

4.12 ELECTRIC FIELD STRENGTH AT CONDUCTOR SURFACES AND AT GROUND LEVEL

When the electric field strength at a conductor surface exceeds the breakdown strength of air, current discharges occur. This phenomenon, called corona, causes additional line losses (corona loss), communications interference, and audible noise. Although breakdown strength depends on many factors, a rough value is 30 kV/cm in a uniform electric field for dry air at

atmospheric pressure. The presence of water droplets or rain can lower this value significantly. To control corona, transmission lines are usually designed to maintain calculated values of conductor surface electric field strength below 20 kV_{rms}/cm.

When line capacitances are determined and conductor voltages are known, the conductor charges can be calculated from (4.9.3) for a single-phase line or from (4.11.10) for a three-phase line. Then the electric field strength at the surface of one phase conductor, neglecting the electric fields due to charges on other phase conductors and neutral wires, is, from (4.8.2),

$$E_r = \frac{q}{2\pi\varepsilon r} \quad \text{V/m} \tag{4.12.1}$$

where r is the conductor outside radius.

For bundled conductors with N_b conductors per bundle and with charge q C/m per phase, the charge per conductor is q/N_b and

$$E_{\text{rave}} = \frac{q/N_b}{2\pi\varepsilon r} \quad \text{V/m} \tag{4.12.2}$$

Equation (4.12.2) represents an average value for an individual conductor in a bundle. The maximum electric field strength at the surface of one conductor due to all charges in a bundle, obtained by the vector addition of electric fields (as shown in Figure 4.26), is as follows:

Two-conductor bundle ($N_b = 2$):

$$E_{r\max} = \frac{q/2}{2\pi\varepsilon r} + \frac{q/2}{2\pi\varepsilon d} = \frac{q/2}{2\pi\varepsilon r}\left(1 + \frac{r}{d}\right)$$

$$= \mathrm{E}_{\text{rave}}\left(1 + \frac{r}{d}\right) \tag{4.12.3}$$

Three-conductor bundle ($N_b = 3$):

$$E_{r\max} = \frac{q/3}{2\pi\varepsilon}\left(\frac{1}{r} + \frac{2\cos 30^\circ}{d}\right) = E_{\text{rave}}\left(1 + \frac{r\sqrt{3}}{d}\right) \tag{4.12.4}$$

Four-conductor bundle ($N_b = 4$):

$$E_{r\max} = \frac{q/4}{2\pi\varepsilon}\left(\frac{1}{r} + \frac{1}{d\sqrt{2}} + \frac{2\cos 45^\circ}{d}\right) = E_{\text{rave}}\left[1 + \frac{r}{d}(2.1213)\right] \tag{4.12.5}$$

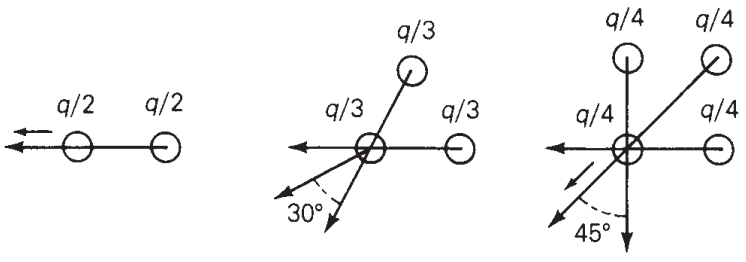

FIGURE 4.26

Vector addition of electric fields at the surface of one conductor in a bundle

TABLE 4.5

Examples of maximum ground-level electric field strength versus transmission-line voltage [1] (© Copyright 1987. Electric Power Research Institute (EPRI), Publication Number EL-2500. *Transmission Line Reference Book, 345-kV and Above, Second Edition, Revised.* Reprinted with permission)

Line Voltage (kV_{rms})	Maximum Ground-Level Electric Field Strength (kV_{rms}/m)
23 (1ϕ)	0.01–0.025
23 (3ϕ)	0.01–0.05
115	0.1–0.2
345	2.3–5.0
345 (double circuit)	5.6
500	8.0
765	10.0

Although the electric field strength at ground level is much less than at conductor surfaces where corona occurs, there are still capacitive coupling effects. Charges are induced on ungrounded equipment such as vehicles with rubber tires located near a line. If a person contacts the vehicle and ground, a discharge current will flow to ground. Transmission-line heights are designed to maintain discharge currents below prescribed levels for any equipment that may be on the right-of-way. Table 4.5 shows examples of maximum ground-level electric field strength.

As shown in Figure 4.27, the ground-level electric field strength due to charged conductor k and its image conductor is perpendicular to the earth plane, with value

$$E_k(w) = \left(\frac{q_k}{2\pi\varepsilon}\right)\frac{2\cos\theta}{\sqrt{y_k^2 + (w - x_k)^2}}$$

$$= \left(\frac{q_k}{2\pi\varepsilon}\right)\frac{2y_k}{y_k^2 + (w - x_k)^2} \quad \text{V/m} \tag{4.12.6}$$

where (x_k, y_k) are the horizontal and vertical coordinates of conductor k with respect to reference point R, w is the horizontal coordinate of the ground-level point where the electric field strength is to be determined, and q_k is the charge on conductor k. The total ground-level electric field is the phasor sum of terms $E_k(w)$ for all overhead conductors. A lateral profile of ground-level

FIGURE 4.27

Ground-level electric field strength due to an overhead conductor and its image

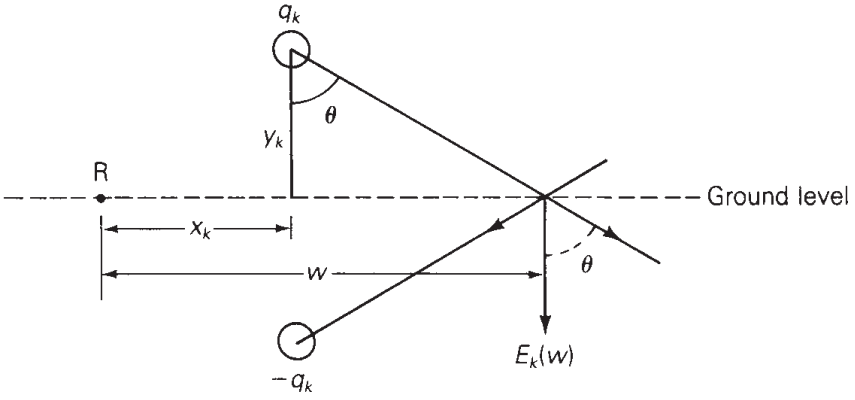

electric field strength is obtained by varying w from the center of the line to the edge of the right-of-way.

EXAMPLE 4.9 Conductor surface and ground-level electric field strengths: single-phase line

For the single-phase line of Example 4.8, calculate the conductor surface electric field strength in kV_{rms}/cm. Also calculate the ground-level electric field in kV_{rms}/m directly under conductor x. The line voltage is 20 kV.

SOLUTION From Example 4.8, $C_{xy} = 5.189 \times 10^{-12}$ F/m. Using (4.9.3) with $V_{xy} = 20\underline{/0^\circ}$ kV,

$$q_x = -q_y = (5.189 \times 10^{-12})(20 \times 10^3 \underline{/0^\circ}) = 1.038 \times 10^{-7} \underline{/0^\circ} \quad \text{C/m}$$

From (4.12.1), the conductor surface electric field strength is, with $r = 0.023$ ft $= 0.00701$ m,

$$E_r = \frac{1.036 \times 10^{-7}}{(2\pi)(8.854 \times 10^{-12})(0.00701)} \frac{\text{V}}{\text{m}} \times \frac{\text{kV}}{1000\ \text{V}} \times \frac{\text{m}}{100\ \text{cm}}$$

$$= 2.66 \quad kV_{rms}/cm$$

Selecting the center of the line as the reference point R, the coordinates (x_x, y_x) for conductor x are (−0.75 m, 5.49 m) and (+0.75 m, 5.49 m) for conductor y. The ground-level electric field directly under conductor x, where $w = -0.75$ m, is, from (4.12.6),

$$E(-0.762) = E_x(-0.75) + E_y(-0.75)$$

$$= \frac{1.036 \times 10^{-7}}{(2\pi)(8.85 \times 10^{-12})} \left[\frac{(2)(5.49)}{(5.49)^2} - \frac{(2)(5.49)}{(5.49)^2 + (0.75+0.75)^2} \right]$$

$$= 1.862 \times 10^3 (0.364 - 0.338) = 48.5 \underline{/0^\circ}\ \text{V/m} = 0.0485\ \text{kV/m}$$

For this 20-kV line, the electric field strengths at the conductor surface and at ground level are low enough to be of relatively small concern. For EHV lines, electric field strengths and the possibility of corona and shock hazard are of more concern. ■

4.13 PARALLEL CIRCUIT THREE-PHASE LINES

If two parallel three-phase circuits are close together, either on the same tower as in Figure 4.3, or on the same right-of-way, there are mutual inductive and capacitive couplings between the two circuits. When calculating the equivalent series impedance and shunt admittance matrices, these couplings should not be neglected unless the spacing between the circuits is large.

FIGURE 4.28

Single-line diagram of a double-circuit line

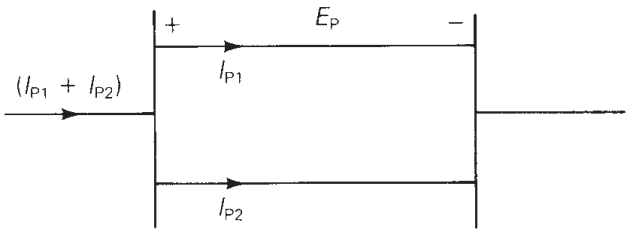

Consider the double-circuit line shown in Figure 4.28. For simplicity, assume that the lines are not transposed. Since both are connected in parallel, they have the same series-voltage drop for each phase. Following the same procedure as in Section 4.7, we can write $2(6+N)$ equations similar to (4.7.6)–(4.7.9): six equations for the overhead phase conductors, N equations for the overhead neutral conductors, and $(6+N)$ equations for the earth return conductors. After lumping the neutral voltage drop into the voltage drops across the phase conductors, and eliminating the neutral and earth return currents, we obtain

$$\begin{bmatrix} \boldsymbol{E}_{\mathrm{P}} \\ \boldsymbol{E}_{\mathrm{P}} \end{bmatrix} = \boldsymbol{Z}_{\mathrm{P}} \begin{bmatrix} \boldsymbol{I}_{\mathrm{P1}} \\ \boldsymbol{I}_{\mathrm{P2}} \end{bmatrix} \tag{4.13.1}$$

where $\boldsymbol{E}_{\mathrm{P}}$ is the vector of phase-conductor voltage drops (including the neutral voltage drop), and $\boldsymbol{I}_{\mathrm{P1}}$ and $\boldsymbol{I}_{\mathrm{P2}}$ are the vectors of phase currents for lines 1 and 2. $\boldsymbol{Z}_{\mathrm{P}}$ is a 6×6 impedance matrix. Solving (4.13.1)

$$\begin{bmatrix} \boldsymbol{I}_{\mathrm{P1}} \\ \boldsymbol{I}_{\mathrm{P2}} \end{bmatrix} = \boldsymbol{Z}_{\mathrm{P}}^{-1} \begin{bmatrix} \boldsymbol{E}_{\mathrm{P}} \\ \boldsymbol{E}_{\mathrm{P}} \end{bmatrix} = \left[\begin{array}{c|c} \boldsymbol{Y}_A & \boldsymbol{Y}_B \\ \hline \boldsymbol{Y}_C & \boldsymbol{Y}_D \end{array}\right] \begin{bmatrix} \boldsymbol{E}_{\mathrm{P}} \\ \boldsymbol{E}_{\mathrm{P}} \end{bmatrix} = \begin{bmatrix} (\boldsymbol{Y}_A + \boldsymbol{Y}_B) \\ (\boldsymbol{Y}_C + \boldsymbol{Y}_D) \end{bmatrix} \boldsymbol{E}_{\mathrm{P}} \tag{4.13.2}$$

where $\boldsymbol{Y}_A$, $\boldsymbol{Y}_B$, $\boldsymbol{Y}_C$, and $\boldsymbol{Y}_D$ are obtained by partitioning $\boldsymbol{Z}_{\mathrm{P}}^{-1}$ into four 3×3 matrices. Adding $\boldsymbol{I}_{\mathrm{P1}}$ and $\boldsymbol{I}_{\mathrm{P2}}$,

$$(\boldsymbol{I}_{\mathrm{P1}} + \boldsymbol{I}_{\mathrm{P2}}) = (\boldsymbol{Y}_A + \boldsymbol{Y}_B + \boldsymbol{Y}_C + \boldsymbol{Y}_D)\boldsymbol{E}_{\mathrm{P}} \tag{4.13.3}$$

and solving for $\boldsymbol{E}_{\mathrm{P}}$,

$$\boldsymbol{E}_{\mathrm{P}} = \boldsymbol{Z}_{\mathrm{Peq}}(\boldsymbol{I}_{\mathrm{P1}} + \boldsymbol{I}_{\mathrm{P2}}) \tag{4.13.4}$$

where

$$\boldsymbol{Z}_{\mathrm{Peq}} = (\boldsymbol{Y}_A + \boldsymbol{Y}_B + \boldsymbol{Y}_C + \boldsymbol{Y}_D)^{-1} \tag{4.13.5}$$

$\boldsymbol{Z}_{\mathrm{Peq}}$ is the equivalent 3×3 series phase impedance matrix of the double-circuit line. Note that in (4.13.5) the matrices $\boldsymbol{Y}_B$ and $\boldsymbol{Y}_C$ account for the inductive coupling between the two circuits.

An analogous procedure can be used to obtain the shunt admittance matrix. Following the ideas of Section 4.11, we can write $(6+N)$ equations similar to (4.11.4). After eliminating the neutral wire charges, we obtain

$$\begin{bmatrix} \boldsymbol{q}_{\mathrm{P1}} \\ \boldsymbol{q}_{\mathrm{P2}} \end{bmatrix} = \mathbf{C}_{\mathrm{P}} \begin{bmatrix} \boldsymbol{V}_{\mathrm{P}} \\ \boldsymbol{V}_{\mathrm{P}} \end{bmatrix} = \left[\begin{array}{c|c} \mathbf{C}_A & \mathbf{C}_B \\ \hline \mathbf{C}_C & \mathbf{C}_D \end{array}\right] \begin{bmatrix} \boldsymbol{V}_{\mathrm{P}} \\ \boldsymbol{V}_{\mathrm{P}} \end{bmatrix} = \begin{bmatrix} (\mathbf{C}_A + \mathbf{C}_B) \\ (\mathbf{C}_C + \mathbf{C}_D) \end{bmatrix} \boldsymbol{V}_{\mathrm{P}} \tag{4.13.6}$$

where $\boldsymbol{V}_{\mathrm{P}}$ is the vector of phase-to-neutral voltages, and $\boldsymbol{q}_{\mathrm{P1}}$ and $\boldsymbol{q}_{\mathrm{P2}}$ are the vectors of phase-conductor charges for lines 1 and 2. $\mathbf{C}_{\mathrm{P}}$ is a 6×6 capacitance matrix that is partitioned into four 3×3 matrices $\mathbf{C}_A$, $\mathbf{C}_B$, $\mathbf{C}_C$, and $\mathbf{C}_D$. Adding $\boldsymbol{q}_{\mathrm{P1}}$ and $\boldsymbol{q}_{\mathrm{P2}}$

$$(\boldsymbol{q}_{\mathrm{P1}} + \boldsymbol{q}_{\mathrm{P2}}) = \mathbf{C}_{\mathrm{Peq}} \boldsymbol{V}_{\mathrm{P}} \tag{4.13.7}$$

where

$$\mathbf{C}_{\mathrm{Peq}} = (\mathbf{C}_A + \mathbf{C}_B + \mathbf{C}_C + \mathbf{C}_D) \tag{4.13.8}$$

Also,

$$\boldsymbol{Y}_{\mathrm{Peq}} = j\omega \mathbf{C}_{\mathrm{Peq}} \tag{4.13.9}$$

$\boldsymbol{Y}_{\mathrm{Peq}}$ is the equivalent 3×3 shunt admittance matrix of the double-circuit line. The matrices $\mathbf{C}_B$ and $\mathbf{C}_C$ in (4.13.8) account for the capacitive coupling between the two circuits.

These ideas can be extended in a straightforward fashion to more than two parallel circuits.

MULTIPLE CHOICE QUESTIONS

SECTION 4.1

4.1 ACSR stands for
(a) Aluminum-clad steel conductor
(b) Aluminum conductor steel supported
(c) Aluminum conductor steel reinforced

4.2 Overhead transmission-line conductors arc barc with no insulating cover.
(a) True (b) False

4.3 Alumoweld is an aluminum-clad steel conductor.
(a) True (b) False

4.4 EHV lines often have more than one conductor per phase; these conductors are called a _____. Fill in the Blank.

4.5 Shield wires located above the phase conductors protect the phase conductors against lightning.
(a) True (b) False

4.6 Conductor spacings, types, and sizes do have an impact on the series impedance and shunt admittance.
(a) True (b) False

SECTION 4.2

4.7 A circle with diameter D in = 1000 D mil = d mil has an area of _____ cmil. Fill in the Blank.

4.8 AC resistance is higher than dc resistance.
(a) True (b) False

4.9 Match the following for the current distribution throughout the conductor cross section:
(i) For dc (a) uniform
(ii) For ac (b) nonuniform

SECTION 4.3

4.10 Transmission line conductance is usually neglected in power system studies.
(a) True (b) False

SECTION 4.4

4.11 The internal inductance L_{int} per unit-length of a solid cylindrical conductor is a constant, given by $\frac{1}{2} \times 10^{-7}$H/m in SI system of units.
(a) True (b) False

4.12 The total inductance L_P of a solid cylindrical conductor (of radius r) due to both internal and external flux linkages out of distance D is given by (in H/m)
(a) 2×10^{-7} (b) $2 \times 10^{-7} \ln(\frac{D}{r})$
(c) $2 \times 10^{-7} \ln(\frac{D}{r'})$
where $r' = e^{-\frac{1}{4}} r = 0.778\, r$

SECTION 4.5

4.13 For a single-phase, two-wire line consisting of two solid cylindrical conductors of same radius, r, the total circuit inductance, also called loop inductance, is given by (in H/m)
(a) $2 \times 10^{-7} \ln(\frac{D}{r'})$ (b) $4 \times 10^{-7} \ln(\frac{D}{r'})$
where $r' = e^{-\frac{1}{4}} r = 0.778r$

4.14 For a three-phase, three-wire line consisting of three solid cylindrical conductors, each with radius r, and with equal phase spacing D between any two conductors, the inductance in H/m per phase is given by
(a) $2 \times 10^{-7} \ln(\frac{D}{r'})$ (b) $4 \times 10^{-7} \ln(\frac{D}{r'})$
(c) $6 \times 10^{-7} \ln(\frac{D}{r'})$
where $r' = e^{-\frac{1}{4}} r = 0.778\, r$

4.15 For a balanced three-phase, positive-sequence currents I_a, I_b, I_c, does the equation $I_a + I_b + I_c = 0$ hold good?
(a) Yes (b) No

SECTION 4.6

4.16 A stranded conductor is an example of a composite conductor.
(a) True (b) False

4.17 $\Sigma \ln A_k = \ln \Pi A_k$
(a) True (b) False

4.18 Is Geometric Mean Distance (GMD) the same as Geometric Mean Radius (GMR)?
(a) Yes (b) No

4.19 Expand $6\sqrt{\Pi_{k=1}^{3} \Pi_{m=1'}^{2'} D_{km}}$

4.20 If the distance between conductors are large compared to the distances between subconductors of each conductor, then the GMD between conductors is approximately equal to the distance between conductor centers.
(a) True (b) False

4.22 For a single-phase, two-conductor line with composite conductors x and y, express the inductance of conductor x in terms of GMD and its GMR.

4.23 In a three-phase line, in order to avoid unequal phase inductances due to unbalanced flux linkages, what technique is used?

4.24 For a completely transposed three-phase line identical conductors, each with GMR denoted D_S, with conductor distance D_{12}, D_{23}, and D_{31} give expressions for GMD between phases, and the average per-phase inductance.

4.25 For EHV lines, a common practice of conductor bundling is used. Why?

4.26 Does bundling reduce the series reactance of the line?
(a) Yes (b) No

4.27 Does $r' = e^{-\frac{1}{4}} r = 0.788\, r$, that comes in calculation of inductance, play a role in capacitance computations?
(a) Yes (b) No

4.28 In terms of line-to-line capacitance, the line-to-neutral capacitance of a single-phase transmission line is
(a) same (b) twice (c) one-half

4.29 For either single-phase two-wire line or balanced three-phase three-wire line, with equal phase spacing D and with conductor radius r, the capacitance (line-to-neutral) in F/m is given by C_{an} = _____. Fill in the Blank.

4.30 In deriving expressions for capacitance for a balanced three-phase, three-wire line with equal phase spacing, the following relationships may have been used.
(i) Sum of positive-sequence charges, $q_a + q_b + q_c = 0$
(ii) The sum of the two line-to-line voltages $V_{ab} + V_{ac}$, is equal to three-times the line-to-neutral voltage V_{an}.

Which of the following is true?
(a) both (b) only (i) (c) only (ii) (d) None

SECTION 4.10

4.31 When calculating line capacitance, it is normal practice to replace a stranded conductor by a perfectly conducting solid cylindrical conductor whose radius equals the outside radius of the stranded conductor.
(a) True (b) False

4.32 For bundled-conductor configurations, the expressions for calculating D_{SL} in inductance calculations and D_{SC} in capacitance calculations are analogous, except that the conductor outside radius r replaces the conductor GMR, D_S.
(a) True (b) False

4.33 The current supplied to the transmission-line capacitance is called _____. Fill in the Blank.

4.34 For a completely transposed three-phase line that has balanced positive-sequence voltages, the total reactive power supplied by the three-phase line, in var, is given by Q_{C3} = _____, in terms of frequency ω, line-to-neutral capacitance C_{an}, and line-to-line voltage V_{LL}.

SECTION 4.11

4.35 Considering lines with neutral conductors and earth return, the effect of earth plane is accounted for by the method of _____ with a perfectly conducting earth plane.

4.36 The affect of the earth plane is to slightly increase the capacitance, an as the line height increases, the effect of earth becomes negligible.
(a) True (b) False

SECTION 4.12

4.37 When the electric field strength at a conductor surface exceeds the breakdown strength of air, current, discharges occur. This phenomenon is called _____. Fill in the Blank.

4.38 To control corona, transmission lines are usually designed to maintain the calculated conductor surface electric field strength below _____ kV_{rms}/cm. Fill in the Blank.

4.39 Along with limiting corona and its effects, particularly for EHV lines, the maximum ground level electric field strength needs to be controlled to avoid the shock hazard.
(a) True (b) False

SECTION 4.13

4.40 Considering two parallel three-phase circuits that are close together, when calculating the equivalent series-impedance and shunt-admittance matrices, mutual inductive and capacitive couplings between the two circuits can be neglected.
(a) True (b) False

PROBLEMS

SECTION 4.2

4.1 The *Aluminum Electrical Conductor Handbook* lists a dc resistance of 0.01558 ohm per 1000 ft (or 0.05112 ohm per km) at 20 °C and a 60-Hz resistance of 0.0956 ohm per mile (or 0.0594 ohm per km) at 50 °C for the all-aluminum Marigold conductor, which has 61 strands and whose size is 564 mm^2 or 1113 kcmil. Assuming an increase in resistance of 2% for spiraling, calculate and verify the dc resistance. Then calculate the dc resistance at 50 °C, and determine the percentage increase due to skin effect.

4.2 The temperature dependence of resistance is also quantified by the relation $R_2 = R_1[1 + \alpha(T_2 - T_1)]$ where R_1 and R_2 are the resistances at temperatures T_1 and T_2, respectively, and α is known as the temperature coefficient of resistance. If a copper wire has a resistance of 50 Ω at 20 °C, find the maximum permissible operating temperature of the wire if its resistance is to increase by at most 10%. Take the temperature coefficient at 20 °C to be $\alpha = 0.00382$.

4.3 A transmission-line cable, of length 3 km, consists of 19 strands of identical copper conductors, each 1.5 mm in diameter. Because of the twist of the strands, the actual length of each conductor is increased by 5%. Determine the resistance of the cable, if the resistivity of copper is 1.72 μΩ·cm at 20 °C.

4.4 One thousand circular mils or 1 kcmil is sometimes designated by the abbreviation MCM. Data for commercial bare aluminum electrical conductors lists a 60-Hz resistance of 0.0880 ohm per kilometer at 75 °C for a 793-MCM AAC conductor. (a) Determine the

cross-sectional conducting area of this conductor in square meters. (b) Find the 60-Hz resistance of this conductor in ohms per kilometer at 50 °C.

4.5 A 60-Hz, 765-kV three-phase overhead transmission line has four ACSR 900 kcmil 54/3 conductors per phase. Determine the 60-Hz resistance of this line in ohms per kilometer per phase at 50 °C.

4.6 A three-phase overhead transmission line is designed to deliver 190.5 MVA at 220 kV over a distance of 63 km, such that the total transmission line loss is not to exceed 2.5% of the rated line MVA. Given the resistivity of the conductor material to be 2.84×10^{-8} Ω-m, determine the required conductor diameter and the conductor size in circular mils. Neglect power losses due to insulator leakage currents and corona.

4.7 If the per-phase line loss in a 60-km-long transmission line is not to exceed 60 kW while it is delivering 100 A per phase, compute the required conductor diameter, if the resistivity of the conductor material is 1.72×10^{-8} Ωm.

SECTIONS 4.4 AND 4.5

4.8 A 60-Hz single-phase, two-wire overhead line has solid cylindrical copper conductors with 1.5 cm diameter. The conductors are arranged in a horizontal configuration with 0.5 m spacing. Calculate in mH/km (a) the inductance of each conductor due to internal flux linkages only, (b) the inductance of each conductor due to both internal and external flux linkages, and (c) the total inductance of the line.

4.9 Rework Problem 4.8 if the diameter of each conductor is: (a) increased by 20% to 1.8 cm, (b) decreased by 20% to 1.2 cm, without changing the phase spacing. Compare the results with those of Problem 4.8.

4.10 A 60-Hz three-phase, three-wire overhead line has solid cylindrical conductors arranged in the form of an equilateral triangle with 4 ft conductor spacing. Conductor diameter is 0.5 in. Calculate the positive-sequence inductance in H/m and the positive-sequence inductive reactance in Ω/km.

4.11 Rework Problem 4.10 if the phase spacing is: (a) increased by 20% to 4.8 ft, (b) decreased by 20% to 3.2 ft. Compare the results with those of Problem 4.10.

4.12 Find the inductive reactance per mile of a single-phase overhead transmission line operating at 60 Hz, given the conductors to be *Partridge* and the spacing between centers to be 20 ft.

4.13 A single-phase overhead transmission line consists of two solid aluminum conductors having a radius of 2.5 cm, with a spacing 3.6 m between centers. (a) Determine the total line inductance in mH/m. (b) Given the operating frequency to be 60 Hz, find the total inductive reactance of the line in Ω/km and in Ω/mi. (c) If the spacing is doubled to 7.2 m, how does the reactance change?

4.14 (a) In practice, one deals with the inductive reactance of the line per phase per mile and use the logarithm to the base 10.
Show that Eq. (4.5.9) of the text can be rewritten as

$$x = k \log \frac{D}{r'} \text{ ohms per mile per phase}$$
$$= x_d + x_a$$

where $x_d = k \log \mathrm{D}$ is the inductive reactance spacing factor in ohms per km

$x_a = k \log \dfrac{1}{r'}$ is the inductive reactance at 1-m spacing in ohms per km

$k = 2.893 \times 10^{-6} f = 1.736$ at 60 Hz.

(b) Determine the inductive reactance per km per phase at 60 Hz for a single-phase line with phase separation of 3 m and conductor radius of 2 cm.
If the spacing is doubled, how does the reactance change?

SECTION 4.6

4.15 Find the GMR of a stranded conductor consisting of six outer strands surrounding and touching one central strand, all strands having the same radius r.

4.16 A bundle configuration for UHV lines (above 1000 kV) has identical conductors equally spaced around a circle, as shown in Figure 4.29. N_b is the number of conductors in the bundle, A is the circle radius, and $\mathrm{D_S}$ is the conductor GMR. Using the distance D_{1n} between conductors 1 and n given by $\mathrm{D}_{1n} = 2\mathrm{A}\sin[(n-1)\pi/N_b]$ for $n = 1, 2, \ldots, N_b$, and the following trigonometric identity:

$$[2\sin(\pi/N_b)][2\sin(2\pi/N_b)][2\sin(3\pi/N_b)]\cdots[2\sin\{(N_b-1)\pi/N_b\}] = N_b$$

show that the bundle GMR, denoted $\mathrm{D_{SL}}$, is

$$\mathrm{D_{SL}} = [N_b \mathrm{D_S} \mathrm{A}^{(N_b-1)}]^{(1/N_b)}$$

Also show that the above formula agrees with (4.6.19)–(4.6.21) for EHV lines with $N_b = 2, 3$, and 4.

FIGURE 4.29
Bundle configuration for Problem 4.16

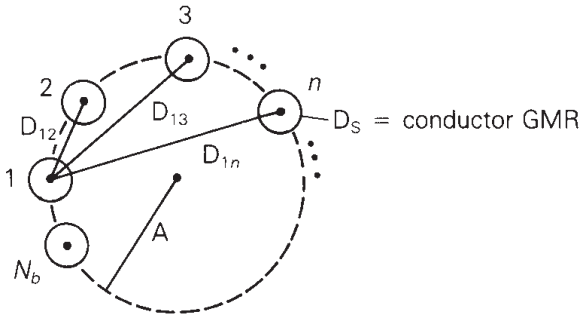

4.17 Determine the GMR of each of the unconventional stranded conductors shown in Figure 4.30. All strands have the same radius r.

FIGURE 4.30
Unconventional stranded conductors for Problem 4.17

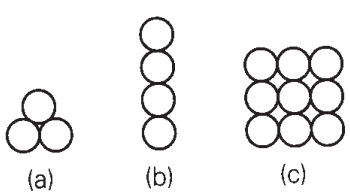

4.18 A 230-kV, 60-Hz, three-phase completely transposed overhead line has one ACSR 954-kcmil (or 564 mm^2) conductor per phase and flat horizontal phase spacing, with 8 m between adjacent conductors. Determine the inductance in H/m and the inductive reactance in Ω/km.

4.19 Rework Problem 4.18 if the phase spacing between adjacent conductors is: (a) increased by 10% to 8.8 m, (b) decreased by 10% to 7.2 m. Compare the results with those of Problem 4.18.

4.20 Calculate the inductive reactance in Ω/km of a bundled 500-kV, 60-Hz, three-phase completely transposed overhead line having three ACSR 1113-kcmil (556.50 mm^2) conductors per bundle, with 0.5 m between conductors in the bundle. The horizontal phase spacings between bundle centers are 10, 10, and 20 m.

4.21 Rework Problem 4.20 if the bundled line has: (a) three ACSR, 1351-kcmil (675.5-mm^2) conductors per phase, (b) three ACSR, 900-kcmil (450-mm^2) conductors per phase, without changing the bundle spacing or the phase spacings between bundle centers. Compare the results with those of Problem 4.20.

4.22 The conductor configuration of a bundled single-phase overhead transmission line is shown in Figure 4.31. Line X has its three conductors situated at the corners of an equilateral triangle with 10-cm spacing. Line Y has its three conductors arranged in a horizontal configuration with 10-cm spacing. All conductors are identical, solid-cylindrical conductors, each with a radius of 2 cm. (a) Find the equivalent representation in terms of the geometric mean radius of each bundle and a separation that is the geometric mean distance.

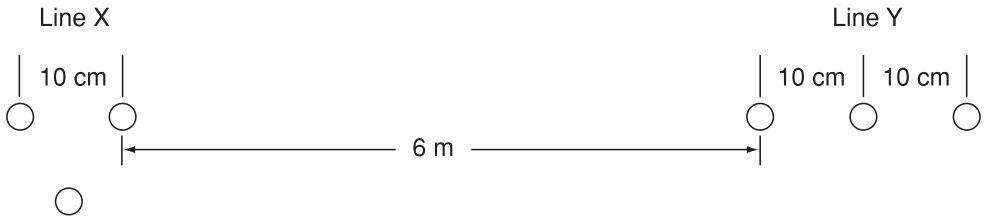

FIGURE 4.31
Problem 4.22

4.23 Figure 4.32 shows the conductor configuration of a completely transposed three-phase overhead transmission line with bundled phase conductors. All conductors have a radius of 0.74 cm with a 30-cm bundle spacing. (a) Determine the inductance per phase in mH/km. (b) Find the inductive line reactance per phase in Ω/km at 60 Hz.

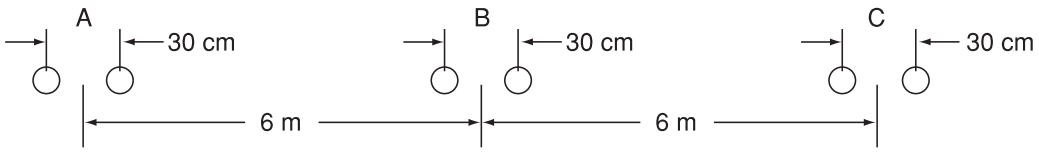

FIGURE 4.32
Problem 4.23

4.24 Consider a three-phase overhead line made up of three phase conductors, Linnet, 336.4 kcmil (170 mm^2), ACSR 26/7. The line configuration is such that the horizontal separation between center of C and that of A is 102 cm, and between that of A and B is also 102 cm in the same line; the vertical separation of A from the line of C–B is 41 cm. If the line is operated at 60 Hz at a conductor temperature of 75 °C, determine the inductive reactance per phase in Ω/km,
(a) By using the formula given in Problem 4.14 (a), and
(b) By using (4.6.18) of the text.

4.25 For the overhead line of configuration shown in Figure 4.33, operating at 60 Hz, and a conductor temperature of 70 °C, determine the resistance per phase, inductive reactance in ohms/km/phase and the current carrying capacity of the overhead line. Each conductor is ACSR Cardinal of Table A.4.

FIGURE 4.33
Line configuration for Problem 4.25

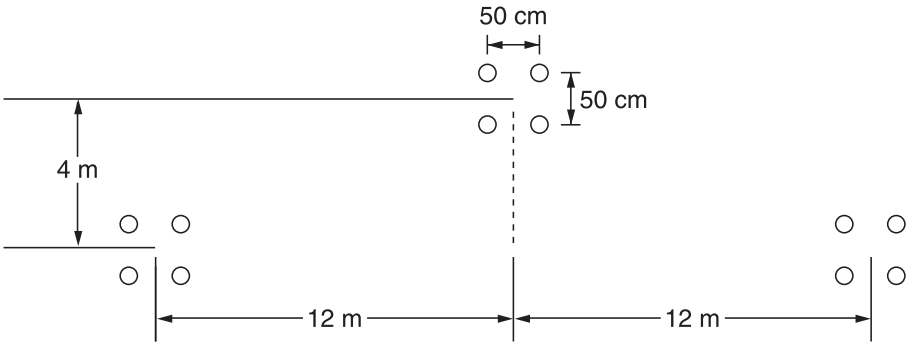

4.26 Consider a symmetrical bundle with N subconductors arranged in a circle of radius A. The inductance of a single-phase symmetrical bundle-conductor line is given by

$$L = 2 \times 10^{-7} \ln \frac{GMD}{GMR} \text{ H/m}$$

where GMR is given by $[Nr'(A)^{N-1}]^{1/N}$

$r' = (e^{-1/4}r)$, r being the subconductor radius, and GMD is approximately the distance D between the bundle centers. Note that A is related to the subconductor spacing S in the bundle circle by $S = 2A \sin(\Pi/N)$
Now consider a 965-kV, single-phase, bundle-conductor line with eight subconductors per phase, with phase spacing D = 17 m, and the subconductor spacing S = 45.72 cm. Each subconductor has a diameter of 4.572 cm. Determine the line inductance in H/m.

4.27 Figure 4.34 shows double-circuit conductors' relative positions in Segment 1 of transposition of a completely transposed three-phase overhead transmission line. The inductance is given by

$$L = 2 \times 10^{-7} \ln \frac{GMD}{GMR} \text{ H/m/phase}$$

where $GMD = (D_{AB_{eq}} D_{BC_{eq}} D_{AC_{eq}})^{1/3}$, with mean distances defined by equivalent spacings

FIGURE 4.34
For Problem 4.27 (Double-circuit conductor configuration)

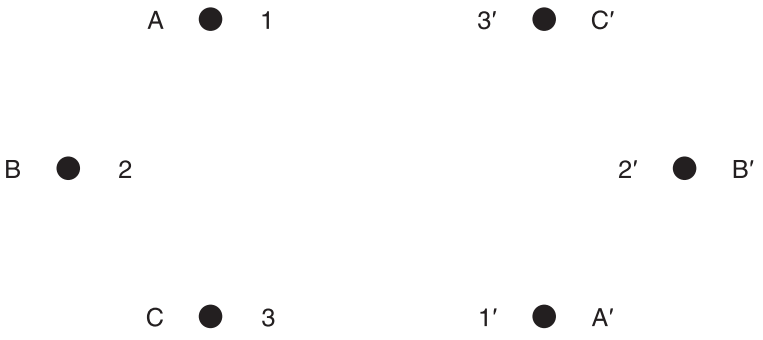

$$D_{AB_{eq}} = (D_{12}D_{1'2'}D_{12'}D_{1'2})^{1/4}$$
$$D_{BC_{eq}} = (D_{23}D_{2'3'}D_{2'3}D_{23'})^{1/4}$$
$$D_{AC_{eq}} = (D_{13}D_{1'3'}D_{13'}D_{1'3})^{1/4}$$

and $GMR = [(GMR)_A(GMR)_B(GMR)_C]^{1/3}$, with phase GMRs defined by

$$(GMR)_A = [r'D_{11'}]^{1/2}; \quad (GMR)_B = [r'D_{22'}]^{1/2}; \quad (GMR)_C = [r'D_{33'}]^{1/2}$$

and r' is the GMR of phase conductors.

Now consider A 345-kV, three-phase, double-circuit line with phase-conductor's GMR of 1.8 cm, and the horizontal conductor configuration shown in Figure 4.35.
(a) Determine the inductance per meter per phase in henries.
(b) Calculate the inductance of just one circuit and then divide by 2 to obtain the inductance of the double circuit.

FIGURE 4.35
For Problem 4.27

Find the relative error involved

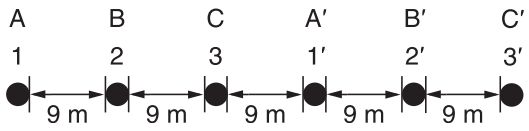

4.28 For the case of double-circuit, bundle-conductor lines, the same method indicated in Problem 4.27 applies with r' replaced by the bundle's GMR in the calculation of the overall GMR.
Now consider a double-circuit configuration shown in Figure 4.36, which belongs to a 500-kV, three-phase line with bundle conductors of three subconductors at 53-cm spacing. The GMR of each subconductor is given to be 1.5 cm.
Determine the inductive reactance of the line in ohms per km per phase. You may use

$$X_L = 0.1786 \log \frac{GMD}{GMR} \ \Omega/\text{km/phase}$$

FIGURE 4.36
Configuration for Problem 4.28

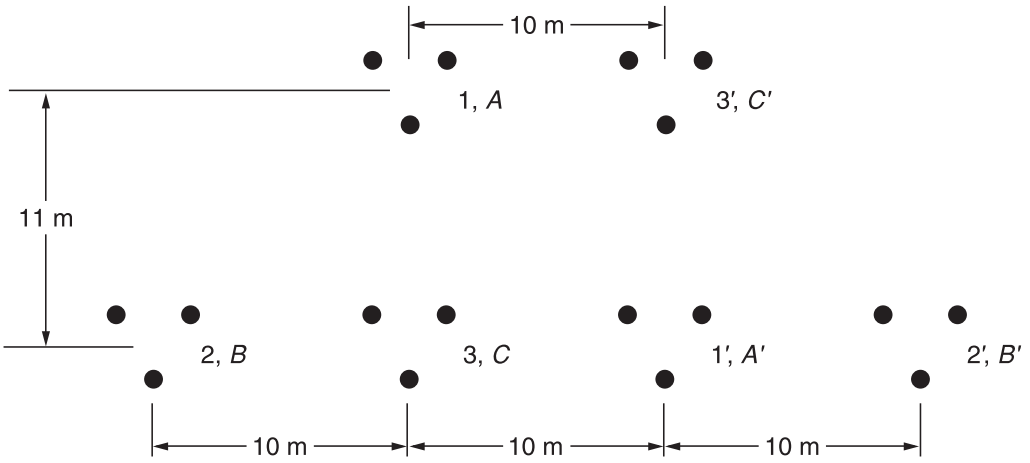

4.29 Reconsider Problem 4.28 with an alternate phase placement given below:

	Physical Position					
	1	2	3	1′	2′	3′
Phase Placement	*A*	*B*	*B′*	*C*	*C′*	*A′*

Calculate the inductive reactance of the line in Ω/km/phase.

4.30 Reconsider Problem 4.28 with still another alternate phase placement shown below.

	Physical Position					
	1	2	3	1′	2′	3′
Phase Placement	*C*	*A*	*B*	*B′*	*A′*	*C′*

Find the inductive reactance of the line in Ω/km/phase.

4.31 Figure 4.37 shows the conductor configuration of a three-phase transmission line and a telephone line supported on the same towers. The power line carries a balanced

FIGURE 4.37
Conductor layout for Problem 4.31

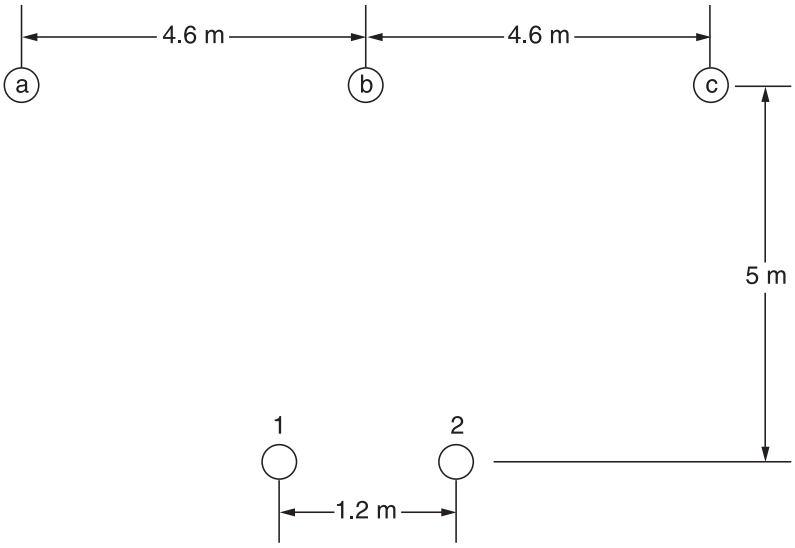

current of 250 A/phase at 60 Hz, while the telephone line is directly located below phase b. Assume balanced three-phase currents in the power line. Calculate the voltage per kilometer induced in the telephone line.

SECTION 4.9

4.32 Calculate the capacitance-to-neutral in F/m and the admittance-to-neutral in S/km for the single-phase line in Problem 4.8. Neglect the effect of the earth plane.

4.33 Rework Problem 4.32 if the diameter of each conductor is: (a) increased by 20% to 1.8 cm, (b) decreased by 20% to 1.2 cm. Compare the results with those of Problem 4.32.

4.34 Calculate the capacitance-to-neutral in F/m and the admittance-to-neutral in S/km for the three-phase line in Problem 4.10. Neglect the effect of the earth plane.

4.35 Rework Problem 4.34 if the phase spacing is: (a) increased by 20% to 146.4 cm, (b) decreased by 20% to 97.6 cm. Compare the results with those of Problem 4.34.

4.36 The line of Problem 4.23 as shown in Figure 4.32 is operating at 60 Hz. Determine (a) the line-to-neutral capacitance in nF/km per phase; (b) the capacitive reactance in Ω-km per phase; and (c) the capacitive reactance in Ω per phase for a line length of 160 km.

4.37 (a) In practice, one deals with the capacitive reactance of the line in ohms-km to neutral. Show that Eq. (4.9.15) of the text can be rewritten as

$$\begin{aligned} X_C &= k' \log \frac{D}{r} \text{ ohms-km to neutral} \\ &= x'_d + x'_a \end{aligned}$$

where $x'_d = k' \log D$ is the capacitive reactance spacing factor

$x'_a = k' \log \frac{1}{r}$ is the capacitive reactance at 1-m spacing

$k' = (21.65 \times 10^6)/f = 0.36 \times 10^6$ at $f = 60$ Hz.

(b) Determine the capacitive reactance in Ω-km for a single-phase line of Problem 4.14. If the spacing is doubled, how does the reactance change?

4.38 The capacitance per phase of a balanced three-phase overhead line is given by

$$C = \frac{0.04217}{\log(GMD/r)} \ \mu f/\text{km/phase}$$

For the line of Problem 4.24, determine the capacitive reactance per phase in Ω-km.

SECTION 4.10

4.39 Calculate the capacitance-to-neutral in F/m and the admittance-to-neutral in S/km for the three-phase line in Problem 4.18. Also calculate the line-charging current in kA/phase if the line is 100 km in length and is operated at 230 kV. Neglect the effect of the earth plane.

4.40 Rework Problem 4.39 if the phase spacing between adjacent conductors is: (a) increased by 10% to 8.8 m, (b) decreased by 10% to 7.2 m. Compare the results with those of Problem 4.39.

4.41 Calculate the capacitance-to-neutral in F/m and the admittance-to-neutral in S/km for the line in Problem 4.20. Also calculate the total reactive power in Mvar/km supplied by the line capacitance when it is operated at 500 kV. Neglect the effect of the earth plane.

4.42 Rework Problem 4.41 if the bundled line has: (a) three ACSR, 1351-kcmil (685-mm^2) conductors per phase, (b) three ACSR, 900-kcmil (450 mm^2) conductors per phase, without changing the bundle spacing or the phase spacings between bundle centers.

4.43 Three ACSR *Drake* conductors are used for a three-phase overhead transmission line operating at 60 Hz. The conductor configuration is in the form of an isosceles triangle with sides of 6 m, 6 m, and 12 m. (a) Find the capacitance-to-neutral and capacitive reactance-to-neutral for each 1-km length of line. (b) For a line length of 280 km and a normal operating voltage of 220 kV, determine the capacitive reactance-to-neutral for the entire line length as well as the charging current per km and total three-phase reactive power supplied by the line capacitance.

4.44 Consider the line of Problem 4.25. Calculate the capacitive reactance per phase in Ω-km.

SECTION 4.11

4.45 For an average line height of 10 m, determine the effect of the earth on capacitance for the single-phase line in Problem 4.32. Assume a perfectly conducting earth plane.

4.46 A three-phase 60-Hz, 125-km overhead transmission line has flat horizontal spacing with three identical conductors. The conductors have an outside diameter of 3.28 cm with 12 m between adjacent conductors. (a) Determine the capacitive reactance-to-neutral in Ω-m per phase and the capacitive reactance of the line in Ω per phase. Neglect the effect of the earth plane. (b) Assuming that the conductors are horizontally placed 20 m above ground, repeat (a) while taking into account the effect of ground. Consider the earth plane to be a perfect conductor.

4.47 For the single-phase line of Problem 4.14 (b), if the height of the conductor above ground is 24 m, determine the line-to-line capacitance in F/m. Neglecting earth effect, evaluate the relative error involved. If the phase separation is doubled, repeat the calculations.

4.48 The capacitance of a single-circuit, three-phase transposed line, and with configuration shown in Figure 4.38 including ground effect, with conductors not equilaterally spaced, is given by

$$C_{an} \frac{2\pi\varepsilon_0}{\ln \dfrac{D_{eq}}{r} - \ln \dfrac{H_m}{H_s}} \text{ F/m Line-to-neutral}$$

where $D_{eq} = \sqrt[3]{D_{12}D_{23}D_{13}} = \text{GMD}$

FIGURE 4.38

Three-phase single-circuit line configuration including ground effect for Problem 4.48

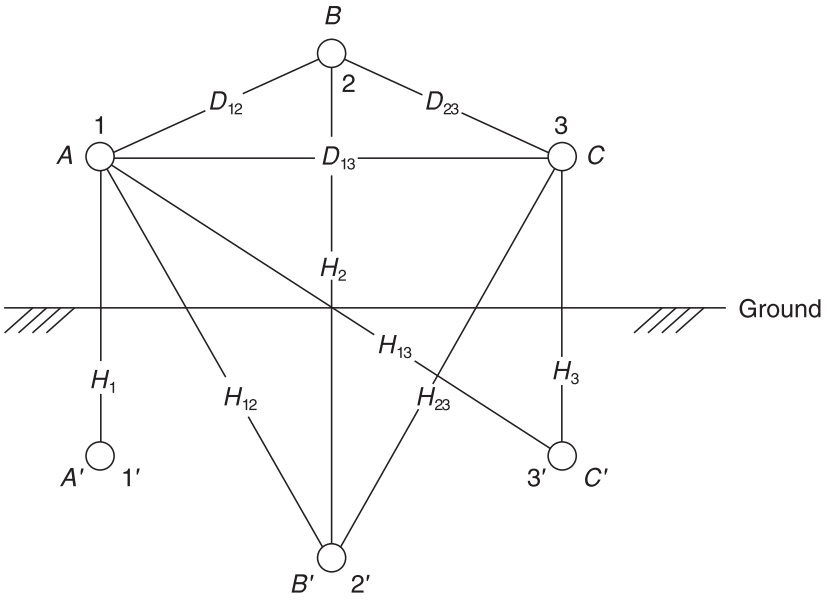

r = conductor's outside radius

$$H_m = (H_{12}H_{23}H_{13})^{1/3}$$

$$H_s = (H_1H_2H_3)^{1/3}$$

(a) Now consider Figure 4.39 in which the configuration of a three-phase, single circuit, 345-kV line, with conductors having an outside diameter of 27.051 mm (or 1.065 in.), is shown. Determine the capacitance to neutral in F/m, including the ground effect.
(b) Next, neglecting the effect of ground, see how the value changes.

FIGURE 4.39

Configuration for Problem 4.48 (a)

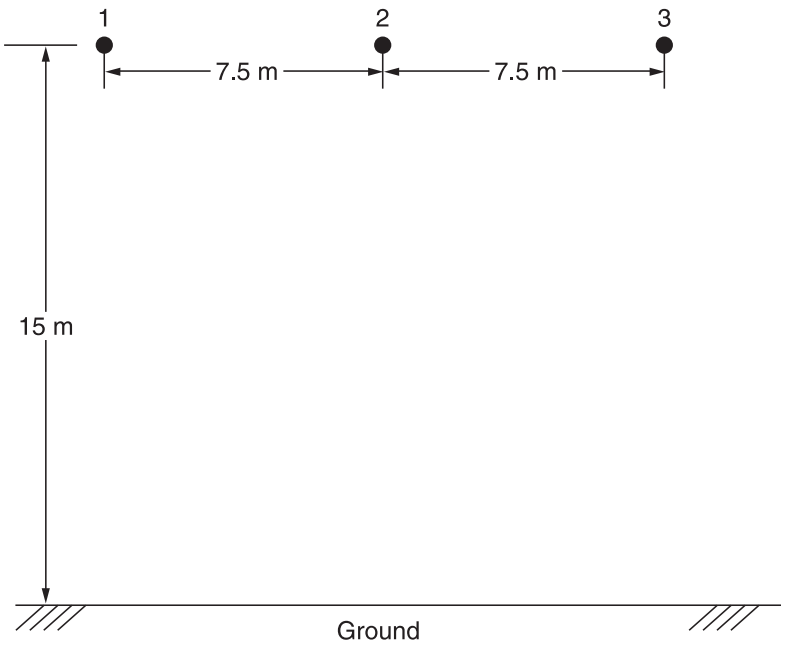

4.49 The capacitance to neutral, neglecting the ground effect, for the three-phase, single-circuit, bundle-conductor line is given by

$$C_{a\eta} = \frac{2\pi\varepsilon_0}{\ell\eta\left(\frac{\text{GMD}}{\text{GMR}}\right)} \text{ F/m Line-to-neutral}$$

$$\text{where} \quad \text{GMD} = (\text{D}_{AB}\text{D}_{BC}\text{D}_{AC})^{1/3}$$

$$\text{GMR} = [rN(\text{A})^{N-1}]^{1/N}$$

in which N is the number of subconductors of the bundle conductor on a circle of radius A, and each subconductor has an outside radius of r.
The capacitive reactance in mega-ohms for 1 km of line, at 60 Hz, can be shown to be

$$X_C = 0.11 \log\left(\frac{\text{GMD}}{\text{GMR}}\right) = X'_a + X'_d$$

$$\text{where} \quad X'_a = 0.11 \log\left(\frac{1}{\text{GMR}}\right) \quad \text{and} \quad X'_d = 0.11 \log(\text{GMD})$$

Note that A is related to the bundle spacing S given by

$$A = \frac{S}{2 \sin\left(\frac{\pi}{N}\right)} \quad \text{for } N > 1$$

Using the above information, for the configuration shown in Figure 4.40, compute the capacitance to neutral in F/m, and the capacitive reactance in Ω-km to neutral, for the three-phase, 765-kV, 60-Hz, single-circuit, bundle-conductor line ($N = 4$), with subconductor's outside diameter of 3 cm and subconductor spacing (S) of 46 cm.

FIGURE 4.40
Configuration for Problem 4.49

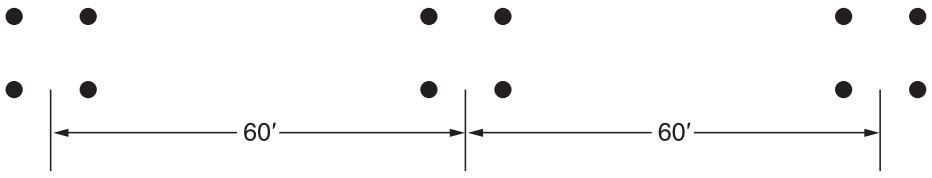

SECTION 4.12

4.50 Calculate the conductor surface electric field strength in kV_{rms}/cm for the single-phase line in Problem 4.32 when the line is operating at 20 kV. Also calculate the ground-level electric field strength in kV_{rms}/m directly under one conductor. Assume a line height of 10 m.

4.51 Rework Problem 4.50 if the diameter of each conductor is: (a) increased by 25% to 1.875 cm, (b) decreased by 25% to 1.125 cm, without changing the phase spacings. Compare the results with those of Problem 4.50.

CASE STUDY QUESTIONS

a. Why is aluminum today's choice of metal for overhead transmission line conductors versus copper or some other metal? How does the use of steel together with aluminum as well as aluminum alloys and composite materials improve conductor performance?

b. What is a high-temperature conductor? What are its advantages over conventional ACSR and AAC conductors? What are its drawbacks?

c. What are the concerns among utilities about porcelain insulators used for overhead transmission lines in the United States?

d. What are the advantages of toughened glass insulators versus porcelain? What are the advantages of polymer insulators versus porcelain? What are the disadvantages of polymer insulators?

REFERENCES

1. Electric Power Research Institute (EPRI), *EPRI AC Transmission Line Reference Book—200 kV and Above* (Palo Alto, CA: EPRI, www.epri.com, December 2005).

2. Westinghouse Electric Corporation, *Electrical Transmission and Distribution Reference Book*, 4th ed. (East Pittsburgh, PA, 1964).

3. General Electric Company, *Electric Utility Systems and Practices*, 4th ed. (New York: Wiley, 1983).

4. John R. Carson, "Wave Propagation in Overhead Wires with Ground Return," *Bell System Tech. J.* 5 (1926): 539–554.

5. C. F. Wagner and R. D. Evans, *Symmetrical Components* (New York: McGraw-Hill, 1933).

6. Paul M. Anderson, *Analysis of Faulted Power Systems* (Ames, IA: Iowa State Press, 1973).

7. M. H. Hesse, "Electromagnetic and Electrostatic Transmission Line Parameters by Digital Computer," *Trans. IEEE* PAS-82 (1963): 282–291.

8. W. D. Stevenson, Jr., *Elements of Power System Analysis*, 4th ed. (New York: McGraw-Hill, 1982).

9. C. A. Gross, *Power System Analysis* (New York: Wiley, 1979).

10. A. J. Peterson, Jr. and S. Hoffmann, "Transmission Line Conductor Design Comes of Age," *Transmission & Distribution World Magazine* (www.tdworld.com, June 2003).

11. ANCI C2. *National Electrical Safety Code*, 2007 edition (New York: Institute of Electrical and Electronics Engineers).

12. R. S. Gorur, "Six Utilities Share Their Perspectives on Insulators," *Transmission & Distribution World Magazine*, (www.tdworld.com, April 1, 2010).